CHALMERS

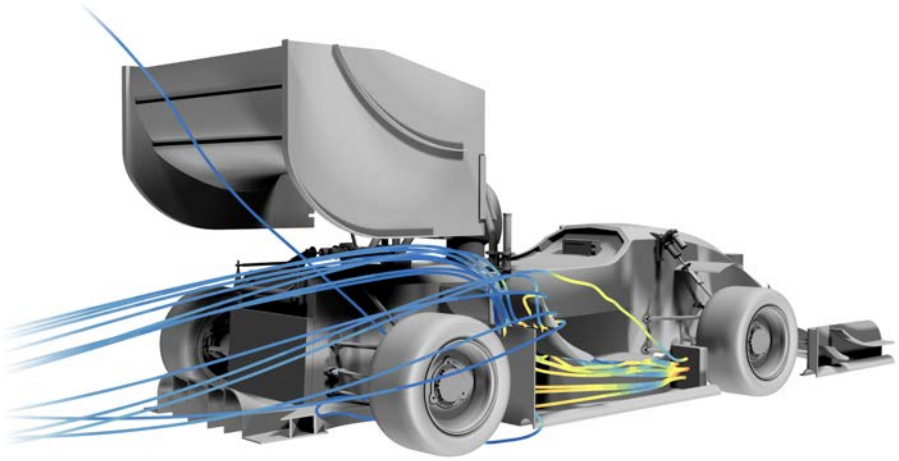

Fan placement on a Formula Student vehicle

A study to evaluate placement of fans for improved aerodynamic performance

Bachelor's thesis in Mechanical Engineering

ANDRÉ AHLBECK

ELIAS HOLMBERG

SVEN KARLSSON

SAMUEL LJUNGQVIST

HANNA LOCKLEY

JOSEF LUNDIN

DEPARTMENT OF MECHANICS AND MARITIME SCIENCES

CHALMERS UNIVERSITY OF TECHNOLOGY

Gothenburg, Sweden 2025

www.chalmers.se

Bachelor's thesis 2025

Fan placement on a Formula Student vehicle

A study to evaluate placement of fans for improved aerodynamic performance

ANDRÉ AHLBECK

ELIAS HOLMBERG

SVEN KARLSSON

SAMUEL LJUNGQVIST

HANNA LOCKLEY

JOSEF LUNDIN

CHALMERS

Department of Mechanics and Maritime Sciences
Division of Vehicle Engineering and Autonomous Systems
Chalmers University of Technology
Gothenburg, Sweden 2025

Fan placement on a Formula Student vehicle
A study to evaluate placement of fans for improved aerodynamic performance
ANDRÉ AHLBECK
ELIAS HOLMBERG
SVEN KARLSSON
SAMUEL LJUNGQVIST
HANNA LOCKLEY
JOSEF LUNDIN

Supervisor: Christian Svensson, PhD student, Division of Fluid Dynamics
Examiner: Simone Sebben, Professor, Division of Vehicle Engineering and Autonomous Systems

Bachelor's thesis 2025
Department of Mechanics & Maritime Sciences
Division of Division name
Chalmers University of Technology
SE-412 96 Gothenburg
Telephone +46 31 772 1000

Cover: Wind visualization on the Chalmers Formula Student car constructed in Star CCM+ showing streamlines of the flow from the cooloing fans.

Typeset in LaTeX
Printed by Chalmers Reproservice
Gothenburg, Sweden 2025

Abstract

Formula Student 2024 saw an increase in teams that used fans for aerodynamic gain instead of just for cooling purposes. This gave a huge performance to the car in terms of downforce and therefore better grip which allows for faster cornering. The sudden performance gain resulted in a rule change for the 2025 Formula Student season where a maximum combined total rated power of any active devices designed to move air is 500 W. This restriction made it more difficult to find aerodynamic advantages from the fans and their positioning became more vital.

The objective for this project is to investigate how a fan system on Chalmers Formula Student's (CFS) current car can be implemented to enhance the aerodynamic performance. Concepts were generated by dividing the aerodynamic components into four regions, front wing, side wing, rear wing and diffuser. Each component could then be investigated by looking at data from past simulations, but also by taking inspiration from other teams.

Having formulated several concepts for each geometrically defined region, they were realized using computer aided design (CAD). The results were then evaluated using computational fluid dynamics (CFD) and numerical values and field plots of several properties were obtained. The result showed that significant downforce can still be found in spite of the new regulation change. The regions that performed best were side wing and diffuser. While the concepts in these regions show potential, future iterative work is still needed to perfect their functionality, depending on the direction of development for the CFS aerodynamic package.

Sammandrag

Säsongen 2024 ökade antalet Formula Student team som använde fläktar för aerodynamisk vinning istället för enbart kyländamål. Detta gav en ansenlig prestandaförbättring för bilen i form av ökad downforce och därmed bättre grepp, vilket möjliggör snabbare kurvtagning. Den avsevärda prestandaökningen ledde till en regeländring för Formula Student-säsongen 2025, där den maximala sammanlagda effekten märkt för alla aktiva system avsedda att flytta luft, begränsades till 500 W. Denna regeländring begränsade möjligheten att nyttja fläktar för aerodynamisk vinning. Där effekt tidigare kunnat kompensera för suboptimal placering, blev placering nu en avgörande faktor i att tillse god aerodynamisk prestanda.

Syftet med detta projekt är att undersöka hur ett fläktsystem kan implementeras på Chalmers Formula Students (CFS) nuvarande bil för att förbättra den aerodynamiska prestandan. Koncepten genererades genom att dela upp de aerodynamiska komponenterna i fyra regioner: framvinge, sidovingar, bakvinge och diffusor. Varje komponent undersöktes sedan med hjälp av data från tidigare simuleringar samt genom inspiration från andra team.

Efter att flera koncept hade tagits fram för varje geometriskt definierad region och realiserats genom datorstödd modellering, evaluerades resultaten med hälp av beräkningsbaserad strömningsmekanik (CFD). Resultat i form av numeriska värden och fältplottar för olika egenskaper erhölls. De visade att signifikant downforce fortfarande kan genereras trots den nya regeländringen. De regioner som presterade bäst var sidovingarna och diffusorn. Även om koncepten i dessa regioner visar potential, krävs fortsatt iterativt arbete för att förfina deras funktionalitet, beroende på vilken riktning CFS aerodynamikpaket tar i framtida utveckling.

Acknowledgments

The group would like to thank our supervisor, Christian Svensson PhD-student at department of Mechanics and Maritime Sciences, for invaluable help, lectures and constant guidance throughout the project.

The group would also like to thank Simone Sebben, Professor at Division of Vehicle Engineering and Autonomous Systems, for accepting this study and allowing us to do it. She assisted us with lectures, experience, and guidance that have been crucial in the study.

Lastly, the group would like to thank Chalmers Formula Student for their constant cooperation and for giving us access to CAD designs and documentation.

-The authors

Nomenclature

Below is the nomenclature of abbreviations and important terms that have been used throughout the thesis.

General terms

AoA	Angle of attack
CAD	Computer aided design
CFS	Chalmers Formula Student
CFD	Computational fluid dynamics
CoP	Center of Pressure
FS	Formula Student
it	Iteration

Fluid dynamics

A	Area $[m^2]$
α	Angle of attack $[rad]$
α_{L0}	Change in angle of attack $[rad]$
C_L	Coefficient of lift $[-]$
C_l	Coefficient of lift for two-dimensional profiles $[-]$
C_D	Coefficient of drag $[-]$
C_d	Coefficient of drag for two-dimensional profiles $[-]$
C_p	Pressure coefficient $[-]$
C_{PT}	Coefficient of total pressure $[-]$
F_L	Lift force $[N]$
g	Gravity constant $[m/s^2]$
m	Mass $[kg]$

μ	Friction coefficient $[-]$
P	Pressure $[Pa]$
P_∞	Ambient pressure $[Pa]$
r	Radius $[m]$
Re	Reynolds number $[-]$
ρ	Fluid density $[kg/m^3]$
U	Velocity $[m/s]$
V_∞	Ambient velocity $[m/s]$

Contents

List of Figures

List of Tables

1
Introduction

This section aims to introduce the project by first explaining what the Formula Student competition is and then go on to state the objective and problem statement of the project. Lastly, the delimitations are discussed.

1.1 Background

Formula Student (FS) is an international design competition where teams of students from different universities around the world design, build and compete with formula style race cars. The underlying objective of the competition is to demonstrate the best possible car concept for a fictitious potential investor. This is done through different static and dynamic competition diciplines. It is therefore important to demonstrate the cars dynamic capabilities as well as the teams knowledge about the underlying physics behind it [1]. Since 2003 there has been an active FS team at Chalmers, namely Chalmers Formula Student (CFS). Today CFS builds four wheel drive electric race cars in accordance with the current technical regulations provided by the competitions. Aerodynamics plays a part in the car's handling providing negative lift (downforce) to enhance grip when cornering.

Downforce refers to the downward acting vertical force created as a result of pressure differences from the air flowing over the car's surfaces. The car relies on friction between the tyres and the ground for changes of direction. With more downforce, the normal load on the tyres increases and subsequently the friction force. The current car built by the 2024 team (CFS24) utilizes fans for cooling purposes. Other than cooling, the fans also affects the airflow around them as the outgoing flow sees a significant increase in momentum. Utilizing this local increase in momentum in the flow could potentially improve the aerodynamic performance of the car. CFS designs an aerodynamic package containing several aerodynamic components placed at different parts of the car. These are dependent on the airflow from the inlet and energy losses from the incoming flow will result in a decrease in performance for a given part. On the other hand, increasing the energy in the oncoming flow could see an increase in performance for the same part. Strategically placing the fans with aerodynamics in mind could therefore be crucial for the aerodynamic behavior of the car which in turn affects its driving characteristics. This means that increasing the generated downforce from the existing aerodynamic components with the help of fans is the primary target.

1.2 Objective

The purpose of the project is to investigate how a fan system on Chalmers Formula Student's current car can be implemented to enhance performance. By analyzing different types of implementations within the given regulations, the aim is to explore how the frictional force between the car and the road surface can be maximized by increasing the downforce generated by the car as it moves through the air. Active components in the form of fans will be used to manipulate the natural airflow over the car with this objective in mind. The primary goal is to increase the car's negative lift, and this will be permitted even at the cost of increased aerodynamic drag.

1.3 Problem Statement

The task of this project is to develop a concept for the implementation of fans on the current CFS car, enabling a future iterative process for maximizing the car's downforce. The term concept refers to a solution that is not yet optimized, where the main positioning of the fans has been determined. Furthermore, the concept must comply with regulations and be feasible for implementation by future CFS teams.

Aerodynamic components utilize the energy of the incoming airflow to generate force. Because these components interact with a fixed mass flow with a given amount of energy, there is a theoretical limit to the achievable performance. With fans, however, energy (in the form of electrical energy converted to kinetic energy) can be added to the airflow, allowing for additional performance gains. With this fundamental principle, the project aims to evaluate various practical implementation possibilities to use the added energy in the most effective way. For example, the risk of flow separation on wing structures with high angles of attack can be reduced by supplying additional energy to the boundary layer, or by decreasing form drag, as air can be moved into regions where low pressure occurs.

1.4 Delimitation

For this specific project, the main limitation is the total power that the fans can use. This restriction is defined in rule T.11.11.1 as: "The maximum combined total rated power of any active devices designed to move air is 500 W [this includes cooling fans but does not apply to CV1.8]." [2]

The concept will not be tested in the real world and will instead be verified solely through computational fluid dynamics (CFD) using the software StarCCM+. This involves simulating airflow behavior when the car is driving straight at 40 km/h. It is assumed that the flow is steady and time-independent (steady-state). Situations such as braking and cornering will be excluded from the project. Although these scenarios frequently occur during driving, this limitation enables comparisons with previously conducted CFS simulations.

No physical implementation on an existing car will be carried out. Instead, the project aims to lay the theoretical foundation required for future implementation.

For a concept to be implementable, the car's cooling must be taken into account. Given the 500 W power limit mentioned above, the highest priority is the cooling of the motors, battery and inverter. A requirement from the cooling system is that a radiator is placed adjacent to the fan, as the fan, from a cooling perspective, is intended to generate airflow through the radiator. This locally slows the airflow, and a concept evaluated with aerodynamics in mind must also consider this. The heat exchanger and fan system will not be altered and the current settings, implemented by CFS will be used. This is due to the ability to compare the result with the CFS team.

Small differences in airflow or how a model is built can have significant effects on how air flows around the model. The Chalmers Formula Student car is complex, with features designed to manipulate and direct airflow, which in turn affects subsequent components and their influence on both drag and downforce. These factors mean that the simulations must be conducted on precise models with a fine mesh on critical components, which makes the simulations computationally demanding and time-consuming given the available resources. This limitation, combined with the tight timeframe, means that the number of simulations per concept will be limited to a maximum of three, with as few exceptions as possible.

2
Theory

In this chapter, the necessary theory to follow the methods, results and conclusion chapters will be presented. The study of fluid dynamics and aerodynamics, which form the largest portion of the overall theory in the project, is complex and finding numerical solution to formalized theories, let alone formalizing those theories can be difficult. Often, a balance between computational load and accuracy needs to be found in order to solve real world problems. With this in mind, the section below will focus on explaining the result of physical theories applied to a problem, rather than trying to explain the theories and fundamental physics. For a deeper understanding of those subjects, the reader is referred to a more comprehensive source of information, for example [3].

2.1 Mechanics of Grip

The mechanical grip of the car is directly related to the maximum speed possible to carry through a corner and therefore related to the laptime. When traveling through a corner, the lateral acceleration component of the total acceleration allows for steady state cornering with the vector pointing to the center of the corner. Without a lateral component, no direction change is possible. For a steady state cornering vehicle generating lift the force equilibrium can be written as follows

$$\mu(mg - F_L) = m\frac{U^2}{r} \tag{2.1}$$

Where μ is the friction coefficient, m is the vehicle mass, g is the gravity of earth, U is the vehicle velocity and r is the radius of the corner. Note that F_L is negative for a vehicle generating downforce. In Equation 2.1 it is shown that the lateral acceleration is given by the normal load scaled with a friction coefficient μ. The coefficient is related to the conditions of the ground on which the vehicle is travelling. In the case where F_L is zero, the lateral acceleration is simply a product of the friction coefficient and the gravitational acceleration. From Equation 2.1 above, the maximum cornering velocity is calculated as

$$V = \sqrt{\frac{\mu mg}{\frac{m}{r} + 0.5\mu C_L A\rho}} \tag{2.2}$$

Where C_L is the coefficient of lift for a three dimensional body, A is the area, μ is the fluid viscosity and ρ is the fluid density. Returning to the case of $F_L = 0$, one can conclude that the the maximum cornering velocity is independent of the vehicle mass, meaning that simply adding mass to the vehicle is not a cornering performance enhancement.

Considering lift in Equations 2.1 and 2.2 above, the lift force is modelled as

$$F_L = 0.5 C_L A \rho V^2 \tag{2.3}$$

An addition of a lift generating aerodynamic device will hence result in an addition to the total vehicle mass as well as an F_L term considering (2.1) above. As previously discussed, only the lift force addition to the overall normal load will affect the possible cornering velocity. This requires, however, that the mass of the wing is small in relation to the total vehicle mass. Finally, it should be mentioned that the mass is still of concern as it greatly affects the longitudinal acceleration.

The increased downforce of a high-downforce vehicle also gives the possibility of maintaining the same cornering speeds with lower slip angles compared to a non-downforce vehicle. With lower slip angle comes less heat and easier tyre temperature management leading to a prolonged tyre life.

2.2 Vehicle Dynamics Theory

In the previous chapter, the fundamental mechanics behind cornering of a vehicle was introduced. This chapter will cover a basic walkthrough of vehicle dynamics, relevant for the Formula Student car. While the simulations in this project are carried out in a straight-line driving scenario, vehicle dynamics parameters have a significant impact on the performance of the aerodynamic devices and are therefore important to keep in mind when performing any kind of aerodynamic design.

2.2.1 Influence of aerodynamics on vehicle dynamics

Driving on track, the motion of the vehicle body in relation to the tyres can be divided into several categories. When considering straight-line driving, the main driving scenarios to be considered are acceleration and braking. Here, aerodynamics plays an important role as the added vertical force impacts the friction force between the tyre and the road. As the force generated by the wings increase with speed, so does the potential braking performance. Adding to this, the longitudinal drag force generated by the wings act in the opposite direction of travel meaning that it enhances the braking performance. Especially at high speeds when the drag force is at its highest. In acceleration, the same concept of adding downforce to increase the longitudinal friction force can be utilized. It should however be mentioned that the lower speeds in the beginning of the acceleration phase translates to less downforce generated by the wings compared to the braking scenario.

Additionally an aerodynamic effect can be noticed in pitch mostly from the devices placed relatively close to the ground plane. A forward load transfer occurs under braking meaning that the front end of the car comes closer to the ground. This has an effect on the front wing, being an aerodynamic device close to the ground. As the wing gets closer to the ground, the area for the air to flow through between the wing and the ground is contracted, resulting in greater amounts of generated downforce. This concept is known

as ground effect and will be expanded upon in the coming chapters. While more grip can be obtained through the front tyre, this downforce increase has a substantial effect on the longitudinal aerodynamic balance shifting the center of pressure forward. This in combination with the load transfer can make for an unstable vehicle that is difficult to control. Furthermore, if the front wing was to get too close to the ground, the area between the wing and the ground could get too small for the wing to get sufficient flow and maintain proper functionality. In this case, the wing will stall and generate considerably less downforce, meaning that although some of the longitudinal balance issues from the load transfer can be countered, the lack of front end downforce could lead to issues turning into the corner. Especially in the case where maximum tyre friction coefficients are used close to the limit of the available grip. In addition to hampering the functionality of the front wing, a reduced ground clearance could also impose issues of distributing air to aerodynamic devices downstream.

While the phenomena above acts symmetrically on the car laterally, describing the aerodynamic impact of yaw, roll and steering angle is far more complicated as they act in an asymmetrical manor and have a longitudinal component in the velocity vector relative to the car. This report will not go into these effects and the reader is referred to [4] for a more extensive explanation.

2.3 Vehicle Aerodynamics

In the previous chapter, it was concluded that the only way to increase the maximum possible cornering velocity for a vehicle is by adding a negative lift component to the total normal load. Having showed how it enhances the vehicle performance, the following section will be dedicated to explaining the fundamentals behind how the energy in the passing airflow can be utilized to generate negative lift.

For any vehicle traveling through a fluid medium, it sees a mass flow of fluid with a finite energy passing through its control volume. This means that a theoretical maximum for the level of extractable performance exists. The fluid flow can be visualized by stream lines, which are the lines formed by the tangent to the velocity vector when looking at single fluid particles. Looking at the flow on a single stream line, and assuming frictionless incompressible flow, the Bernoulli equation can be formulated as

$$\frac{\rho V^2}{2} + P = const. \tag{2.4}$$

where P is the static pressure, and $\frac{\rho V^2}{2}$ the dynamic pressure. Derived from the energy conservation equation, Equation 2.4 states that at all points along the streamline, the sum of all energy forms is the same. While only applicable to fluid flows without viscous forces, the equation is important as it shows the relation between the static pressure and the velocity. At a point along the stream line with high velocity, the static pressure will be low and vice versa.

While Equation 2.4 provides a measure to correlate velocity and pressure, aerodynamic

load is a consequence of a difference in surface pressures. The static pressure (P in Equation 2.4) is often expressed as a non-dimensional coefficient, C_p, defined as

$$C_p = \frac{P - P_\infty}{0.5\rho V_\infty^2} \tag{2.5}$$

A benefit of the pressure coefficient is its theoretical independence of the vehicle velocity and the density of the fluid around the car.

So far, this section has been dedicated to flows without viscous forces (losses). This is possible in theory, but as viscous forces are taken into account, the right hand side in Equation 2.4 can no longer be seen as constant. An energy loss, or loss of total pressure will occur. Similar to the coefficient of pressure, a coefficient of total pressure is normally used to get a normalized description of the total pressure. Coefficient of total pressure is defined as

$$C_{p_T} = \frac{0.5\rho V^2 - P}{0.5\rho V_\infty^2} \tag{2.6}$$

To understand how these losses of total pressure occur, the concept of a boundary layer has to be introduced. Boundary layer theory describes the interaction between a surface of a solid, and a fluid flowing past it. A fundamental assumption for boundary layer theory is the no slip condition which when considering a velocity profile of a fluid near a wall, assumes that the velocity at the wall is zero. This is regardless of whether the flow is turbulent or laminar. At a certain distance from the wall, the velocity is no longer affected by the wall. This means that there must be a velocity distribution profile that spans from zero velocity at the wall (due to the no-slip condition) to the free stream velocity. The shape of this profile depends on several factors and can vary downstream along the wall. In general the transition from boundary layer to the free stream is considered to take place at the point from the wall where 99 percent of the free stream velocity is reached.

In general, the boundary layer on a submerged body can be divided into a laminar region, a transition region and a turbulent region in the longitudinal direction. To analyze the properties and point of transition between these regions, the Reynolds number is commonly used. It is a dimensionless property describing the relation between viscous and inertial forces in a fluid defined as

$$Re = \frac{\rho U L}{\mu} \tag{2.7}$$

where ρUL describes the inertial part, and μ describes the viscous part. This relation is applicable outside the boundary layer as well, and for a given geometry, one can find a critical Re where flow goes from laminar to turbulent. In essence a transition to turbulence occurs when the viscous forces can no longer dampen out disturbances in the flow as it becomes more unstable. Turbulence in the boundary layer implies higher velocity fluctuations which results in an increased exchange of momentum. Increasing the degree of turbulence increases the level of mixing.

Going back to loss of total pressure, another important concept to understand is pressure gradients. When plotting the pressure distribution over a geometry, the pressure gradient is basically the gradient in every point on the graph. A favorable pressure gradient means that the pressure is decreasing in the direction of the fluid motion.

As the fluid moves along a surface with an adverse pressure gradient, it experiences increasing resistance to motion, the flow moving from a low-pressure region to a high-pressure region. Due to the velocity near the surface being low as a result of the no slip condition, the momentum of the flow is not large enough to overcome the increase in pressure which in turn can cause the flow nearest to the wall to reverse. When this happens, the flow can no longer follow the path of the surface, a phenomena commonly known as separation. With more mixing and higher momentum near the wall, a turbulent boundary layer can delay the separation mechanism compared to a laminar boundary layer.

2.3.1 Airfoils

A generic airfoil has geometry similar to that shown in Figure 2.1. This specific airfoil is classified as a cambered airfoil while if the chord and camber lines defined in Figure 2.1 would be collinear it would be a symmetric airfoil.

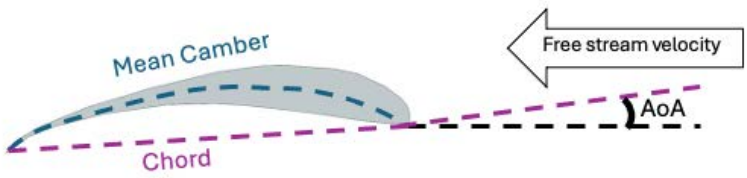

Figure 2.1: An airfoil with mean camber, chord and angle of attack

Looking at the streamlines over a generic airfoil, one can find a point close to the leading edge at which the flow stagnates. The point is known as the stagnation point and as the flow is generally slowed down by the absence of direction changes, causing a pressure increase on the surface. Consequently, as can be seen in Figure 2.2 a pressure side and suction side is introduced. The pressure side is where the flow decelerates and thus ac-

cording to Equation 2.4 the pressure increases. In contrast the suction side is where the flow increases velocity and that causes the pressure to decrease. The physical background to these effects are widely debated and for a more detailed explanation of the concepts behind how lift is generated by an airfoil, see [3].

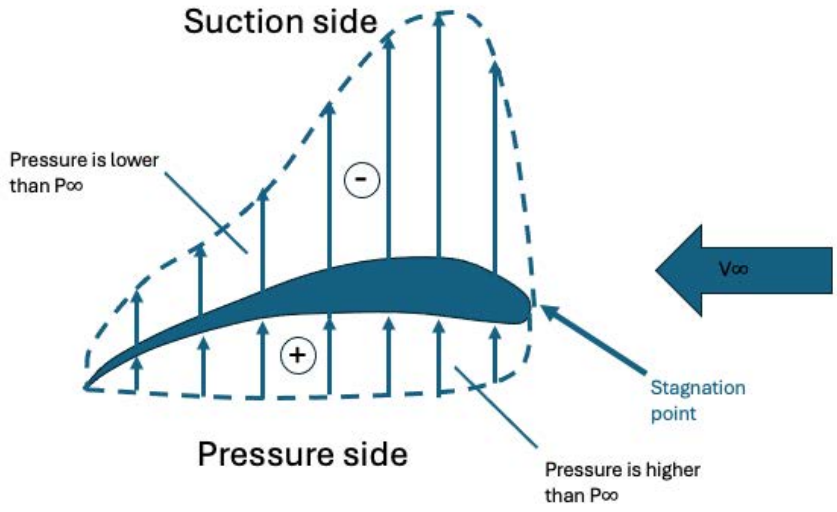

Figure 2.2: Airfoil with suction and pressure side.

Looking at the general pressure distribution in Figure 2.2, one can conclude that the pressure difference between the suction and pressure side will result in a force acting on the body. This force is per definition a function on the magnitude of the pressure difference as well as the surface area on which the pressures act. In general, the pressure distribution of an airfoil is portrayed using the dimensionless parameter C_p defined in Equation 2.5. By looking at the pressure distribution in dimensionless form, one can make direct comparisons between experiments of different profiles regardless of parameters such as chord length and free stream velocity.

There are several measures to alter the pressure distribution and increase the lift force generated by an airfoil. One of which is to alter the angle of the airfoil's chord line relative to the tangent vector of the free stream velocity. This angle is commonly refereed to as Angle of Attack (AoA) and an example can be seen in Figure 2.1 above. Similar to how pressure is nondimensionalized for ease of comparison, the lift generated by a body can be nondimensionalized as

$$C_l = \frac{F_l}{0.5\rho U^2 A} \tag{2.8}$$

where F_l refers to the lift force (2D) and $0.5\rho U^2 A$ refers to the dynamic force. Further-

more, the effect on C_l from altering the angle of attack, α can be formulated as

$$C_l \approx 2\pi(\alpha + \alpha_{L0}) \tag{2.9}$$

with α being the AoA measured in radians and α_{L0} being the effective change in AoA by the airfoil's camber.

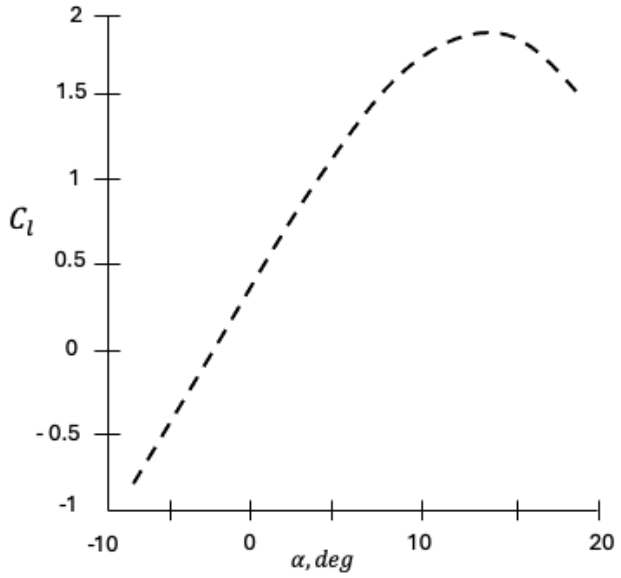

Figure 2.3: C_l as a function of AoA for an arbitrary airfoil, where separation induced lift reduction is seen to occur at around 10 degrees and more

Figure 2.3 shows a generic plot of C_l as a function of the AoA. While Equation 2.9 would suggest that C_l could be increased to infinity simply by increasing the AoA infinitely, the equation does not take viscous forces into account. As mentioned above, a loss of total pressure will occur once the momentum in the boundary layer is unable to overcome the adverse pressure gradient and looking at Figure 2.3, this is what happens once the increase in C_l starts to drop off. The flow on the suction side will separate from the airfoil body and not meet up with the flow on the pressure side, causing a region of recirculation around the trailing edge.

A similar effect can be obtained by altering the camber line of the airfoil section. The most noteworthy effects are observed when the camber line is altered close to the trailing edge [4]. The fundamental mechanics works in the same way as when altering the AoA and granted attached flow, Equation 2.9 is still applicable. In the same way that too big of an AoA will cause separation, too steep of a camber line will result in the same effect. One way to avoid the separation is to introduce multiple wing elements.

2.3.1.1 Multielement wing

Adding multiple wing elements is one way to obtain the same effects as when altering the camber line or increasing the AoA. The multi-element wing shown in Figure 2.4 achieves the same effect as a single airfoil with the leading edge of the first element and the trailing edge of the last element, but without separating. The reason for not separating is the injection of air with high momentum into the boundary layer at every transition between two flaps. Separation occurs as a result of a lack of momentum in the boundary layer and gradually injecting new momentum delays the separation mechanism as well as making steeper net changes in camber possible.

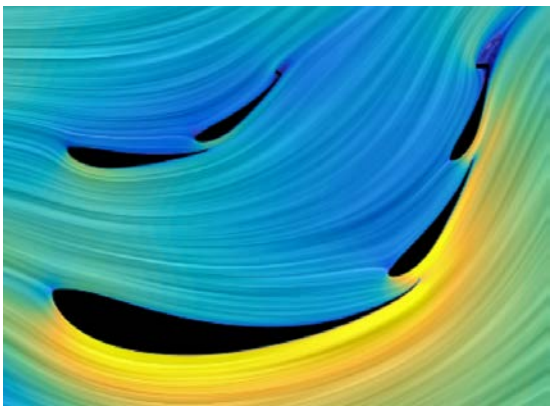

Figure 2.4: CFS current multielement rear wing

Another important feature of the multielement wing becomes evident when observing a plot of the pressure coefficient over the cord length like the one in Figure 2.2. For a single cambered airfoil, the pressure recovery to around ambient pressure takes place over a relatively long distance resulting in a thick boundary layer with low kinetic energy. Introducing multiple elements could be seen as distributing the total pressure recovery over multiple smaller elements. This implies that every individual element has a more gentle pressure gradient with a relatively thin and high energy boundary layer, making for higher resilience towards phenomena such as separation.

2.3.2 Airfoil Drag

In addition to the pressure distribution in the normal direction to the airfoil, another aspect to consider is the drag generated as a consequence of air passing over the body. It is formally in general terms, the force in the streamwise direction. The total drag force can be divided into two categories. Friction drag and pressure drag. Non dimensionalizing the total drag force F_D given by adding the two contributions together, one can obtain the drag coefficient C_D as

$$C_D = \frac{F_D}{0.5\rho U^2 A}$$

Beginning with friction drag, the viscous forces in the boundary layer slow down the fluid and the friction adds to the tangential drag force. As the boundary layer is defined as the region where the viscous forces slows down the flow, a thicker boundary layer will cause greater drag. With more mixing and higher wall shear stresses as a result, higher friction drag figures are to be expected from a turbulent boundary layer compared to a laminar boundary layer.

For a submerged body with flow separation, loss of total pressure means a difference in pressure between the front and rear most part. This will result in a longitudinal pressure drag force adding to the total drag force of the body. As a higher degree of pressure recovery will result in less pressure drag, the point of separation and the resulting wake region is the decisive factor with regards to magnitude of the pressure drag. A later point of separation will result in a smaller wake region and greater pressure recovery, meaning less pressure drag, and vice versa. This means that the actions to decrease pressure drag can increase friction drag, and the relative importance of the two components are case specific.

2.3.3 Vorticity

For a wing with non-infinite span, the pressure differential on the tips (side edge) of the wing is significantly lower as flow from the side with higher pressure flows to the one with lower pressure. Other than counteracting the mechanism behind the lift generation, the rotating flow between the two sides create a vortex with the air circulating around the vortex core as shown in Figure 2.5.

While the case above is one example of a rotating velocity field, it's far from the only one where the phenomena is found, and controlling vorticity in the flow field when carrying out design work is key.

Figure 2.5: Graphic representation of end tip vortex

The aspect ratio AR, defined as $\frac{\text{span width}}{\text{cord length}}$, is a fundamental geometrical property of a wing in this context, as a wing with lower aspect ratios will see a larger share of the overall

span width being affected by the effects of the end tip vorticies. While the lift generated by a certain wing profile is reduced, the vorticies can sometimes be a sought after feature as the rotating movement results in a subsequent movement of the air around it downstream. As seen in Figure 2.6, the rotational movement of the vortex does not simply stop at the trailing edge of the wing, but can rather continue far downstream interacting with the flow. This further means that careful consideration is needed when adding a wing element to a given geometry as the resulting vorticies can lead to unpredicted results downstream.

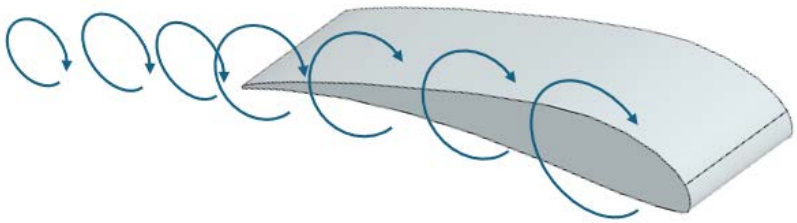

Figure 2.6: Graphic representation of vortex downstream of airfoil

2.3.4 Ground effect

Previously, airfoils have been discussed in the context of undisturbed freestream laminar flow. However, when considering the parameter of ground proximity, one finds that properties such as lift generation and flow deflection are affected. Moving the wing in such a way that the ground proximity is half of the cord length could see a potential increase in lift by 50% [4]. Furthermore, the proximity to the ground also affects the flow deflection where, for a downforce generating airfoil, the upwash is significantly reduced [5]. This is an important design parameter, especially for devices far upstream, as a lower degree of flow deflection could allow other devices down stream to use the same air to a greater extent. Overall, the concept of lift increase as a result of closer ground proximity, ground effect, is closely related to the Venturi tube and a visual representation of the effect can be seen in Figure 2.7.

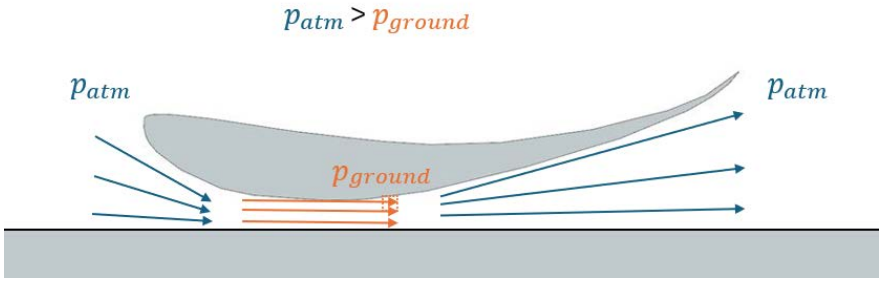

Figure 2.7: Illustrated example of an inverted airfoil in ground effect

2.4 Aerodynamics devices

The effect of an aerodynamic component is greatly affected by the air that flows around the component. Generally, energized flow is preferred to increase the desired effect of the component. If a component were to be placed directly downstream of an obstructing component, it would sit in the wake, which could also be described as a zone of low dynamic pressure. This means that the air moves slowly compared to the component, meaning that the component has a decreased aerodynamic performance. This could be utilized to minimize the drag caused by a component, however, it also means that performance from a downforce generating component can be lost if the airflow is sub-optimal. On a Formula Student car the drag penalty of a component is mostly overlooked since the performance gain from downforce gains more laptime.

2.4.1 Front wing

Depending on the current rules and category of race cars, the size and shape of the front wings of the race cars vary greatly, see the CFS front wing in Figure 2.8a, but they all share a few common things. The front wing always receives clean energized air. This is beneficial for producing local downforce. As the front wing is upstream of every other aerodynamic component of the car, the produced upwash and vortexes must be carefully studied and controlled so that components further downstream can produce the desired downforce. At each end of the main segment there are endplates, these are designed to stop high pressure air at the pressure side from escaping to the suction side. However, these can be used to achieve several different effects as they produce a top and bottom vortex.

Upwash can be controlled by suspension arms and components such as *bullhorns* or *bunny ears* that was used by Honda and several other teams in F1 between 2007 and 2008 [5] (see Figure 2.8b). These components are designed to reduce the upwash from the front wing at the cost of locally produced lift. To maximize effectiveness, these components must be designed in tandem as they are greatly affected by each other. The vortexes produced by the front wing can achieve several different aerodynamic phenomenons. Vortexes can be used to seal off a low pressure zone under the car. This sealing effect is obtained as the inwashing airflow is obstructed by the outwashing part of the vortex. A vortex can also be used to create a suction that draws clean energized air from the surrounding air that can be used to enhance performance downstream. It is not only upwash that needs to be controlled when designing a front wing. Since almost all air heading to the floor and diffuser passes underneath or over the front wing the design also needs to take this into consideration. To maximize the downforce produced by the floor, the floor needs to receive as much air as possible, see Section 2.4.3. This is usually achieved by raising the front wing slightly in front of the floor inlet to alow for a greater airflow. To maximize the total downforce and minimize lap time the front wing needs to be a compromise between producing downforce and helping other aerodynamic components downstream. Due to the amount of downforce produced and the distance between the front wing and *Center of Pressure* (CoP) the front wing greatly affects the CoP. This means that the car balance and handling is greatly affected by slight increases or decreases in the downforce produced

by the front wing.

The current Formula Student rules state that the front wing is limited to a maximum of 700 mm in front of the leading edge of the front wheels, up to 250 mm from the ground and can theoretically stretch all the way back to the center of the front wheels However, the wheels must have a 75 mm clearance from the front wing and no component can be placed above the wheels. There are however, no limits to the width of the front wing.

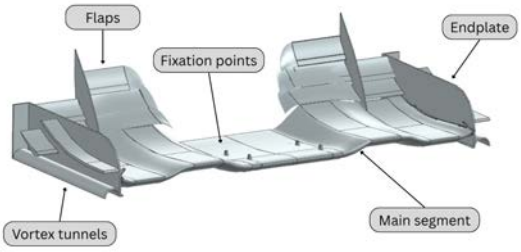

(a) Overview of the front wing and its components

(b) Chalmers formula student bullhorns

Figure 2.8: Chalmers Formula Student front wing and bullhorns

2.4.2 Side Wings

Side wings are common on formula-style vehicles. According to the boundary volumes specified in [2], aerodynamic devices need to allow a 75mm clearance to the wheels and a 30mm clearance to the ground. The rules also state that the aerodynamic device needs to be within the outside of the wheels if they are closer than 500mm to the ground (and within the inside of the wheels if they are higher than 500mm above the ground). As the side wings are placed centrally on the car, they must be designed with close regards to the front wing, rear wing and diffuser. The main segment of the side wings is an airfoil in close proximity to the ground, leading to a strong ground effect influencing the performance, see Section 2.3.4. This concept was firstly introduced to F1 in the late 70's [4]. To enhance performance, the side wings are sensitive to high pressure air entering the wing from the side. This led to the introduction of side skirts to seal the underfloor from ambient air, see Figure 2.9a. Today, these skirts are usually replaced by vortex tunnels, or similar components as side skirts were banned. See CFS vortex tunnels in Figure 2.9b. The vortices created in these tunnels resemble a virtual wall that keeps air from entering the side wing from the sides.

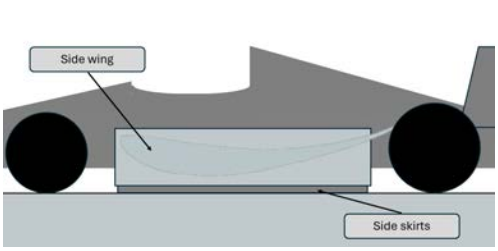

(a) 70's-80's F1 side wings and skirts

(b) Vortex tunnels on CFS

Figure 2.9: Side Wings

The side wings are also sensitive to wheel wake entering the inlet, as the de-energized air can not accelerate as much, and therefore the pressure difference between the pressure and suction side is not as prominent, and therefore downforce is lost. This could be minimized by implementing vertical wings, deflector plates, inwards of the front wheel to keep wheel wake from entering the side wings. Zakspeed implemented a set of large deflector plates on their 1986 F1 car [4]. The side wings can have a great performance effect on the diffuser as the side wings, if designed correctly, can cause a sealing effect on the diffuser, as the diffuser edges are located mostly downstream of the side wings.
At the leading edge of the side wings there are inlet strakes, similar to the outlet strakes on a diffuser. These are important to reduce the side wings sensitivity to low energy air. When high-energy air is contaminated with lower-energy air, there is a risk of creating turbulence and reduce the total energy. The strakes at the leading edge help separate the air and reduces the risk of an energy loss. These strakes also help the airflow stay attached, crucial for the performance of the side wings. Furthermore the strakes contribute by creating vortices on the low pressure side of the side wing.

2.4.3 Diffuser

A significant portion of the total downforce is generated by the low-pressure region beneath the car. The fundamental concept is that the car operates similarly to a Venturi tunnel. According to the Bernoulli principle, this results in a high-velocity, low-pressure airflow. The diffuser is the component responsible for managing the expansion of this low-pressure flow back to atmospheric pressure downstream of the car. This is illustrated in Figure 2.10, which presents a 2D representation where the diffuser expands vertically. However, the same effect can also be achieved through horizontal expansion or a combination of both.

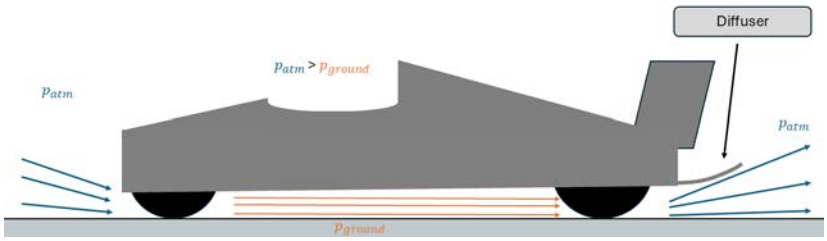

Figure 2.10: 2D illustration of the venturi effect of a race car with a diffuser.

The optimal expansion angle of a diffuser varies from car to car, but in motorsport applications it can exceed 20 degrees. However, the effectiveness of a diffuser also depends heavily on its geometric shape and the quality of the airflow passing through it. A major challenge in many race cars is that turbulent wakes from the tyres and other components spill underneath the floor, disrupting the intended flow. To counter this, strakes are often added to the diffuser. Since downforce is generated by the pressure differential, any intrusion of higher-pressure air into the diffuser or underfloor region reduces this differential, thereby diminishing downforce. Additionally, this unwanted airflow can disturb the expansion process and cause flow separation. Strakes act as vertical barriers that limit the intrusion of external air into the diffuser. Furthermore, they generate vortices along their lower edges, which help energize the flow and delay separation by keeping low-energy air away from the surface. Figure 2.11 shows the CFS 2025 diffuser, where the main segment, as well as the inner and outer strakes, can be seen. For the CFS car the diffuser is not allowed to extend further rearward than 250 mm from the rearmost part of the rear tires and not extend more than the outside of the back wheel.

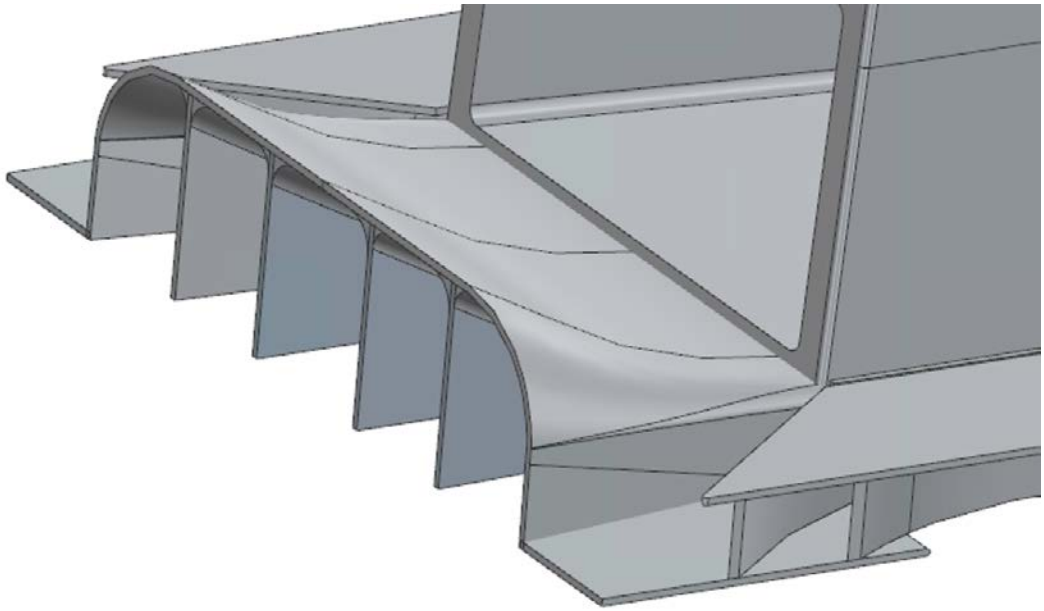

Figure 2.11: CAD of the CFS25 Diffuser

2.4.4 Rear Wing

The rear wing is generally the main contributor to downforce and drag on the rear portion of the vehicle. According to the boundary volumes specified in [2], aerodynamic devices are allowed to be placed up to 1200mm over the ground plane and 250mm behind the rear wheels on a formula student vehicle. This means that the rear wing is placed relatively far back and high up in comparison to other devices. While placed far downstream, the height compared to previous aerodynamic devices means that the rear wing often sees air

of ambient pressure and velocity. Its functionality can therefore be described largely as the multi-element wings in Section 2.3.1.1, with the main practical difference being that the previous description assumed an infinite span. As rear wings in general do not have sufficient span widths for this assumption to be valid, a device commonly implemented to minimize the effect of the previously mentioned end tip vorticies are end plates. These are plates placed at the tips of the wing acting as a physical blockade for the flow between the suction and pressure sides. While three dimensional effects exists in the flow even after adding end plates, they are severely dampened by the addition. The three dimensional effects can be a result of different energy levels in the oncoming air with losses caused by for example tyre wake present in some cases. On the same note, the cross section of the wing does not necessarily have to be the same through the span width with differences in the oncoming flow and desired pressure distribution being possible reasons to alter camber or relative placement.

By nature, relatively high downforce figures as well as the placements means that the rear wing has a significant impact on the longitudinal aerodynamic balance of the vehicle. In addition to the front wing flaps, adjusting the downforce levels on the rear wing is therefore a common measure to alter the balance in a bid to as previously described, adapt the aerodynamic load distribution to suit the overall vehicle dynamics.

While not so common in the context of Formula Student, some racing disciplines like Formula 1 races on tracks with such variety in downforce requirements that rear wings of different specification has to be designed. The different designs are mostly related to the lift/drag ratio of the wing with different airfoil profiles and endplates being used depending on the specification. While some tracks contains long straights calling for lower drag, other contains long corners of varying radius calling for higher downforce [5].

2.5 Fans and radiators

A fan is defined as a mechanical device that generates kinetic energy to surrounding air due to rotating blades. The fan can also be observed as a fluid dynamic system that creates a pressure difference in the flow. The blades convert rotational mechanical energy to increased velocity and momentum. The principle is based on Newton's second law of motion [6].

Certain parts of a car need to be cooled to prevent overheating. A common method is to circulate relatively cold water through the car, where it absorbs heat. The heated coolant is then directed to a radiator, where it is cooled before recirculating. Inside the radiator, the hot coolant flows through thin tubes while a fan forces or draws air across them. The cold air absorbs heat from the coolant, lowering its temperature. The efficiency of the radiator depends on several factors, including its size, design, airflow, and the mass flow rate of the coolant.

2.6 Computational Fluid Dynamics

In this chapter, general aspects of computational fluid dynamics (CFD), used for solving all fluid equations in this project, is introduced together with its applications.

2.6.1 Navier-Stokes equations

The Navier-Stokes equations are a set of partial differential equations that describe the motion of fluids. The equations describe how the properties of a fluid are related, specifically the pressure, temperature and density. In an educational article by NASA, the equations are described to consist of "a time-dependent continuity equation for conservation of mass, three time-dependent conservation of momentum equations and a time-dependent conservation of energy equation" [7]. The equation in the x-direction is formulated as follows:

$$\rho\left(\frac{\partial \mathbf{u}}{\partial t} + (\mathbf{u}\cdot\nabla)\mathbf{u}\right) = -\nabla p + \mu\nabla^2\mathbf{u} + \mathbf{f}$$

$$\nabla\cdot\mathbf{u} = 0$$

where ρ is the fluid density, u is the velocity vector field, p is pressure, μ is the dynamic viscosity and f is the body force per unit volume (e.g gravity).

2.6.2 Reynolds-Averaged Navier-Stokes Equations (RANS)

While the Navier-Stokes equations are exact independent of laminar or turbulent flow, the latter can result in significant gradients which makes analytical analysis impossible. Reynolds averaging is a method where velocity and pressure are decomposed into an average ($\bar{u}$) and a fluctuation (u'). With this, the velocity in the x-direction can be written as $u = \bar{u} + u'$. The RANS-equations are given by splitting these properties and inserting them in the Navier-Stokes equations. In the x-direction, the resulting equation becomes:

$$\rho\left(\frac{\partial \overline{u}}{\partial t} + \overline{u}\frac{\partial \overline{u}}{\partial x} + \overline{v}\frac{\partial \overline{u}}{\partial y} + \overline{w}\frac{\partial \overline{u}}{\partial z}\right) = -\frac{\partial \overline{p}}{\partial x} + \mu\nabla^2\overline{u} - \rho\left(\frac{\partial \overline{u'u'}}{\partial x} + \frac{\partial \overline{u'v'}}{\partial y} + \frac{\partial \overline{u'w'}}{\partial z}\right)$$

2.6.3 Finite Volume Method

Solving the differential equations within fluid dynamics requires a numerical solution method. For this purpose, the finite volume method (FVM) was used. FVM makes numerical solution possible, by discretizing the domain. This means that the calculation domain does not fully match the geometry of the actual domain, and a remaining error is inevitable. However, with appropriate settings, the error can be minimized to the point where the overall result is not significantly affected. It can be used for numerical solutions of conservation laws that are needed to solve fluid dynamic problems [8].

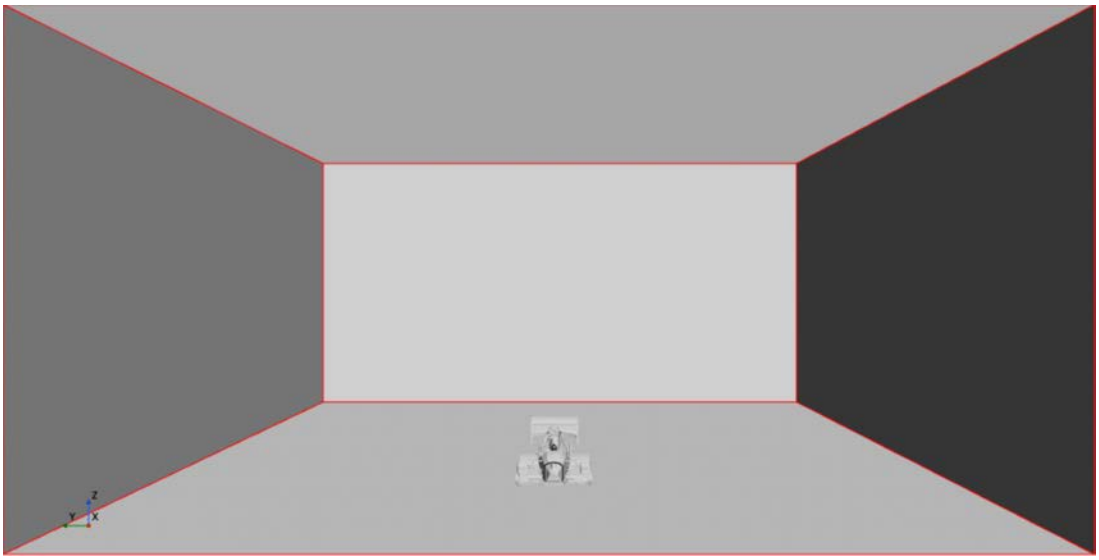

Figure 2.12: CFS simulation setup of a windtunnel and car in StarCCM+

2.6.4 Pre-processing

This section includes the pre-processing and all the geometry preperations needed for a CFD solver to be executable.

2.6.4.1 Physics models

The selection of physics models for the simulations determines which fields and governing equations that the solver will interpret into its calculations. This can involve a mix of fluid, particulate, thermal or chemical physics and the aim with their settings is to match the physics of the environment that is to be simulated upon.

2.6.4.2 Surface wrapper

Since the simulation model cannot handle geometries with gaps and unclean surfaces, a surface wrapper is used on all imported geometries. The surface wrapper applies a continuous surface on top of the geometries, aiming towards not changing the overall shaping of them. This process can be compared to vacuum forming the geometry, where the settings control how close the process will be to reach vacuum and match the geometry while sealing all unwanted imperfections from the CAD process of the geometry.

2.6.4.3 Subtract

A subtract operation is used to generate the geometry which is then to be discretized. For external flow, such as a car, the geometry of interest is then the simulation domain (or virtual windtunnel) minus the car geometry. This way a wall boundary condition can be put on the car's external surface

2.6.4.4 Mesh operations

In CFD, the fluid flow equations are solved numerically using iterative methods. In order for that to be possible, the domain on which the calculations are done on (in this case the subtracted surface described in part 2.6.4.3) needs to be discretized. This is done by generating a mesh on the domain that approximates its surface.

2.6.4.5 Regions

To define volumes in which different types of airflow will occur, so called Regions are used. Regions are domains of, in this case volumes, that are enclosed by boundaries [9] on which boundary conditions are applied. Between different regions, interfaces are used to transfer information between adjacent regions.

2.6.5 Post Processing

After a simulation is complete, it is necessary to present the CFD calculation with understandable data and images. This project will generate numerical values and two types of images. The first type is a boundary plot, which presents the physical quantity on the surface of the simulated geometry. An example of this type of plot is the skin friction coefficient, where the skin friction coefficient is represented at each point on the geometry. The second type of plot is a field plot, where the physical quantity is represented over the field around the car. An example of this plot is the LIC (line integral convolution) which is a method to get streamlines at each point in the air around the car.

As a compliment to the images, for every simulation, a set of data is produced, see Table 2.1.

Physical quantity	Unit
$-F_z$ total	N
Cd	-
$-C_L$	-
$-C_L/C_D$	-
$-F_z$ body/diffuser	N
$-F_z$ Front Wing	N
$-F_z$ Rear Wing	N
$-F_z$ Side Wing	N

Table 2.1: Physical quantities and their corresponding units

3
Method

This section explains the general workflow for generating, designing, simulating, and analyzing a concept. This process was repeated for every concept or for further iterations. This workflow can be visualized in Figure 3.1 below.

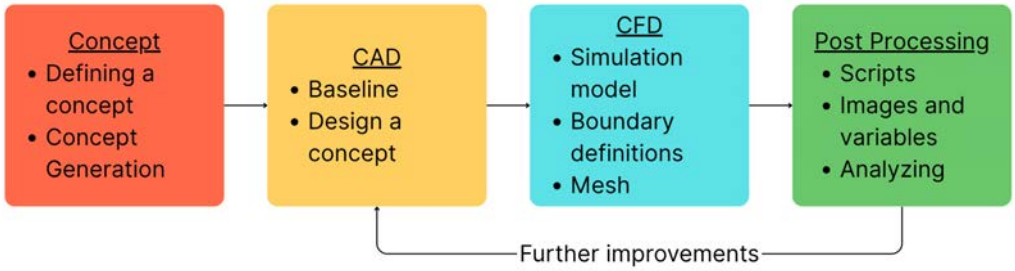

Figure 3.1: Diagram illustrating the design workflow

3.1 Concepts

In this section the process of defining and generating a concept is described. This must be done before moving on and finalizing the design later in the process.

3.1.1 Defining a concept

To keep the design and work process structured, the definition of a concept was decided. Firstly, the car was divided into four initial geometric boxes. The specific regions were a result of the method used by CFS to define different areas of the aerodynamic package having one project engineer in charge of each region. These regions were the front wing, side wings, rear wing and diffuser, see figure 3.2 below.

With the areas of the car defined, a basic study of where the top 50 Formula student teams placed their fans on their most recent cars was conducted (see Appendix A and B). This was done to verify that no potential important placement was overlooked. The study showed that most of the teams had placed their fans on the diffuser or side structures. It was also evident that not a single team had placed their fans on the front wing. A decision was taken that despite this fact, this study would still consider a fan placement on the front wing, since it might discover something new or simply to exclude the front wing from further fan placement studies.

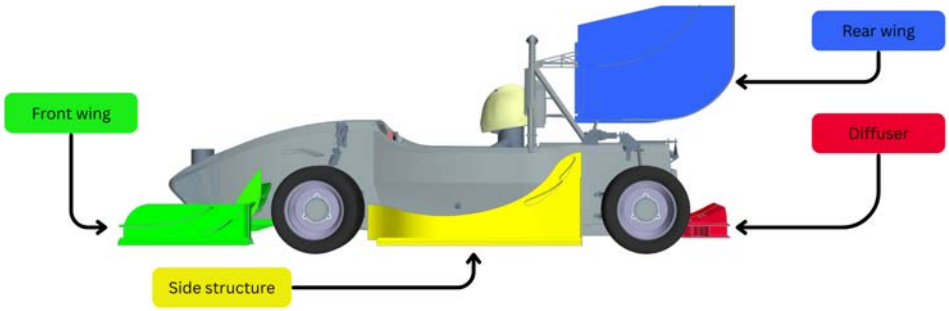

Figure 3.2: Full car with defined areas

A decision was taken to define a concept by how it wants to introduce or strengthen the mass flow within the defined geometric box. This was done to easily separate and keep track of the different concepts throughout the design process, which was important to be able to maintain a consistency in the workflow and thereby ensuring objectivity in the result evaluations.

3.1.2 Concept generation

Initially the defined areas in Section 3.1.1 were analyzed on the already existing Chalmers Formula Student car. If a possible improvement was found, a concept was sketched, named and a short description of the purpose and how the concept seeks to improve the airflow was formulated.

3.2 Computer-aided design

In this chapter, the computer-aided design (CAD) baseline model will be presented. The software Siemens NX was used in the project since it is the CAD-software used by CFS.

3.2.1 Baseline geometry

A baseline is the reference design with which all other designs are compared against. In this report, the baseline was taken directly from CFS25 with a minor change that their fan concept was removed. This was done to only see the results that the implemented fans are performing and not relative to the CFS25 fan concept. Note that a comparison to the CFS25 fan concept will still be made. The new baseline that was a consequence of removing the CFS25 fan concept is now designated as design iteration 1, or "it001" for short. Basic geometrical and aerodynamic data can be seen in Table 3.1, where the values are the average of the last 500 iterations, and the CAD geometry in Figure 3.3.

Parameter	Value	Unit
Wheel base	1530	mm
Front track	1250	mm
Rear track	1250	mm
Frontal area	1.17	m^2
-F_z	382.8	N
-F_x	130.7	N
C_D	1.5	-
-C_L	4.5	-
-C_L/C_D	2.9	-
Balance % rearwards (weight on the rear)	54.5	-
-F_z body/diffuser	56.1	N
-F_z FW	133.3	N
-F_z RW	106.8	N
-F_z SW	98.6	N

Table 3.1: Aerodynamic data of it001

Figure 3.3: Geometry of baseline, it001

In Figure 3.4 boxes with measurements can be seen in which all aerodynamic components must fit. Note that this might not be the same as in the rulebook to account for tolerances when manufacturing in real life.

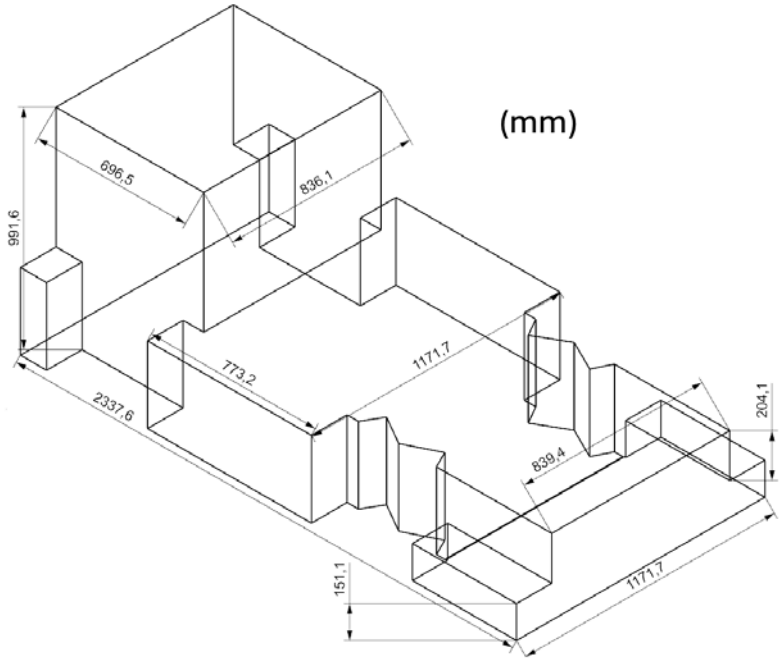

Figure 3.4: Geometric description of the volumes in which all aerodynamic components must fit

3.2.2 Concept design

CFS uses the product lifecycle management (PLM) software Siemens Teamcenter, which allows for collaborative design. When working with the individual concepts, a more detailed description of each concept will be presented later in the Section 4. After a concept has been generated as explained in Section 3.1 a CAD must be constructed. A concept can be realised in multiple ways and it is in the CAD where the decision has to be made about how and where to implement it. This will in no case be the most optimal for the given concept but the idea is to come close and show a trend of performance. It is also worth mentioning again that minimal change will be done to the curent CAD in terms of changing main aerodynamic devices since there is a time limit (see Section 1.4), however, ducts, flaps and simple geometry changes will be made when necessary.

3.3 Computational Fluid Dynamics

To analyze each concept's aerodynamic performance, computational fluid dynamics (CFD) was used to create models for computational simulations.

3.3.1 The simulation model

All CFD modeling was done using the software Simcenter STAR-CCM+ [10]. CAD geometries were imported and prepared before being meshed and the computational calcula-

tions were thereafter performed on the generated mesh. The solved simulation model was thereafter post processed to extract relevant simulation images and numbers, a process more thoroughly described in Section 2.6.5.

3.3.2 Physics models

The following physics models were used in the simulation:

- All y^+ Wall Treatment
- Cell Quality Remediation
- Constant Density
- Gas
- Gradients
- k-ω Turbulence
- Reynolds–Averaged Navier–Stokes
- Segregated Flow
- Solution Interpolation
- SST (Menter) k-ω
- Steady
- Three Dimensional
- Turbulent
- Wall Distance

3.3.3 Boundary conditions

In the simulation model, the initial velocity is set to 40 km/h and constant. The model has a moving ground with the same velocity. All four tyres (including rims) are assigned Moving Reference Frames (MRFs) with a rotational velocity according to Equation 3.1:

$$\omega = \frac{v}{r} \tag{3.1}$$

Where ω is the tyre and rim's rotational velocity, v is the velocity of the car and r is the radius of the tyre (including the rim).

Initial gauge pressure is constant at 0.0 Pa. The Turbulence intensity in the model is set to 0.01, the Turbulence Telocity Scale is set to 1 m/s and the Turbulent Viscosity Ratio is set to 200.

3.3.4 Surface wrapper

The surface wrapper settings used were:

- Base size: 32 mm
- Target Surface size: 50% of Base
- Minimum Surface size: 6.25% of Base
- Surface curvature: 280 points per circle
- Volume of Interest: External
- Under Custom Controls, Mesh controls were set on some of the surfaces
- Contact Prevention and Wrapper Defeature settings were also used

These settings proved to be sufficient for an adequate representation of the geometry in the discretized domain, in particular the leading and trailing edges.

3.3.5 Subtract

The subtracting of the imported geometries from the full domain is executed using the subtract operation, a boolean operation that simply removes all parts of the full domain that intersects with imported geometries.

3.3.6 Mesh operations

For the generated mesh, the used settings were:

- Meshers
  - Surface Remesher
  - Automatic Surface Repair
  - Trimmed Cell Mesher
  - Prism Layer Mesher
- Default Controls:
  - Base size: 32 mm
  - Target Surface size: 75% of Base
  - Minimum Surface size: 8% of Base
  - Surface curvature: 280 points per circle
  - Surface Growth Rate: Slow
  - Prism Layer Controls:
    - Number of Prism Layers: 12
    - Prism Layer Near Wall Thickness: $6.255 * 10^{-5}$m
    - Prism Layer Total Thickness: 10mm, absolute size
- Custom controls

Within the Custom Controls, Mesh Controls were set inside closed volumes. These volumes were placed in areas with more complex geometries, that needed finer mesh settings than the rest of the domain. Some examples of mesh refinement boxes are seen in Figure 3.5 and all refinement boxes are thereafter listed in Table 3.2.

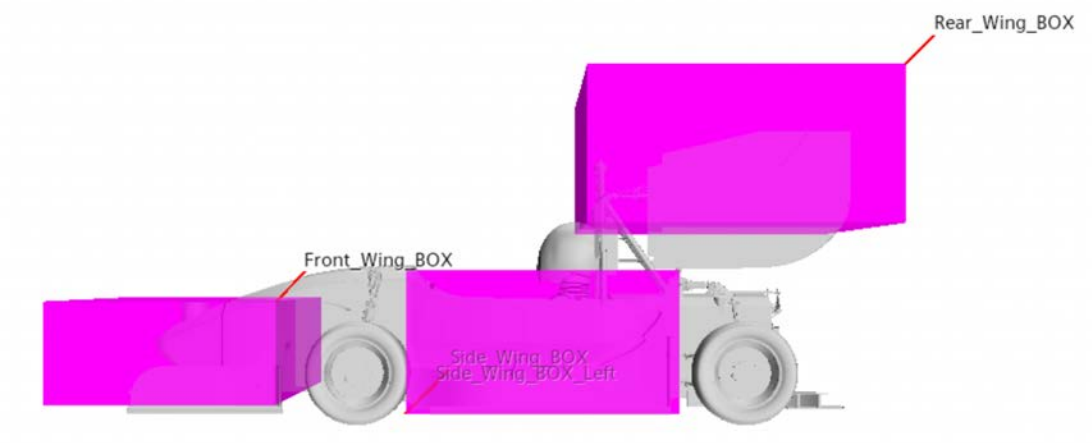

Figure 3.5: Refinement boxes for front wing, side wing and rear wing

Table 3.2: Custom Controls

Mesh refinement part	**Placement**	**Percentage of base size** [%]
Diffuser	Floor of the car	25
Far Rear Wake	Behind rear wing	90
Front Wheels	Around front wheels	50
Front Wing	Above front wing	25
Main	Around the entire car	70
Mid Rear Wake	Behind rear wing	80
Near Rear Wake	Rear part of the car	75
Rear wheel	Around rear wheels	50
Rear Wing	Upper part of rear wing	25
Side wing	Around side wings	25

3.3.7 Fan and radiator

The fan and radiator need to be defined in StarCCM+ to function correctly and as explained in Section 2.5. The naming for each geometry can be seen in Figure 3.6.

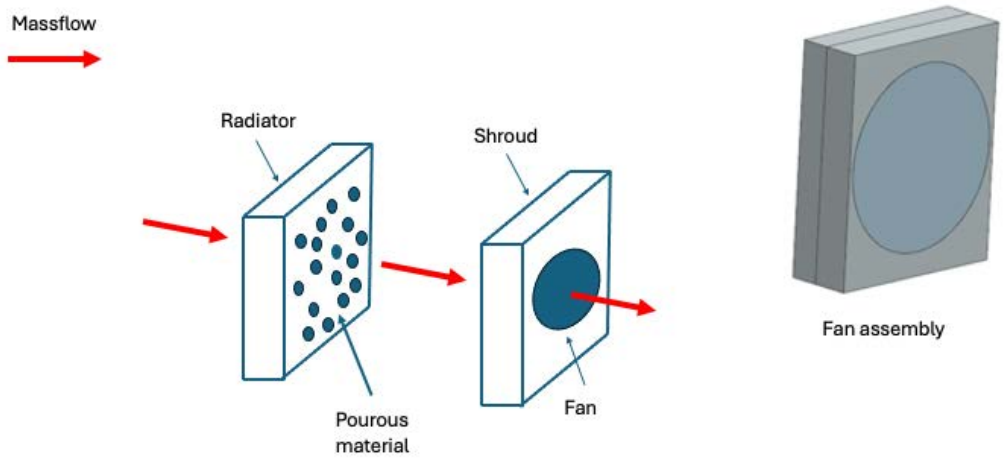

Figure 3.6: Fan assembly and naming of parts

- Radiator
  - The Radiator type is defined as a pourous material and has all its surfaces defined as walls.
- Shroud
  - The shroud also has all its surfaces defined as walls and is only meant to seal the fan and keep it in place.
- Fan
  - The fan is only one surface and is defined as a "fan interface boundary" and the interface as a "fan interface" where the the specifics of the fan can be seen in Table 3.3

Table 3.3: Fan Curve Table

Parameter	**Value/Setting**
Units: X	m^3/s
Fan Curve Table Units: P	Pa
Method	Volumetric Flow Rate
Pressure Rise	Static to Static
Operating Rotation Rate	9805.5rpm
Data Rotation Rate	11000.0rpm

Fan curves are used to plot how the pressure produced by the fan changes as the airflow rate through the fan changes. This is used in CFD to define the fan's properties. The fan curves make it possible to adjust parameters for different conditions. However, since the flow rate varies in real world the pressure will also vary which is important when deciding parameters in CFD software.

3.3.8 Regions

In this model, the regions are mainly divided into whether the airflow is coming from the surrounding air or from the fans on the car.
The regions used are:

- Air: contains the main mesh, including the full car geometry in which the flow from surrounding air goes through.
- Fan Duct Left: contains the left fan duct, in which the fan airflow goes through
- Fan Duct Right: contains the right fan duct, in which the fan airflow goes through
- Radiator Left: contains the left radiator, in which the airflow sucked from the left fan duct flows through
- Radiator Right: contains the right radiator, in which the airflow sucked from the right fan duct flows through

In the wind tunnel, there is an inlet, an outlet, ground, ceiling and walls. The inlet is defined as a velocity inlet and its velocity is set to the velocity of the car (40 km/h). The air from the inlet is then passed to the outlet, defined as a pressure outlet. The wind tunnel ceiling and walls are set as symmetry regions, while the ground is defined as a wall region, with a no-slip condition. The geometry of the car is defined as a wall region with a no slip-condition.

3.3.9 Reports

To track and save computed parameters, reports were created and enabled saving the chosen values in .csv-format. Some computed parameters included, but were not limited to:

- C_L [-]: a dimensionless parameter used to describe how much lift force that a geometry generates.
- C_D [-]: the same as for C_L but for drag force instead of lift force.
- C_LA [m^2] ($= C_L * A$): a parameter that gives a better comparison of the lift force generated by two bodies of differencing areas.
- C_DA [m^2]: the same as for C_LA but for drag force instead of lift force.
- F_L [N] ($= \frac{1}{2} * C_L * \rho * A * V^2$): The negative force acting on the car in vertical direction.
- F_D [N] ($= \frac{1}{2} * C_D * \rho * A * V^2$): The force acting on the

Where ρ is the air density, A is the projected area in the direction the force is calculated on, and V is the vehicle's velocity.

3.4 Post processing

After each finished simulation the result was processed into specific variable values and images so that the simulated geometry could be analyzed. If further improvements could be found or if the desired effect was not obtained a new iteration was created.

3.4.1 Scripts

A post-processing script was used to automate the process of producing images of the averaged fields from the simulations.

3.4.2 Images and variables

In the post processing, each report listed in Section 3.3.9 was converted ino a .csv file, with future handling further mentioned in Section 3.4.3.

For plotting graphic results, clip planes were generated on which the desired parameter could later on be visualized on. The planes were enerated in the following coordinates that almost fully encapsule the car geometry:

- YZ-planes: from X = 0.6m to 3.6m with 0.05m between each plane
- XZ-planes: from Y = 0.0m to 0.8m with 0.025m between each plane
- XY-planes: from Z = 0.05m to 1.25m with 0.025m between each plane

Where the X vector is in the car's longitudinal direction, Y vector is in the car's lateral direction and Z vector is in normal (upward) direction of the ground plane. In the car's lateral direction, the coordinate origin is placed right in the middle of the car. In longitudinal direction it is placed in front of the car and in vertical direction it is placed on the ground plane.

On each plane listed above, each of the following parameters were plotted and thereby visualized:

- Field Mean Velocity Vector (m/s)
- Mesh (-)
- Pressure Coefficient (-)
- Total Pressure Coefficient (-)
- Vorticity vector (-)

Field Mean Velocity Vector is in this project used with LIC-picture (line integral convolution) which is the method to get streamlines.

A few 3-dimensional views were also used for a few parameters. These viewing angles included:

- Front view of car
- Side view of car
- Rear view of car
- Bottom view of car
- Top view of car
- Isometric front view of car
- Isometric rear view of car
- Isometric side view of car

On the listed 3-dimensional views, the following parameters were plotted:

- Skin Friction Coefficient (-)
- Pressure Coefficient (-)

3.4.3 Concept evaluation

After executing the scripts in Section 3.4.1 the values of the specific variables in section 3.4.2 was compared to the baseline values and previous simulations. The values gave a great understanding whether the desired effect was obtained or if some misjudgment had occurred. After this, the newly generated images were analyzed to determine what went wrong or why the iteration was a step forward. To learn from each iteration, the images were thoroughly analyzed and discussed. If the desired airflow was not obtained, a decision had to be made if a change in geometry could solve the issue or if the concept itself was unsuccessful or fully developed. If a concept was deemed fully developed, the fucus could be moved to the next concept since more iterations were thought to be abundant and unnecessary. If a different geometry was thought to be able to solve the problem, a new iteration was created, and the process was restarted. This was done to maximize performance gained from the previously declared concepts.

4
Results and Analysis

The following sections explain and analyze the results for the different concepts and iterations for all geometric areas.

4.1 Front Wing

In this section, concepts concerning the geometrical region including the front wing and its close surroundings are discussed. For all concepts, the major constraint was the lack of space in the predefined region. This was made clear in the results.

4.1.1 Concept 1 Ground effect and near wall momentum

The aim of this concept was to increase the mass flow through the front wing main segment using the suction effect from the fan. The duct was designed in such a way that the outgoing flow was directed upward and outward to energize the boundary layer of the front wing flaps and minimize recirculation ahead of the front wheels.

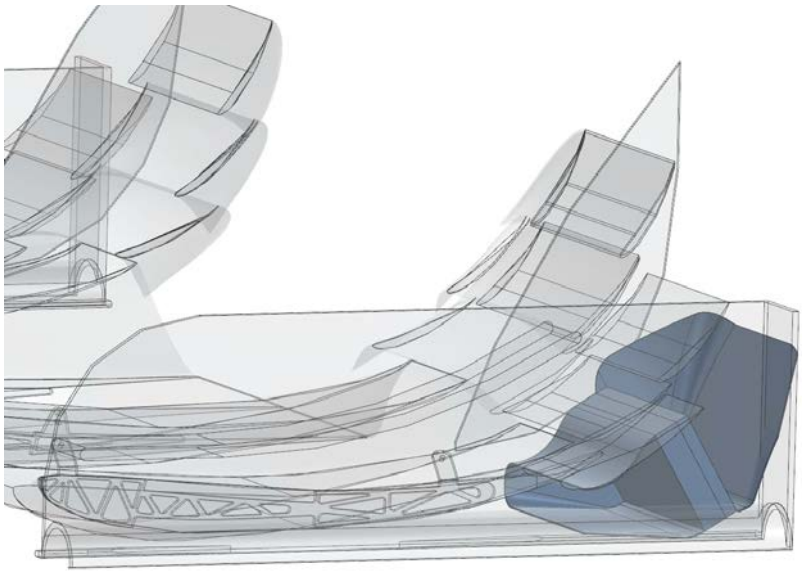

Figure 4.1: CAD of Front Wing Concept 1

A front duct was added to control the volume from which to suck air and allow for placement of the fan outside of the boundary layer. On the outlet, another duct was added to redirect the flow from the fan. The concept CAD can be seen above in Figure 4.1.

Simulation	**-F_z Body/Diffuser**	**$-F_z$ FW**	**$-F_z$ Side Wings**	**$-F_z$ RW**	**$-F_z$ Total**
Baseline	56.1 N	133.3 N	98.6 N	106.8 N	382.8 N
FW1	50.5 N	95.1 N	93.0 N	102.2 N	327.3 N

Table 4.1: Results for Front Wing Concept 1

The introduction of the fan and duct package led to significantly less mass flow on the suction side of the flaps, causing the flaps to stall with not enough energy in the boundary layer. Subsequently, this caused the front wing to lose downforce. As seen in Figures 4.2b and 4.2a, there is a significant difference in velocity in the boundary layer on the suction side of the flaps. Furthermore, a recirculation bubble can be seen on the trailing edge of the top flap in Figure 4.2b. This was thought to be an effect of the airflow not having enough energy to stay attached to the suction side of the flaps. The steep exit duct angle caused the air to separate and create a large recirculation bubble. The exit duct guides the air over the front wheel as intended. This causes the air to interact with the wheel further up. This would probably have caused a slight decrease in drag. Since the concept lost a great amount of downforce in all areas of the car and no obvious solution was found the concept was scraped and no further iterations were designed.

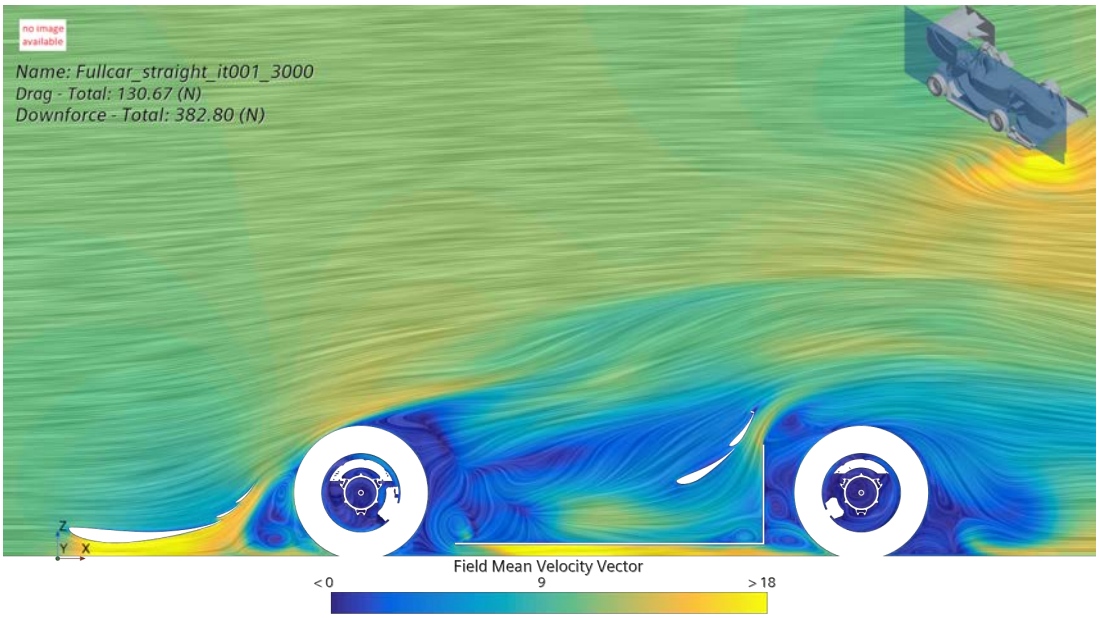

(a) Velocity vector field plot for Baseline at y = 0.6 m plane

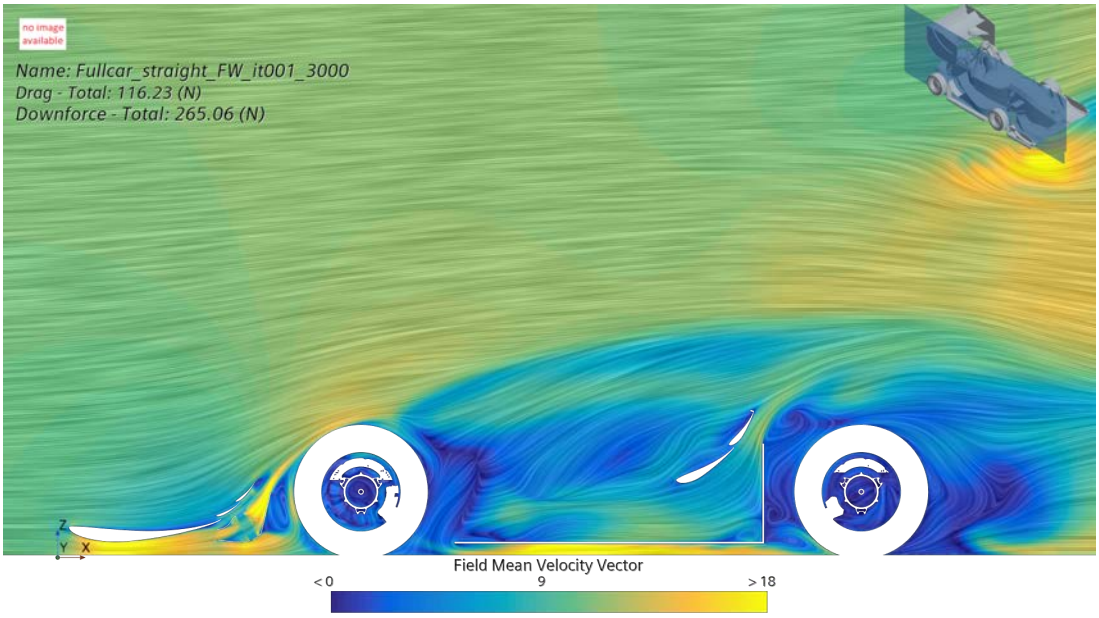

(b) Velocity vector field plot for FW1 it001 at y = 0.6 m plane

Figure 4.2: LIC plots for Baseline and FW1

4.1.2 Concept 2 Ground effect and outwash

The goal with this design was to reduce the effect of the low energy wheel wake and force energized air inward to gain performance from the side wings and rear wing. This was thought to be possible by placing the fan such that its suction effect could be used to

increase the mass flow through the main segment while outwashing the outgoing air to generate flow of high energy downstream to mix with the low energy wake generated by the tyres. Since the air exiting the fans is energized and therefore having high dynamic pressure, it was thought that it could result in a static pressure lower than that of the tyre wake, and therefore cause a mixing effect with the wheel wake.

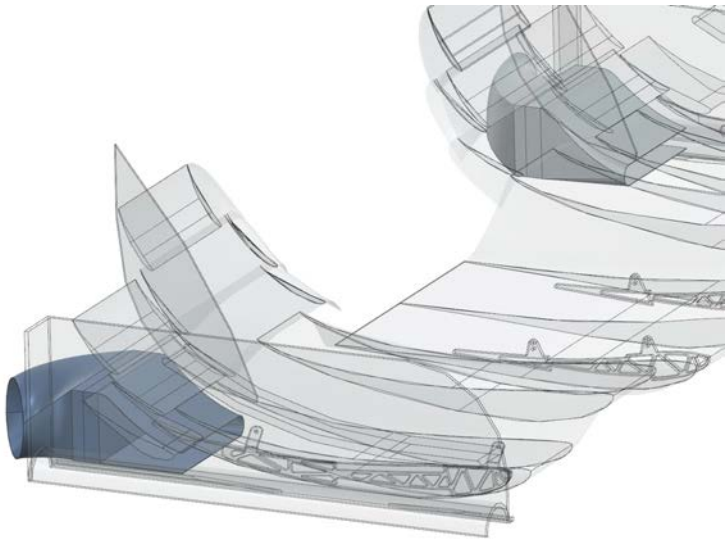

Figure 4.3: CAD of Front Wing Concept 2

Similarly to concept 1, a front duct was added to manage the suction region. Relative to the first concept, the entire fan and duct assembly was moved downwards and backwards to reduce interference with the front wing flaps. As seen in Figure 4.3, the outlet of the rear duct was angled outwards horizontally to redirect the air outboard of the front wheels.

Simulation	**-F_z Body/Diffuser**	**$-F_z$ FW**	**$-F_z$ Side Wings**	**$-F_z$ RW**	**$-F_z$ Total**
Baseline	56.1 N	133.3 N	98.6 N	106.8 N	382.8 N
FW Concept 2	50.7 N	117.5 N	90.4 N	103.2 N	348.4 N

Table 4.2: Results of FW Concept 2

Looking at Figures 4.4b and 4.4a, the added fan assembly interacts with an originally inwashing flow and therefore the effect is reduced. The airflow in the baseline has approximately the same properties as the air exiting the outlet duct. The inwash manages to attract some of the tyre wake, however, its not fully effective and the effect was not obtained to the desired extent. Some losses appear near the exit ducts, these losses continue downstream until they enter the side wing main segment. This causes the side structures to lose downforce compared to the baseline. The side structure main segments exit is upstream of the diffuser which means that the diffuser is greatly effected by the side structures. As seen in Table 4.2 the diffuser loses some amount of downforce, this

was thought to be due to the worsened airflow though the side structures. In Figure 4.4b the jet of energized air exiting the main segment is clearly worsened. This was thought to cause a decreased sealing effect of the diffuser and therefore more unwanted wake could slip into the diffuser, and therefore cause a loss of downforce.

The sought after downstream suction effect from outwashing air upstream was not strong enough and the initial flow structure is deemed to achieve the effect to a larger extent. Since this concept outwashes the baseline effect was opposed leading to a drastic loss of inwash downstream of the front wheels. As the functionality of the outer side wing flaps rely heavily on this inwash effect, this method of outwashing is not deemed to be incompatible with the existing geometry. However, with an altered side wing geometry, this concept prove beneficial as different effects such as tyre sqirt and tyre wake could be handled. Overall though, the concept causes a downforce loss as seen Table 4.2.

The concept cause to front wing to lose around 12% of its downforce. It is evident in Figure 4.5 that the air stagnates after the ducts which causes the front wing to stall, leading to decreased performance. Since the concept lost a great amount of downforce and the idea behind the concept proved to be a failure, no further iteration were designed.

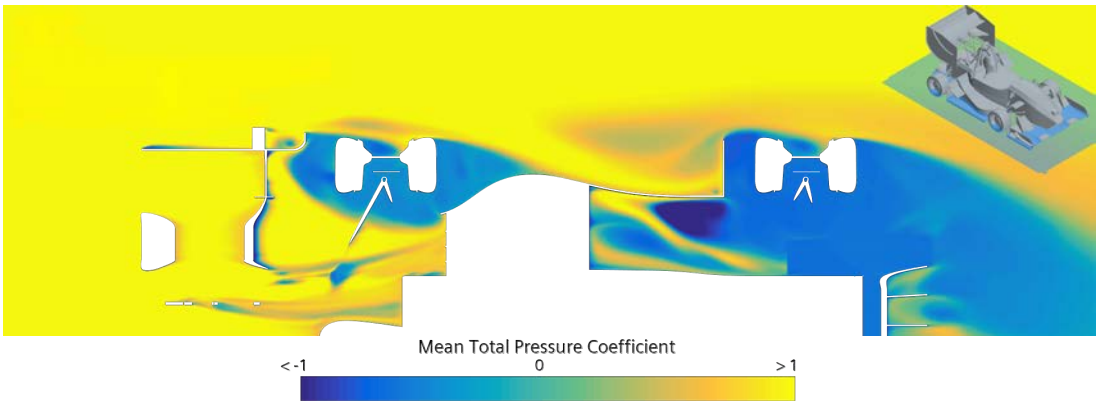

(a) Total Pressure Coefficient Plot for Baseline at z = 0.15 m plane

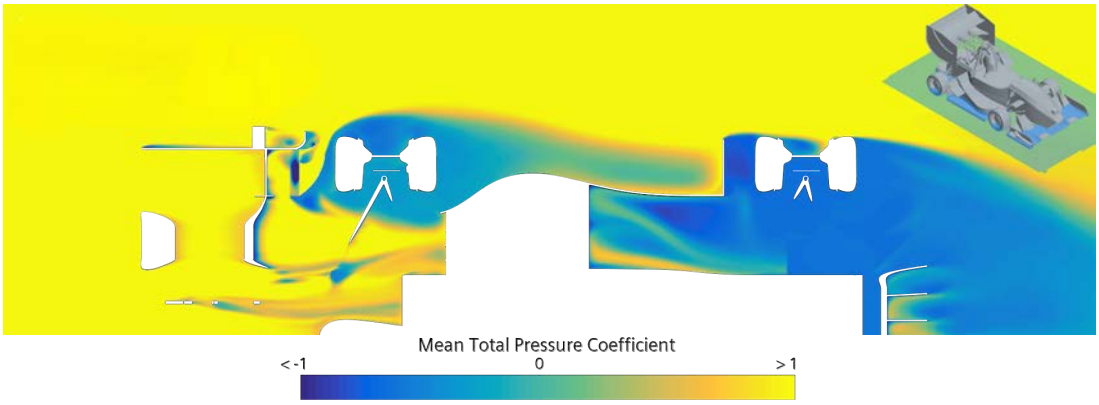

(b) Total Pressure Coefficient plot for FW2 it001 at z = 0.15 m plane

Figure 4.4: Total Pressure Coefficient plots for Baseline and FW2 it001

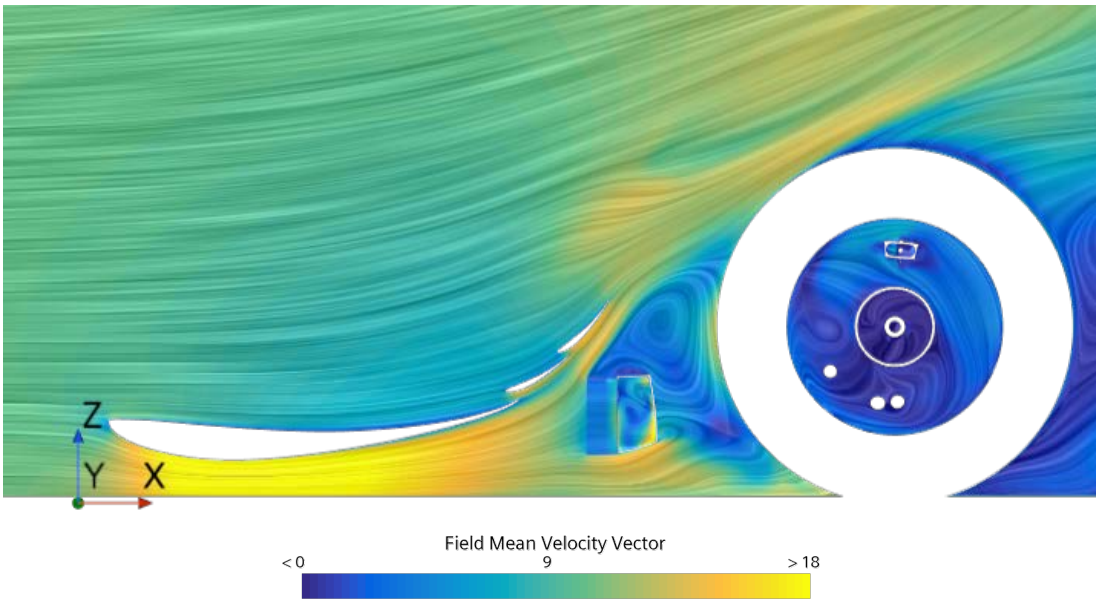

Figure 4.5: Velocity vector field plot for FW2 it001 at y = 0.55 m plane

4.1.3 Concept 3 outwash

Similar to Concept 2, this concepts aims to outwash air at the endplates of the front wing, and by conservation of mass, use the lower pressure generated downstream to achieve an inwash of ambient air with which to mix the losses coming from the tyres.

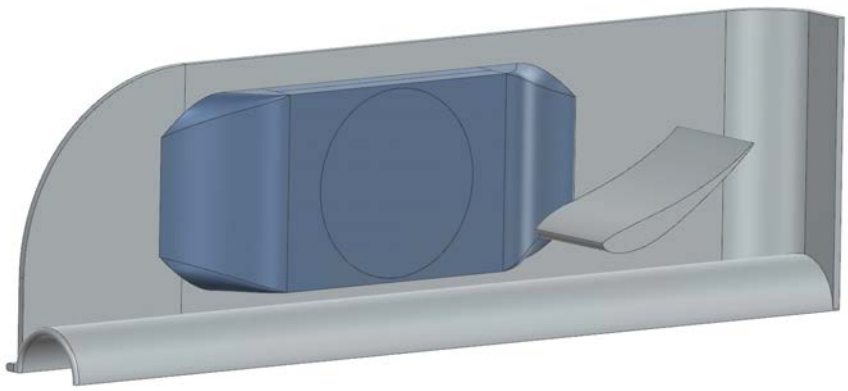

Figure 4.6: CAD of Front Wing Concept 3

The fan assembly was placed on the endplate of the front wing main segment with the outlet pointing outwards perpendicular to the car's traveling direction. A hole was made in the original endplate geometry to allow for airflow through it while no inlet or outlet ducts were added to the assembly. The placement of the fan assembly in CAD can be seen in figure 4.6 above.

Simulation	$-F_z$ **Body/Diffuser**	$-F_z$ **FW**	$-F_z$ **Side Wings**	$-F_z$ **RW**	$-F_z$ **Total**
Baseline	56.1 N	133.3 N	98.6 N	106.8 N	382.8 N
FW Concept 3	51.0 N	97.0 N	88.9 N	97.6 N	322.0218 N

Table 4.3: Results for Front Wing Concept 3

Similarly to the previous concept, the outgoing air from the fan disrupted the inwashing of ambient air to the side wing region, which as seen in Figure 4.7 lead to less overall energy in the region compared to the baseline. Additionally, losses of energy losses came from behind the jet of outwashing air. Despite some mixing of ambient air which resulted in less local losses (lighter blue) in the front tyre wake region, the negative effects far outweigh the positive. Since the fan sucked air from the pressure side of the front wing, the pressure difference between the pressure side and the suction side decreased and therefore the downforce produced drastically decreased. This problem was identified in the design phase, but since it was not possible to achieve fan suction on the wings suction side without drastically changing the front wing, nothing was done to prevent this from happening.

As shown by Figure 4.7 and the numbers in table 4.3, the aim of the concept to reduce the losses in the region behind the front wheels was not achieved and the performance loss was deemed significant enough not to perform further iterations on the concept.

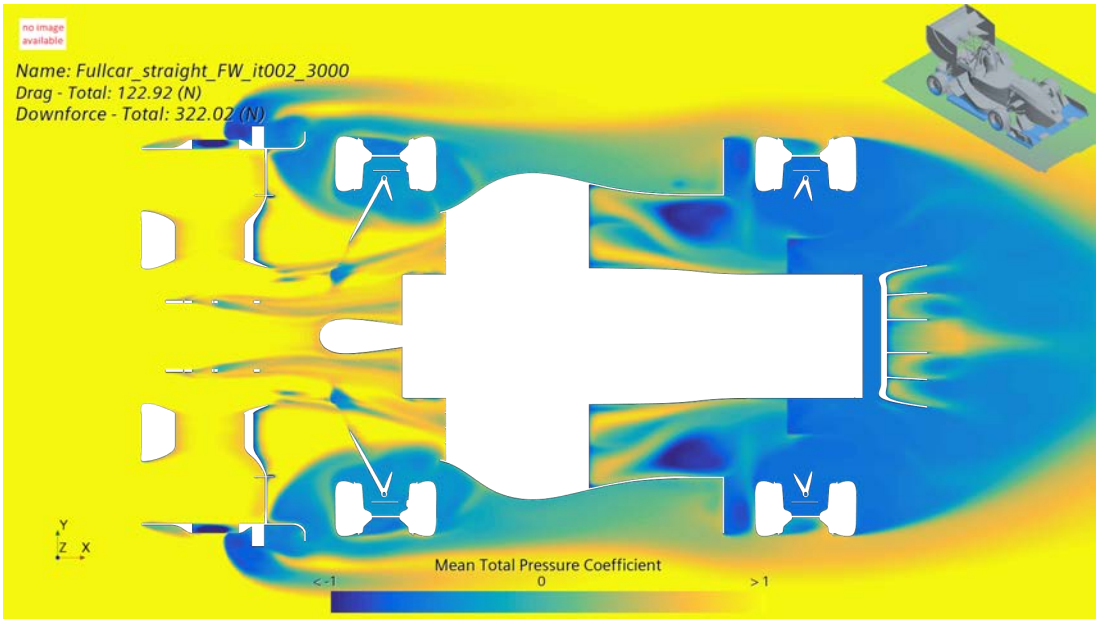

Figure 4.7: Total Pressure Coefficient plot for FW3 it001 at z = 0.15 m plane

4.1.4 Concept 4 Enhanced underfloor mass flow it001

This concept aims to improve the airflow under the monocoque, leading to a greater mass flow through the diffuser as well as enhanced suction on the suction side the front wing main segment. The fans are placed centrally, behind the trailing edge of the main segment of the front wing, see Figure 4.8 below. In iteration 001 no ducts or winglets were added.

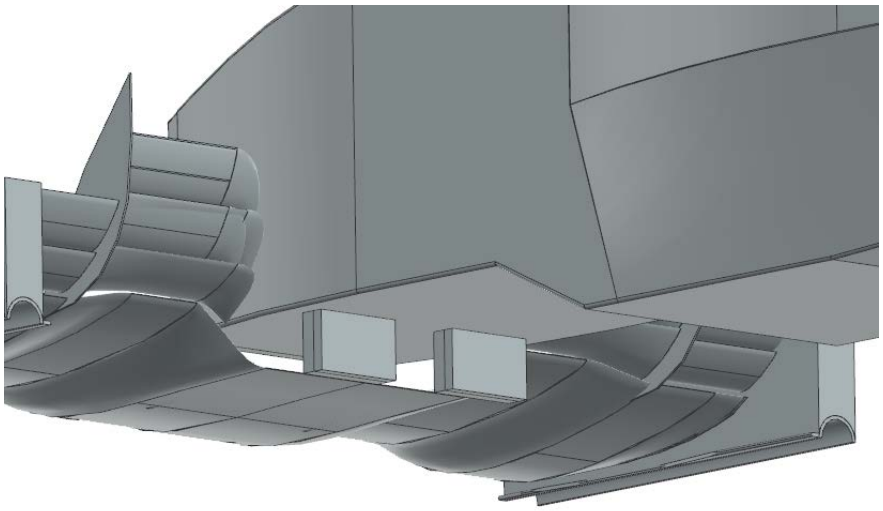

Figure 4.8: CAD of Front Wing Concept 4 iteration 1

Simulation	DF Body/Diffuser	$-F_z$ FW	$-F_z$ Side Wings	$-F_z$ RW	$-F_z$ Total
Baseline	56.1 N	133.3 N	98.6 N	106.8 N	382.8 N
FW Concept 4 it001	62.2 N	132.0 N	101.0 N	101.8 N	386.1 N

Table 4.4: Results for Front Wing Concept 4 it001

The fans improved the mass flow through the diffuser as intended. This can be seen as an increase in velocities in Figures 4.9b and 4.9a. To achieve this effect was the main focus of the concept, so that means that the idea behind the concept was a success. There are however, still a few troublesome areas that were negatively effected by the introduction of fans and radiators in this area. Losses were found near the trailing edges of the fans, leading to increased drag and most importantly a reduction in mass flow. The losses could be minimized by introducing some sort of duct that guides the airflow so that less separation occurs. The concept increased downforce in the two focus areas, diffuser and side wings, but lost downforce on both the front wing and rear wing. The loss of downforce produced by the front wing is due to an increase in mass flow on the pressure side of the main segment of the front wing. This means that the pressure difference between the pressure side and the suction side was decreased and because of this the downforce produced decreased in the center of the main segment. This problem was identified in

the design phase, but due to a lack of space, no plausible solution was found. As seen in Table 4.4 the rear wing loses around 5% of its downforce. The reason behind this is hard to find in any of the images, but one theory is that the suction from the fans guides the stagnated air at the front of the monocoque downward, meaning that slightly less air follows the upper side of the monocoque, leading to a decreased mass flow over the rear wing. Another identified problem was the trailing edge of the fan-radiator assembly where some losses occur. As only a portion of the surface ejects high energy air through the fans, the rest is the source of losses, which subsequently spread through the floor.

Despite this, the concept generated a greater total downforce than the baseline. Due to this fact, the concept was thought to have some potential, and it002 was designed.

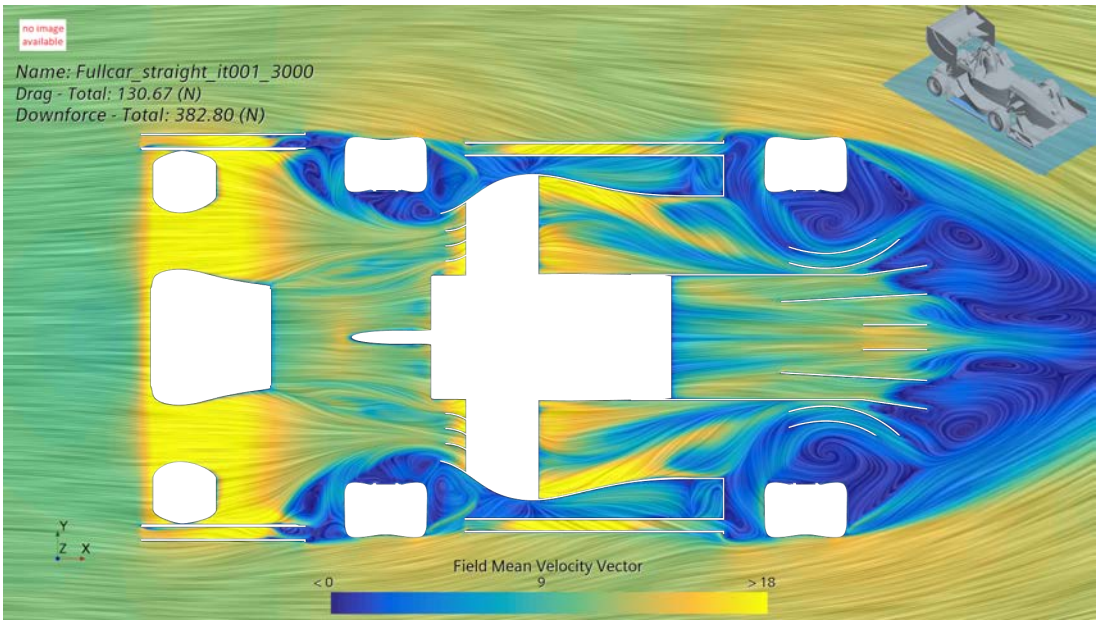

(a) Velocity vector field Plot for Baseline at z = 0.1 m plane

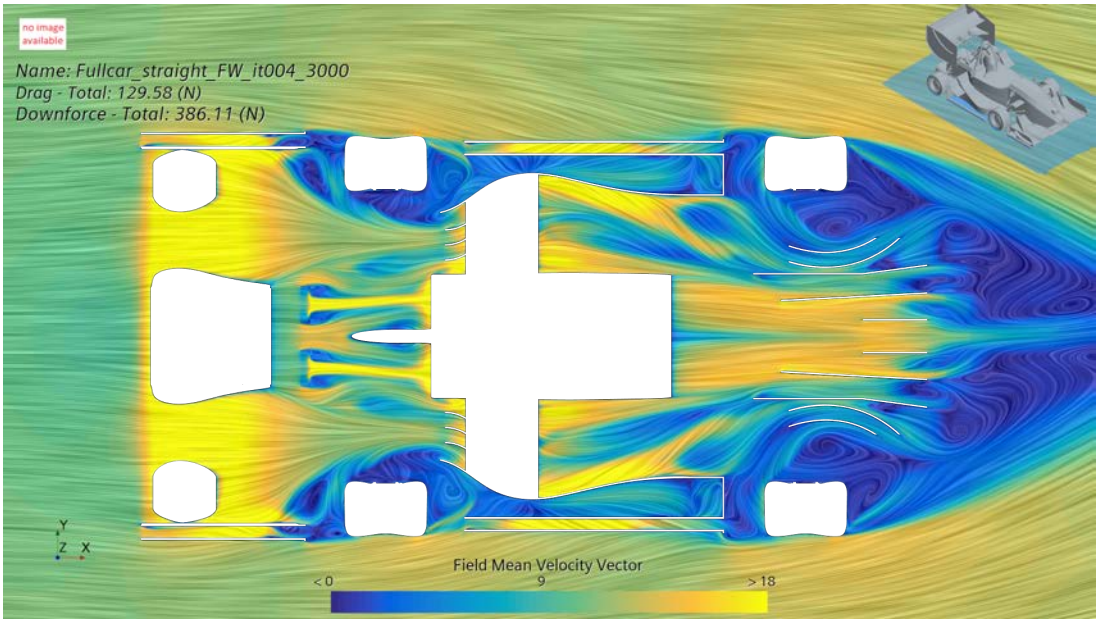

(b) Velocity vector field plot for FW1 it001 at z = 0.1 m plane

Figure 4.9: Velocity vector field plots for Baseline and FW4 it001

4.1.5 Concept 4 Enhanced underfloor mass flow it002

This iteration is based upon concept 4 it001 as described in Section 4.1.4, and aims to remove the previous losses near the trailing edge of the fans. The placement of the fans is not changed, however a duct placed behind the fans is introduced to remove losses and

clean up the airflow.

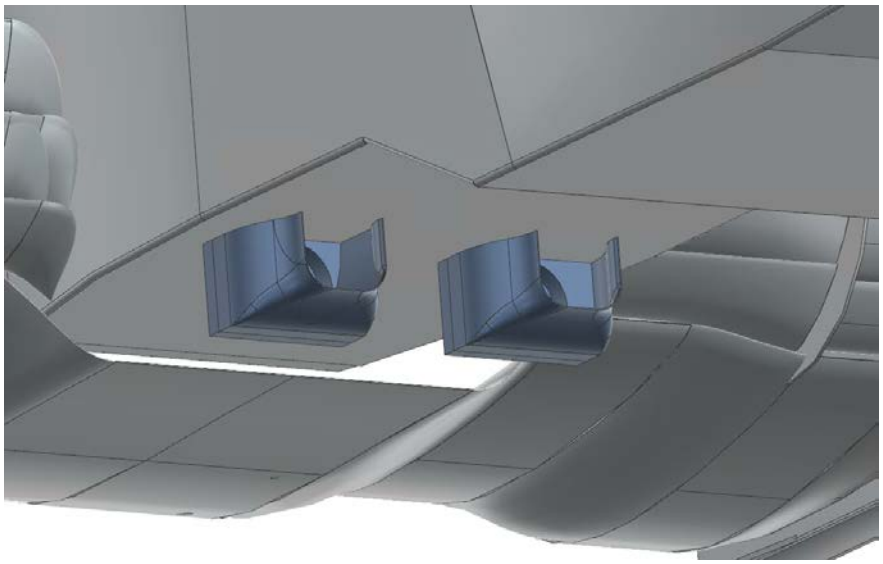

Figure 4.10: CAD of Front Wing Concept 4 iteration 2

Simulation	DF Body/Diffuser	$-F_z$ FW	$-F_z$ Side Wings	$-F_z$ RW	$-F_z$ Total
Baseline	56.1 N	133.3 N	98.6 N	106.8 N	382.8 N
FW Concept 4 it001	62.2 N	132.0 N	101.0 N	101.8 N	386.1 N
FW Concept 4 it002	62.5 N	132.5 N	104.4 N	98.7 N	387.0 N

Table 4.5: Results for Front Wing Concept 4 it002

The ducts improved the downforce produced by the diffuser, side wings and front wing, but the rear wing lost 3.03 N compared to it001 and more than 8 N compared to the baseline. Despite improved airflow, there were still losses within the ducts and separation along the outer duct surface, see Figure 4.11. Since no duct were added upstream of the fan and radiator setup the cause separation at the trailing edge of the fan despite the ducts. A shallower duct angle could probably have caused slightly less separation. However, no separation at all may be very difficult and would require several iterations. No further iterations were made with different duct angles as areas with greater improvement potential had been identified. The new iteration saw an increase of around 0.2% in total downforce compared to iteration 1.

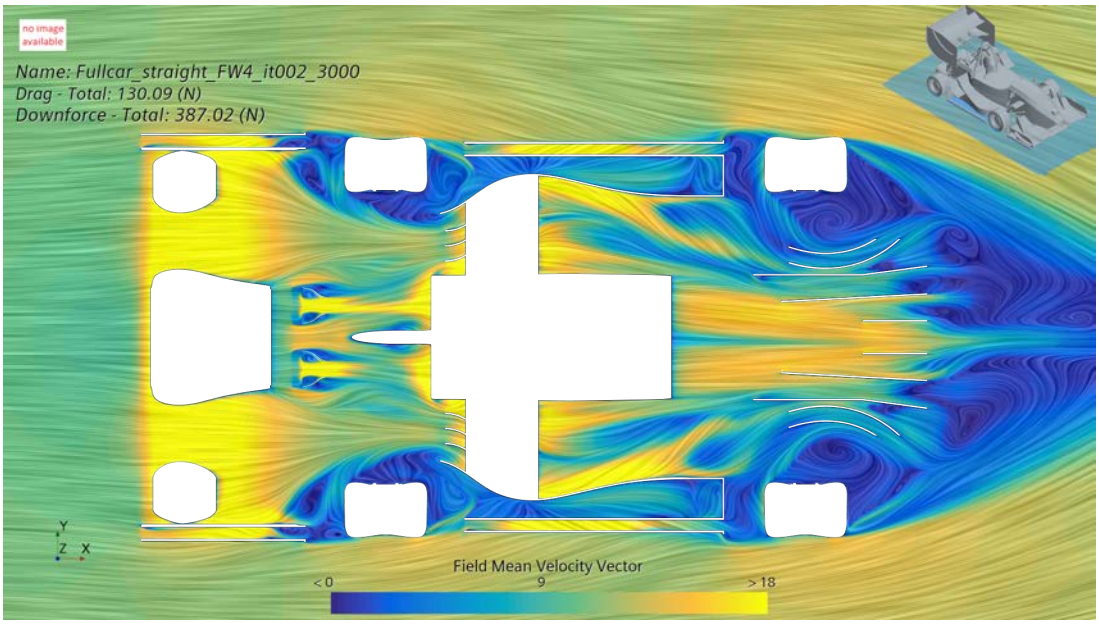

Figure 4.11: Velocity vector field plot for FW4 it002 at z = 0.1 m plane

4.1.6 Concept 4 Enhanced underfloor mass flow it003

Iteration 3 aimed to solve the issue with greater mass flow on the pressure side of the front wing and the issue with a loss of mass flow over the rear wing. Ducts upstream of the radiator were introduced to force air from the suction side of the front wing into the radiator. The improved mass flow on the suction side was thought to allow for a greater mass flow over the upper side of the monocoque, causing the rear wing to gain performance subsequently. A central splitter was introduced on the upper side of the duct. This was designed to minimize stagnation near the underside of the monocoque. This could increase mass flow through the diffuser and therefore improve performance. The duct downstream of the fan was also slightly redesigned to reduce separation and turbulence within the duct itself. In it002 an outer duct was introduced to improve the airflow outside of the duct, in this iteration however, an inside to the duct was added to improve mass flow exiting the duct. The aim of this iteration was to achieve the positive effects of it001 and it002 without the negative effects that caused them to barely outperform the baseline. See Figure 4.10.

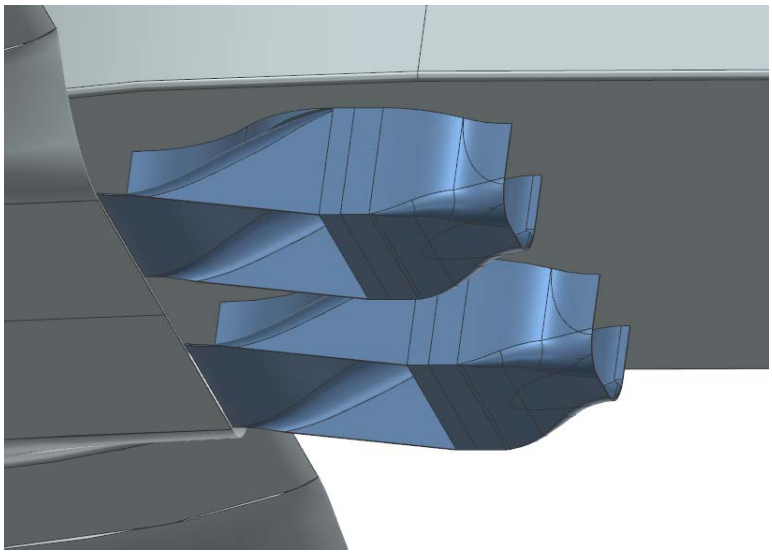

Figure 4.12: CAD of Front Wing Concept 4 iteration 3

Simulation	DF Body/Diffuser	$-F_z$ FW	$-F_z$ Side Wings	$-F_z$ RW	$-F_z$ Total
Baseline	56.1 N	133.3 N	98.6 N	106.8 N	382.8 N
FW Concept 4 it001	62.2 N	132.0 N	101.0 N	101.8 N	386.1 N
FW Concept 4 it002	62.5 N	132.5 N	104.4 N	98.7 N	387.0 N
FW Concept 4 it003	57.2 N	137.2 N	104.1 N	98.1 N	387.5 N

Table 4.6: Results for Front Wing Concept 4 it003

The ducts upstream of the radiator had the desired effect of improving the mass flow on the suction side of the front wing. However, the ducts were not ideal as the flow separated before the radiator due to the steep angle, see Figure 4.14. Despite this, a 3.5% increase in front wing downforce was noted. As presented in Table 4.6, the diffuser lost around 8.5% of its downforce. This was thought to be because the new duct had a blocking effect on the underside of the body. The added obstacle for the airflow caused a reduced mass flow through the diffuser, leading to the reduced downforce. The new ducts downstream of the fans improved the airflow as they managed to keep the airflow attached more than in it002, see Section 4.1.5 and Figure 4.15. The fan and radiator setup were forced to be moved rearwards to allow for the leading duct. This appears to have caused separation further downstream near the steering motor cover. This was thought to be due to an outwashing effect which split the air exiting the fans, and therefore separate from the steering motor cover. This effect can be seen in Figure 4.15. This causes the diffuser and the underbody to lose performance. The new iteration did not have the desired effect on the rear wing as it lost even more than downforce than it002. The reasons for which are difficult to establish, but similar to the previous iterations, it is thought to correlate with the added suction on the underside of the car resulting in less mass flow on the overside. Overall, the iteration was considered to be a step forward, but not the solution to all problems with the concept. Since the total downforce produced still was not as great as

some other concepts and the idea of improving the mass flow though the diffuser could be implemented in a simpler way by placing the fan and radiator setup in the diffuser. See Section 2.4.3. No further iterations were designed or simulated.

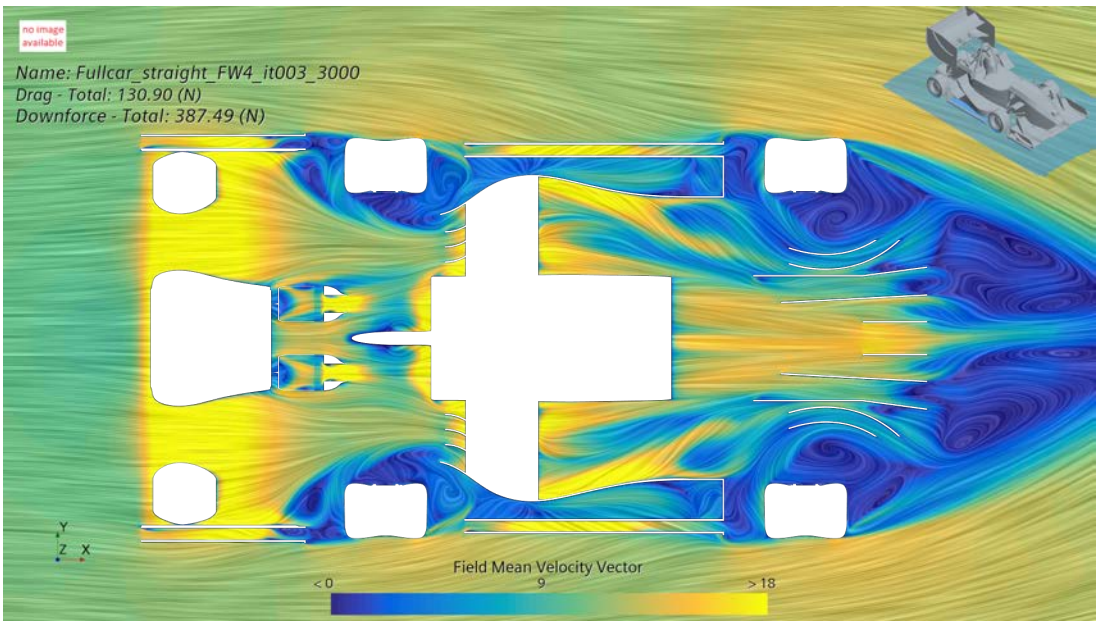

Figure 4.13: Velocity vector field plot for FW4 it003 at z = 0.100m plane

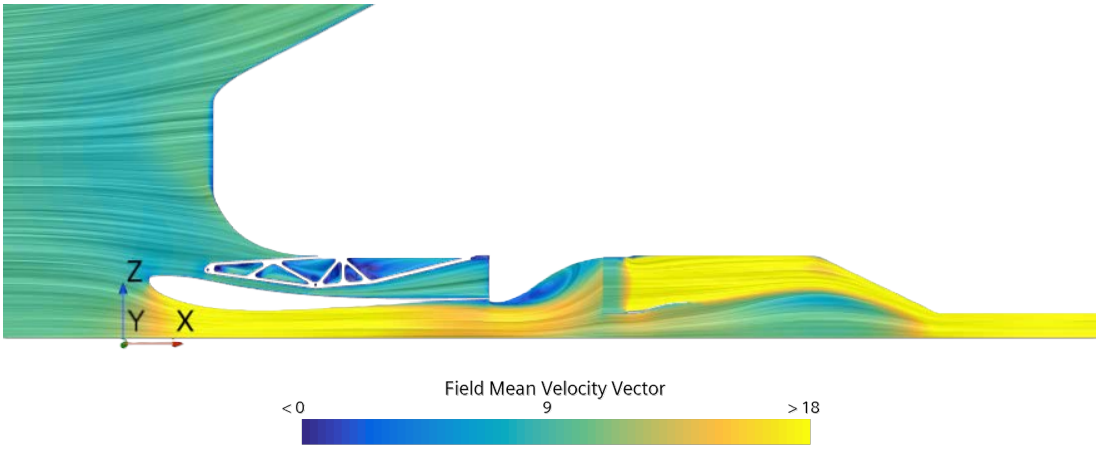

Figure 4.14: Velocity vector field plot for FW4 it003 at y = 0.125 m plane

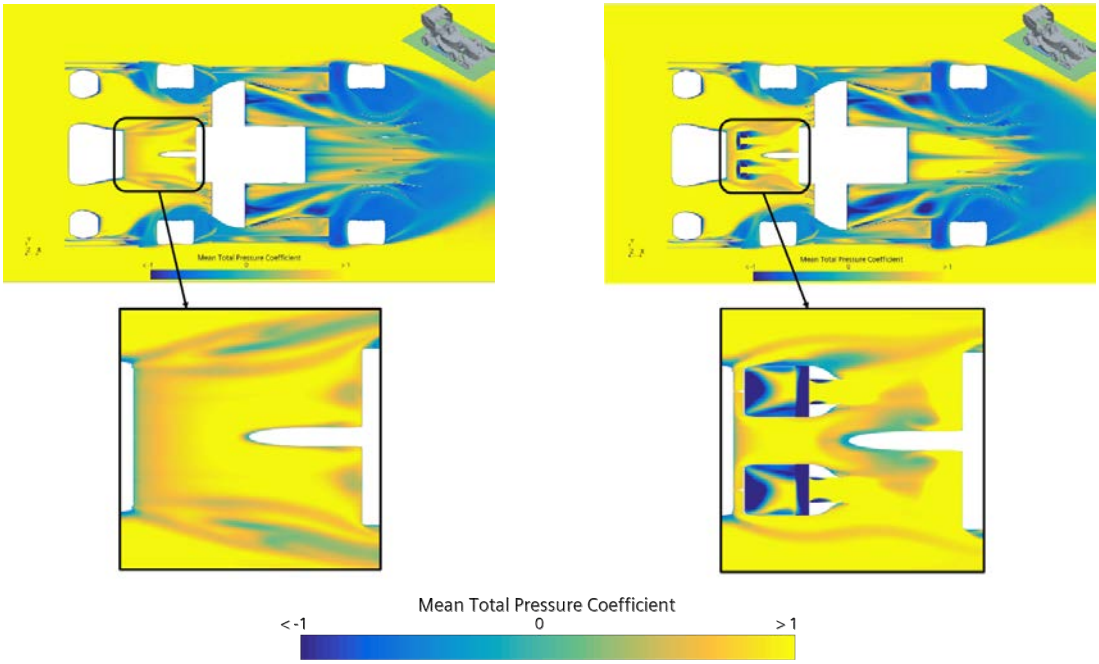

(a) Total Pressure Coefficient plot for Baseline at z = 0.1 m plane

(b) Total Pressure Coefficient plot for FW4 it003 at z = 0.1 m plane

Figure 4.15: Total Pressure Coefficient plots for Baseline and FW4 it003 underneath the front of the monocoque.

4.2 Side Wing

In this section, concepts of fan implementation on the side wings and the results of their are discussed.

4.2.1 Concept 1 Airflow through stagnation plate

This concept, pictured in Figure 4.16, is currently implemented in the Chalmers Formula Student project. It consists of the fans being attached to the stagnation plates at the end of the side wings with a hole to allow air to flow through. This relocates air that was previously flowing above and around the stagnation plates, to go through the plates instead.

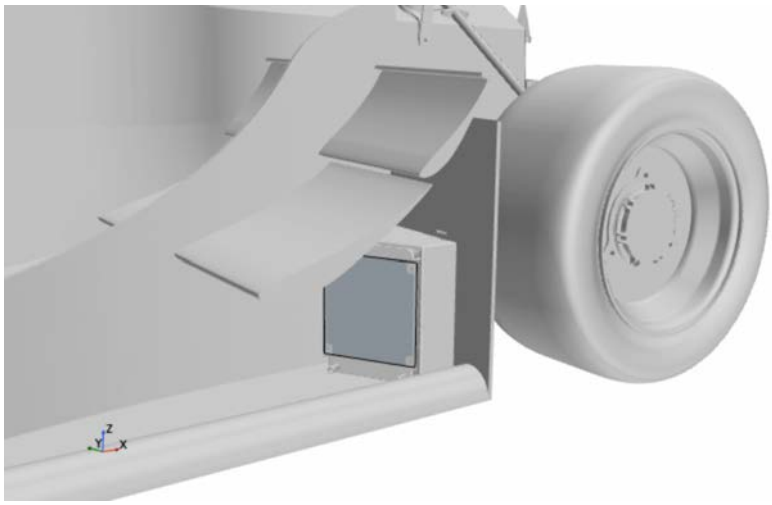

Figure 4.16: CAD of Side Wing Concept 1, Airflow through stagnation plate

As can be seen when comparing the concept with the baseline in Figure 4.17, the air flowing from the outside of the side wing attaches to the air flowing under the main segment after passing through the fan at the endplate, creating a streamlined transition. The suction of the fan increases the velocity of the airflow on the suction side which in turn lowers the pressure, generating more downforce in the side wings. The blow of the fan redirects the air to the diffuser and takes advantage of the otherwise stagnated air on the stagnation plate.

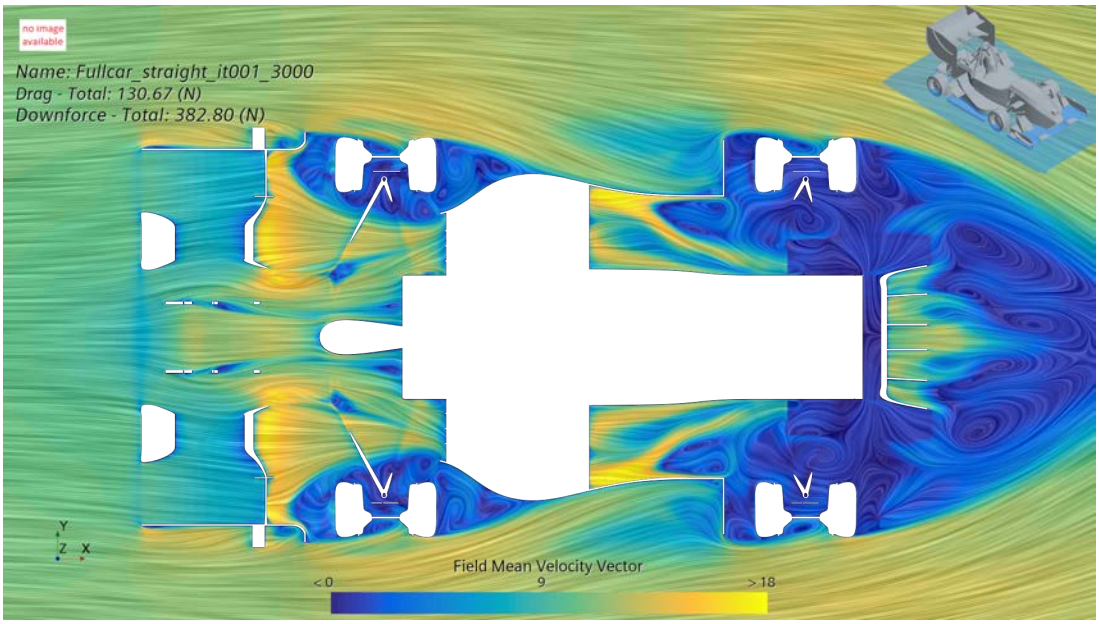

(a) Velocity vector field plot for Baseline at z = 0.15 m plane

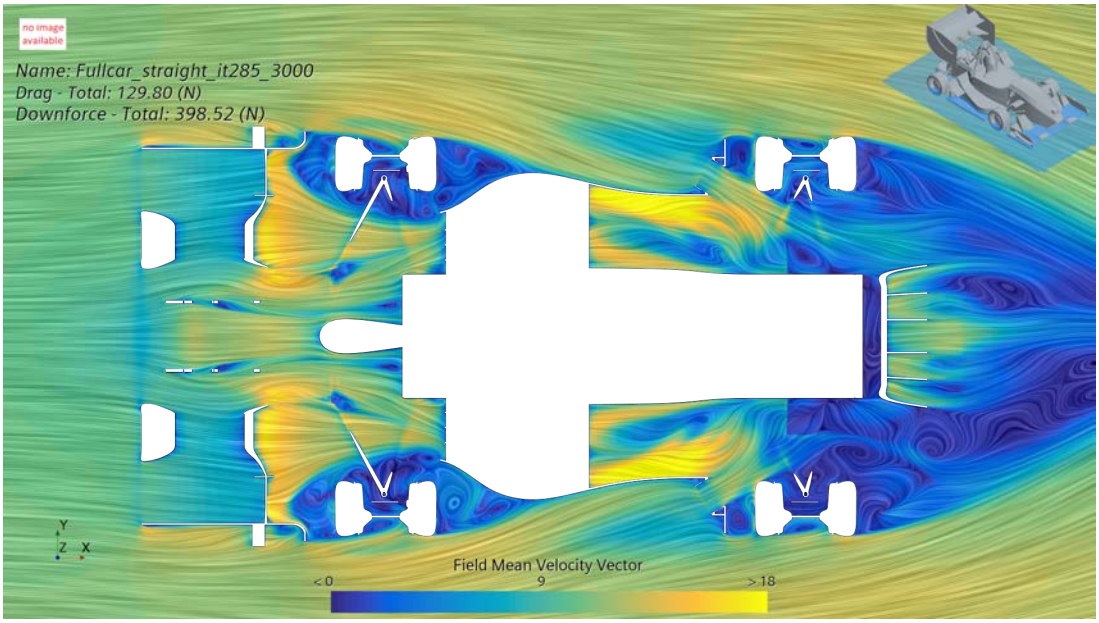

(b) Velocity vector field plot for SW1 it001 at z = 0.15 m plane

Figure 4.17: Velocity vector field plots for Baseline and SW1 it001

Simulation	$-F_z$ **Body/Diffuser**	$-F_z$ **FW**	$-F_z$ **SW**	$-F_z$ **RW**	$-F_z$ **Total**
Baseline	56.1 N	133.3 N	98.6 N	106.8 N	382.8 N
SW Concept 1	62.7 N	133.7 N	110.3 N	103.5 N	398.5 N

Table 4.7: Results for Side Wing Concept 1 it001

The increased downforce in the side wings can be verified in Table 4.7. Furthermore, by energizing the stagnated wheel wake around the rear wheels, this concept improved the air flow to the diffuser, increasing its generated downforce. The relocation of air to the diffuser had a cost of worsened airflow to the rear wing, but the total downforce was an increase with this concept.

4.2.2 Concept 2 Ground effect in side wing main segment

In the second side wing concept, pictured in Figure 4.18, the fan and radiator package was placed under the side wings, in what is called the main segment of the side wings. The theory behind this concept is first to increase the mass flow through the main segment by using the suction effect from the fan which in turn has the capability of increasing the downforce of the car through Bernoulli's principle. In the first iteration of this concept, the fans were placed close to the flaps of the main segment in order to increase the mass flow along them. The fans were angled in order to keep the air flow attached along the side wing and allow the air to continue to flow naturally downstream, similar to the baseline simulation. The resulting airflow is illustrated in Figure 4.19b and the baseline in Figure 4.19a

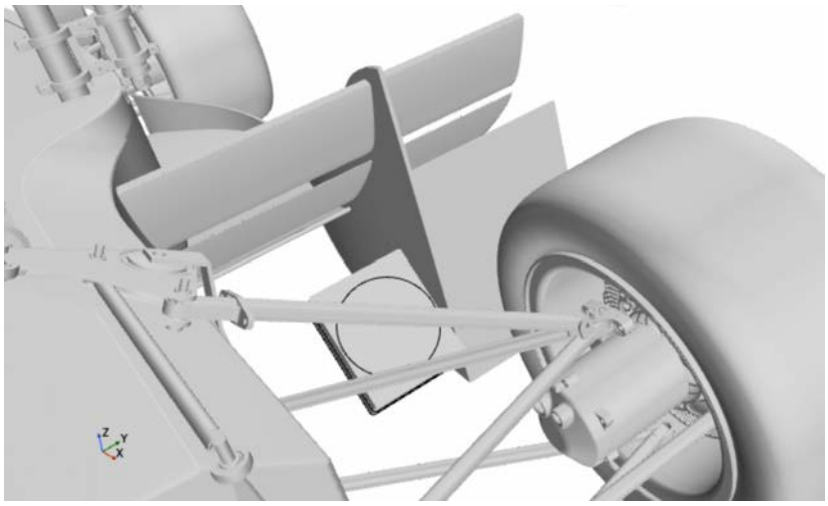

Figure 4.18: CAD of Side Wing Concept 2, Ground effect in side wing main segment

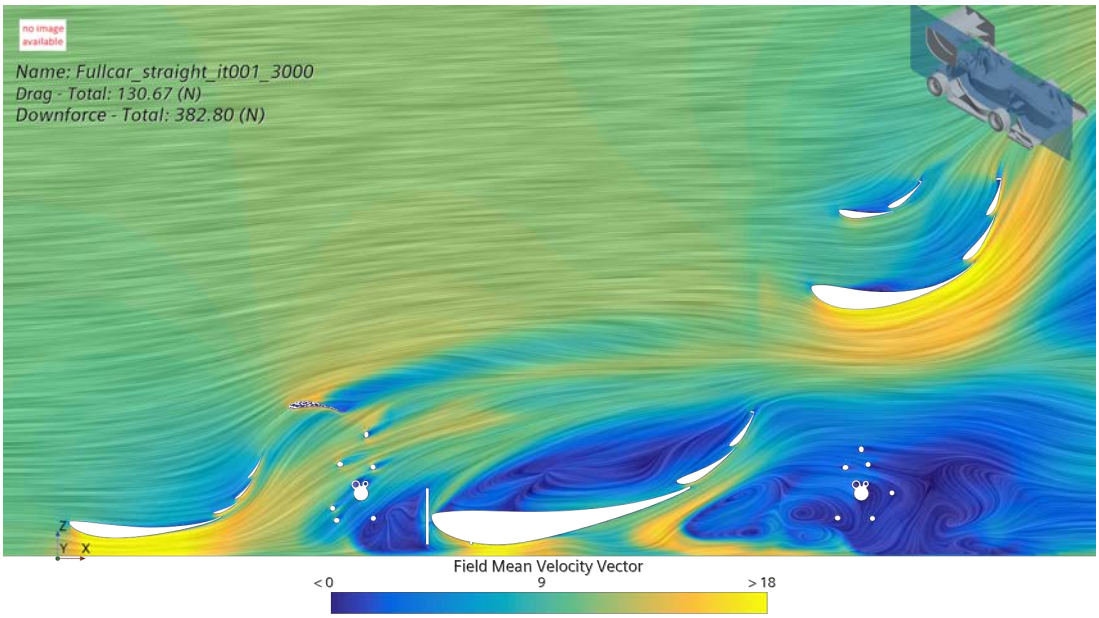

(a) Velocity vector field plot for Baseline at y = 0.45 m plane

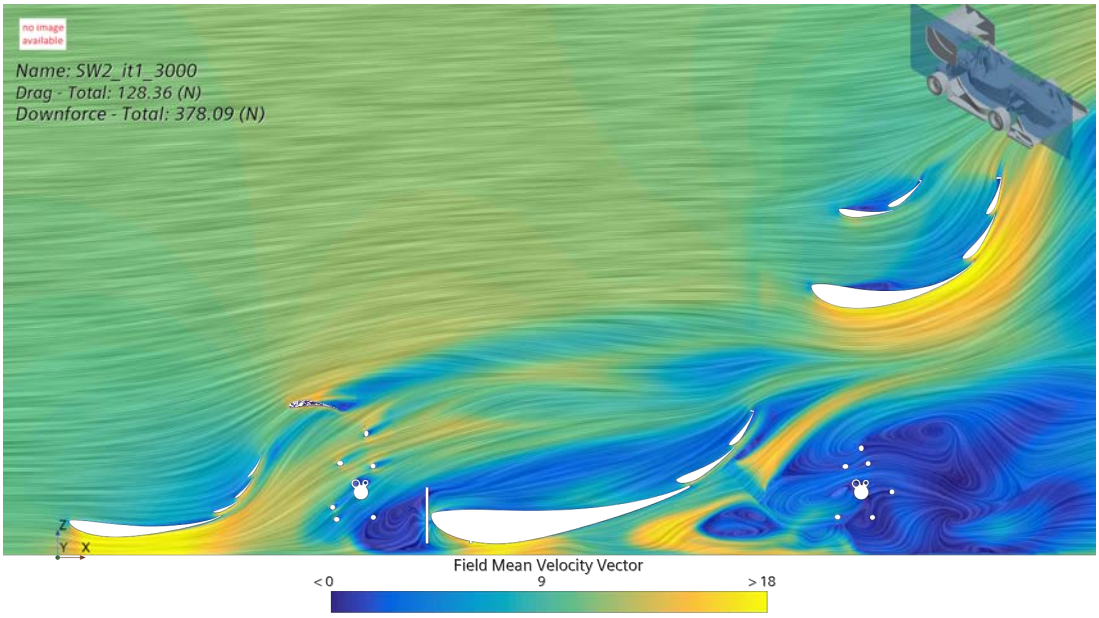

(b) Velocity vector field plot for SW2 it001 at y = 0.45 m plane

Figure 4.19: Velocity vector field plots for Baseline and SW2 it001

As can be seen in Figure 4.19b the fan has been placed in a way that stagnates the air at the upper edge of the fan resulting in a disturbance in the flow along the main segment wing. At the last element of the multi-element wing, furthest downstream, the flow has detached resulting in worse performance. This disturbs the airflow and reduces its energy without gaining any downforce which is undesirable. The downforce in newton for each

major part of the car and the total downforce of the car can be seen in Table 4.8

Simulation	$-F_z$ **Body/Diffuser**	$-F_z$ **FW**	$-F_z$ **Side Wings**	$-F_z$ **RW**	$-F_z$ **Total**
Baseline	56.1 N	133.3 N	98.6 N	106.8 N	382.8 N
SW Concept 2	57.8 N	130.9 N	102.4 N	99.8 N	378.1 N

Table 4.8: Results for Side Wing Concept 2 it001

From Table 4.8 we can see that the resulting downforce over the car has all been reduced except for the downforce of the side wings. This indicates that the concept itself has potential of creating more downforce since the downforce did not reduce drastically despite poor implementation.

4.2.3 Concept 2 Ground effect in side wing main segment iteration 2

The resulting plots from the first iteration showed that the airflow separated along the airfoil due to the fan being located to close to the airfoil, making the airflow unable to flow naturally along the segment. Due to this, the fan and radiator package was relocated further from the pressure side of the side wing flap with the aim of increasing the massflow through the flaps. Similarly to iteration 1, the aim was to push the airflow along the bottom of the main airfoil in the side wing without making the flow detach.

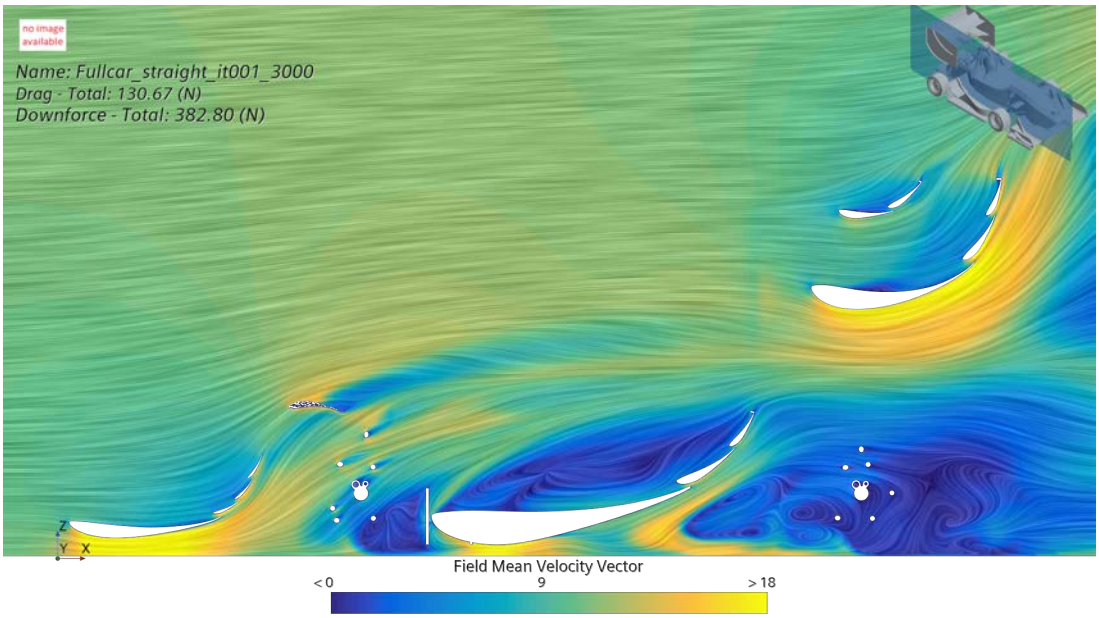

(a) Velocity vector field plot for Baseline at x = 0.7 m plane

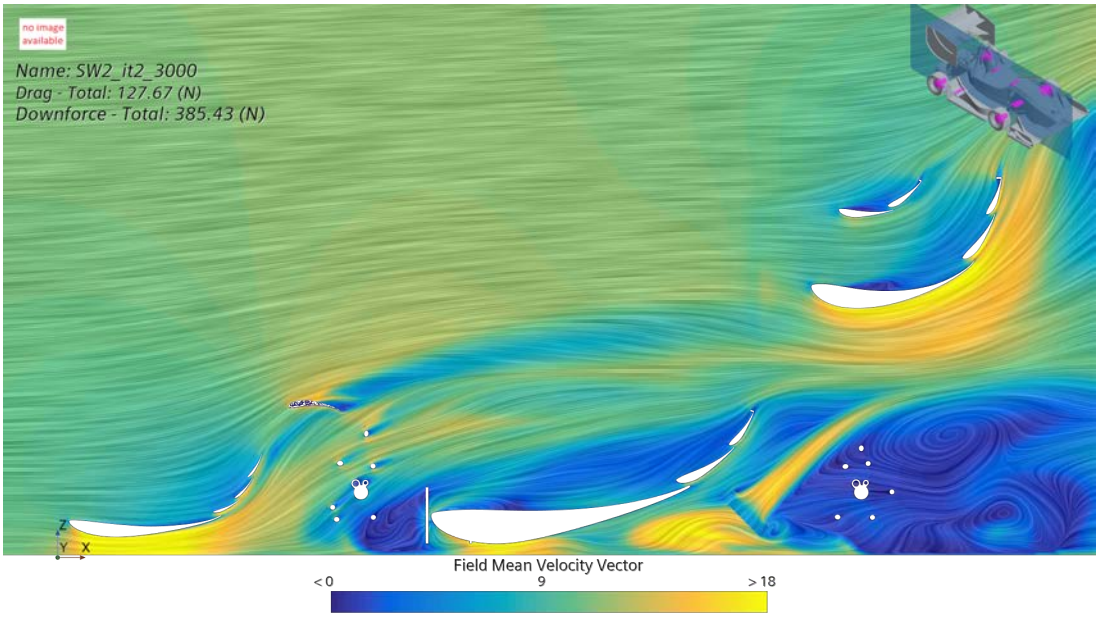

(b) Velocity vector field plot for SW2 it002 at x = 0.7 m plane

Figure 4.20: Velocity vector field plots for Baseline and SW2 it002

In the comparison between the baseline simulation and iteration 2 of SW concept 2 as can be seen in Figure 4.20, there is an improvement with a larger high velocity area in the main segment although the increase is may not be as large as desired. Furthermore, the detached flow along the wing caused by the position of the fan has been avoided.

Simulation	$-F_z$ Body/Diffuser	$-F_z$ FW	$-F_z$ Side Wings	$-F_z$ RW	$-F_z$ Total
Baseline	56.1 N	133.3 N	98.6 N	106.8 N	382.8 N
SW Concept 2	58.7 N	131.5 N	106.0 N	101.9 N	385.4 N

Table 4.9: Results for Side Wing Concept 2 it002

As can be seen in Table 4.9 the concept creates small differences in downforce on the front wing and diffuser and an increase in downforce on the side wings along with a decrease on the rear wing resulting in a small increase in total downforce. From these results there is a clear increase in downforce from the side wings indicating that the basic principle of the concept is working although the increase might not be as large as desired. When overviewing all the simulations the rear wing appears to be sensitive to change in airflow indicating that it might be better to implement the concept in a straight configuration as opposed to the angle it is set to in concept 2 where it might disturb the airflow around the rear wing.

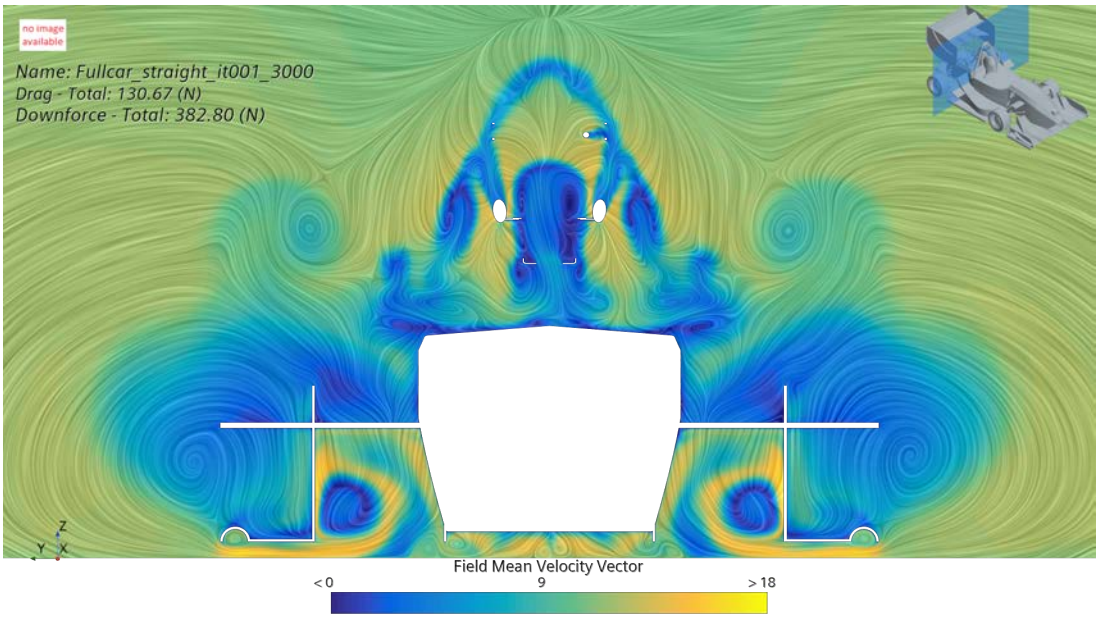

(a) Velocity vector field plot for Baseline at x = 2.7 m plane

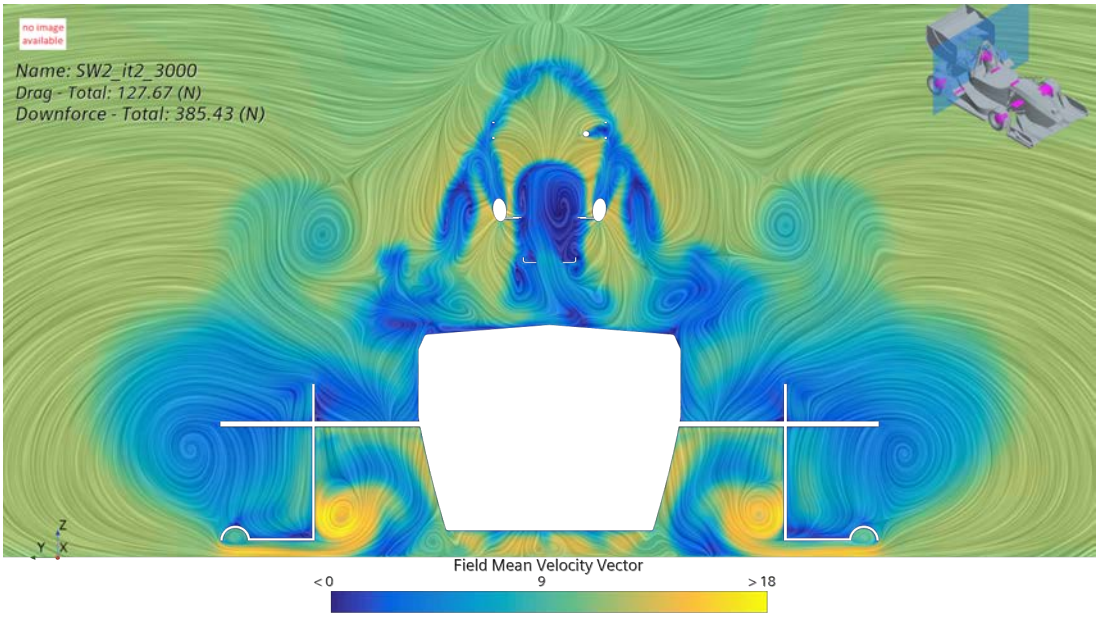

(b) Velocity vector field plot for SW2 it002 at x = 2.7 m plane

Figure 4.21: Velocity vector field plots for Baseline and SW2 it002

When looking at the simulation in Figure 4.21 there is a clear indication of a vortex inside the main segment as can be seen in Figure 4.21a for the baseline. This could make the airflow more complicated to gain downforce from since it has lost momentum in the downstream direction. In Figure 4.21b the indications of a vortex remains with implemented fans.

In summary there are potential gains to be made from a concept similar to this but it might require more precision or as likely is the case, simply require more power from the fans.

4.2.4 Concept 3: Accelerate low energy wheel wake along side structures

The aim of the third concept, that is pictured in Figure 4.22, is to increase the airflow along the sidestructures, accelerating stagnated, low energy air from the tyre wake of the front tyres, to match the naturally flowing air along the sidestructures sidewall and along the top of the floor.

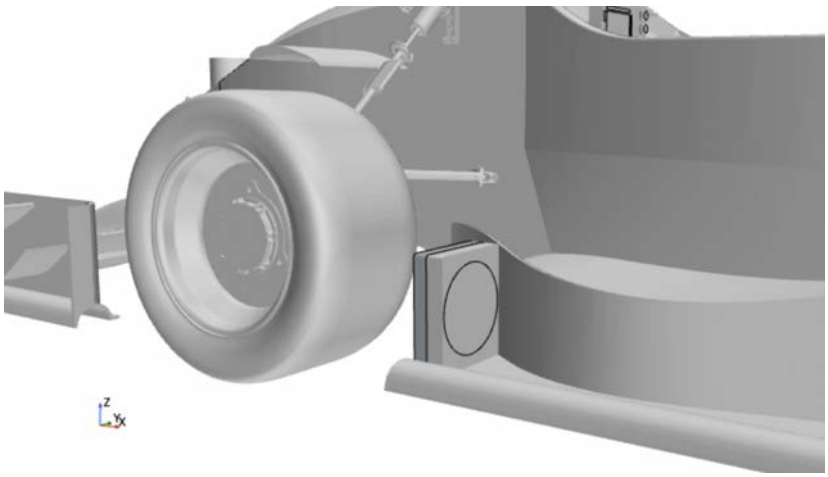

Figure 4.22: CAD of Side Wing Concept 3, Accelerate low energy wheel wake along side structures

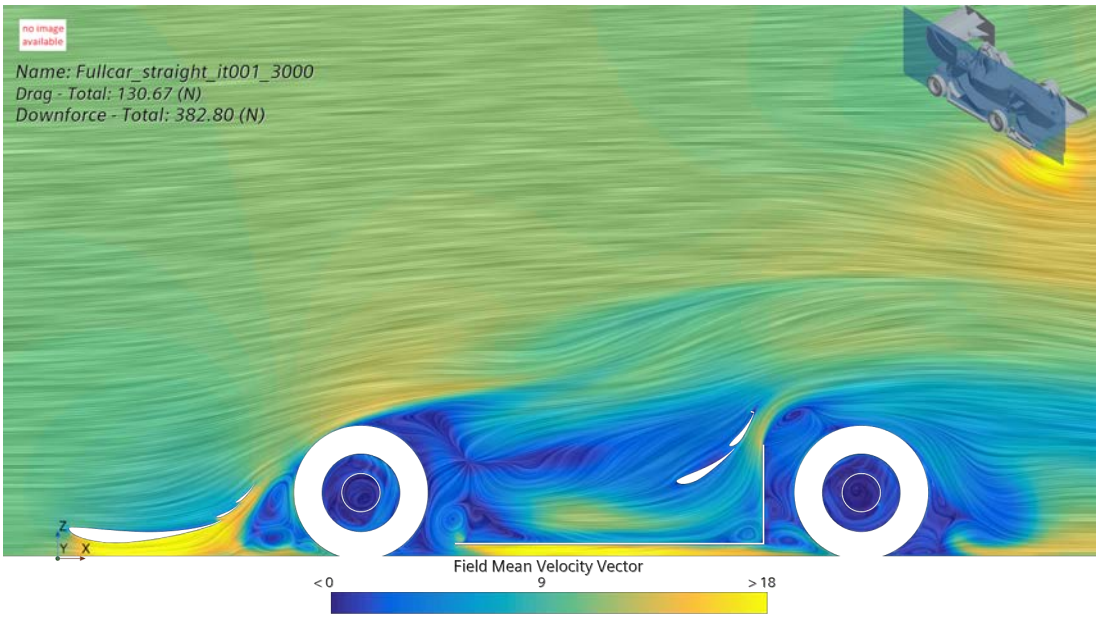

(a) Velocity vector field plot for Baseline at y = 0.625 m plane

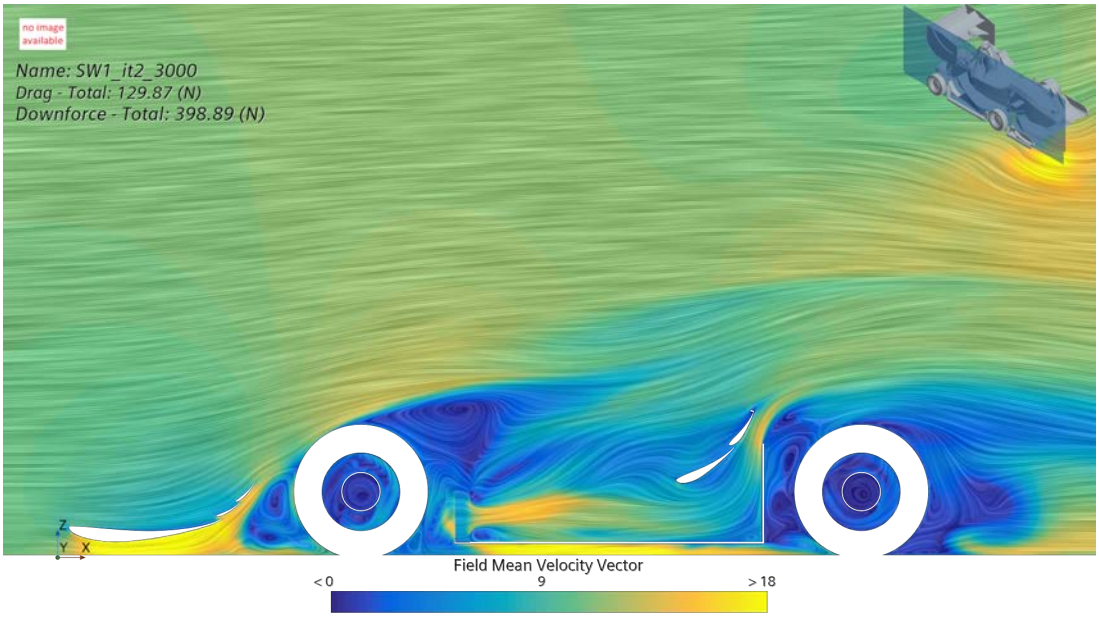

(b) Velocity vector field plot for SW3 it001 at y = 0.625 m plane

Figure 4.23: Velocity vector field plots for Baseline and SW3 it001

In Figure 4.23, there is a clear increase in airflow velocity in the wake of the front tyres when comparing the first iteration of concept 3 with the baseline simulation. The most prominent difference in this plot can be seen along the whole side wing where the velocity of the airflow has increased on the side wing, mainly upstream of the wing but also in between the flaps and the stagnation plate. As previously described, in cases when

downforce is desired, the velocity should be higher on the bottom of the wing, creating lower pressure. This is exactly what happens when the velocity is increased between the wing elements and the stagnation plate. There is also a visible difference in the airflow above the side wings where the wheel wake looks to have risen slightly higher up and further downstream. This in turn could cause changes on performance on other parts of the car, as we in this case can see later in Table 4.10.

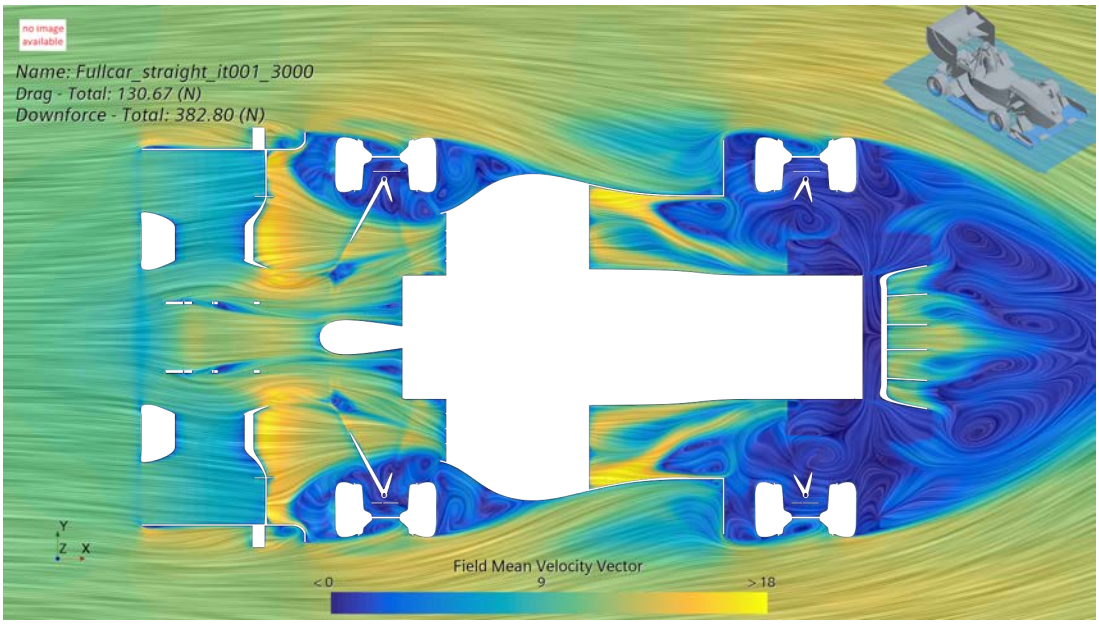

(a) Velocity vector field plot for Baseline at z = 0.15 m plane

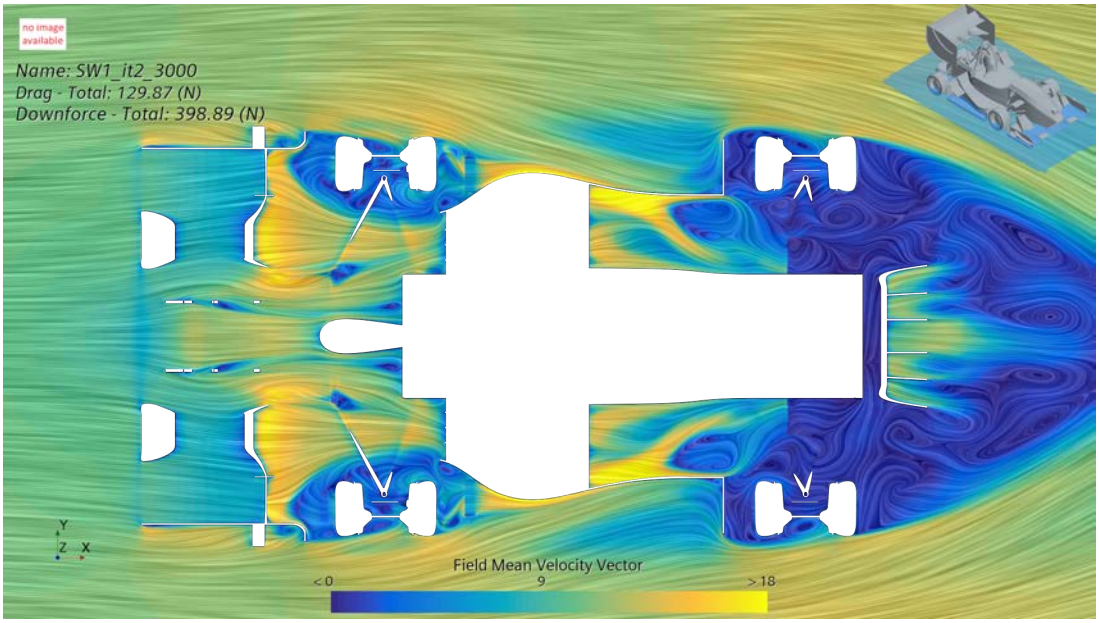

(b) Velocity vector field plot for SW3 it001 at z = 0.15 m plane

Figure 4.24: Velocity vector field plots for Baseline and SW3 it001

From the z-plane plots in Figure 4.24, there is a clear difference in the wheel wake of the front tyres. The integration of the fans has managed to speed up the airflow surrounding the front wheels, utilizing otherwise stationary air for the outside of the side wings and reducing blockage of flow around the front tyres. This appears to have considerably increased the performance of the side wings while also promoting the performance of the

front wing, as we can see in Table 4.10.

Simulation	$-F_z$ Body/Diffuser	$-F_z$ FW	$-F_z$ Side Wings	$-F_z$ RW	$-F_z$ Total
Baseline	56.1 N	133.3 N	98.6 N	106.8 N	382.8 N
SW Concept 3	63.2 N	135.5 N	115.6 N	94.6 N	398.9 N

Table 4.10: Results for Side Wing Concept 3 it001

This concept gave increased downforce in several areas of the car, with side wings and body/diffuser getting the largest increase. A pretty significant decrease can be seen in the rear wing, however the increases on all other parts on the car weigh up for it. In total, the downforce generated by this concept was the highest of all simulated concepts.

A further four iterations were made with concept 3, all with the aim of moving more air from the front tyre wake and front wheel suspension components. This was accomplished through positioning the fan and radiator package at an angle at the front of the side structures. These proved to perform worse and their results can be seen in Table 4.11, direction (out and in) defined by direction of outlet, see Figure 4.25 for reference.

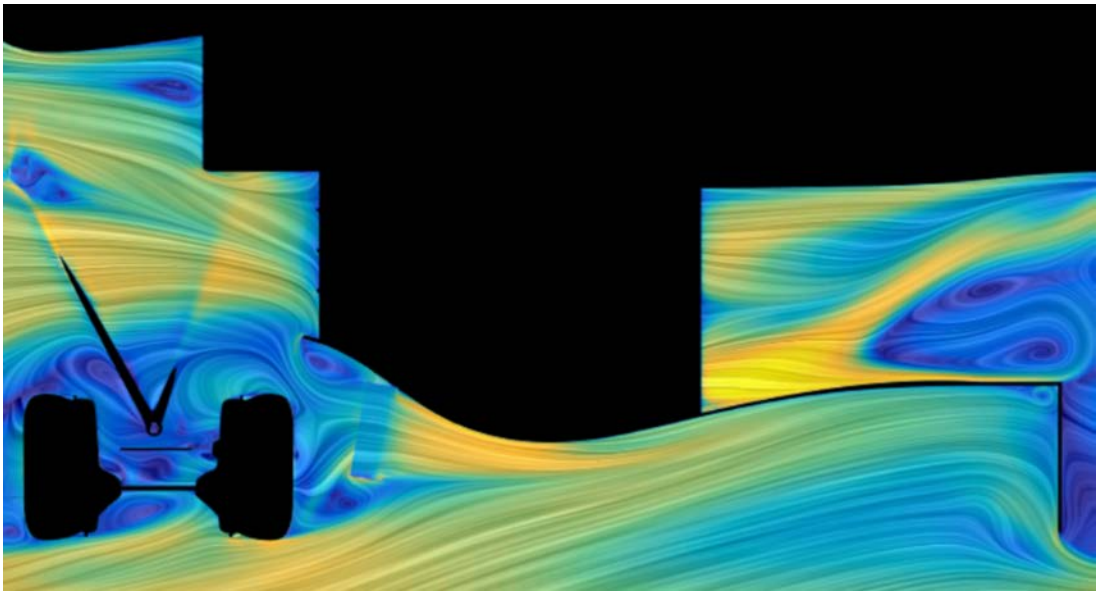

Figure 4.25: Fan in outwards direction

Simulation	$-F_z$ Body/Diffuser	$-F_z$ FW	$-F_z$ Side Wings	$-F_z$ RW	$-F_z$ Total
30 deg. out	59.8 N	135.6 N	108.0 N	96.5 N	389.9 N
10 deg. out	61.5 N	134.9 N	108.0 N	94.9 N	388.7 N
5 deg. out	57.8 N	130.9 N	102.4 N	99.8 N	378.1 N
0 deg.	63.2 N	135.5 N	115.6 N	94.6 N	398.9 N
5 deg. in	62.5 N	135.7 N	112.1 N	96.2 N	396.8 N

Table 4.11: Results for Side Wing Concept 3, all angles

4.2.5 Concept 4 Accelerate air over stagnation plate

The purpose of the stagnation plate in front of the rear wheels is to stop the tyres from creating turbulence and a large wheel wake which in turn can disturb the airflow in the diffuser, rear wing and other important parts of the car. These stagnation plates creates stationary air which sits at the end of the side structures. In concept 4, pictured in Figure 4.26, the fan package was positioned in order to push the air up and above the stagnation plate, trying to make use of the air that otherwise would hit the stagnation plate.

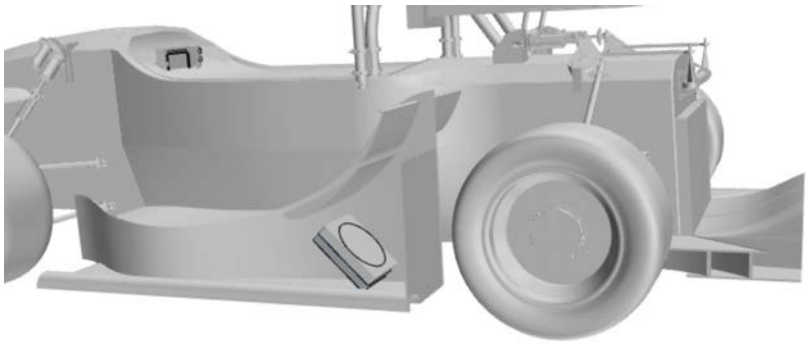

Figure 4.26: CAD of Side Wing Concept 4, Accelerate air over stagnation plate

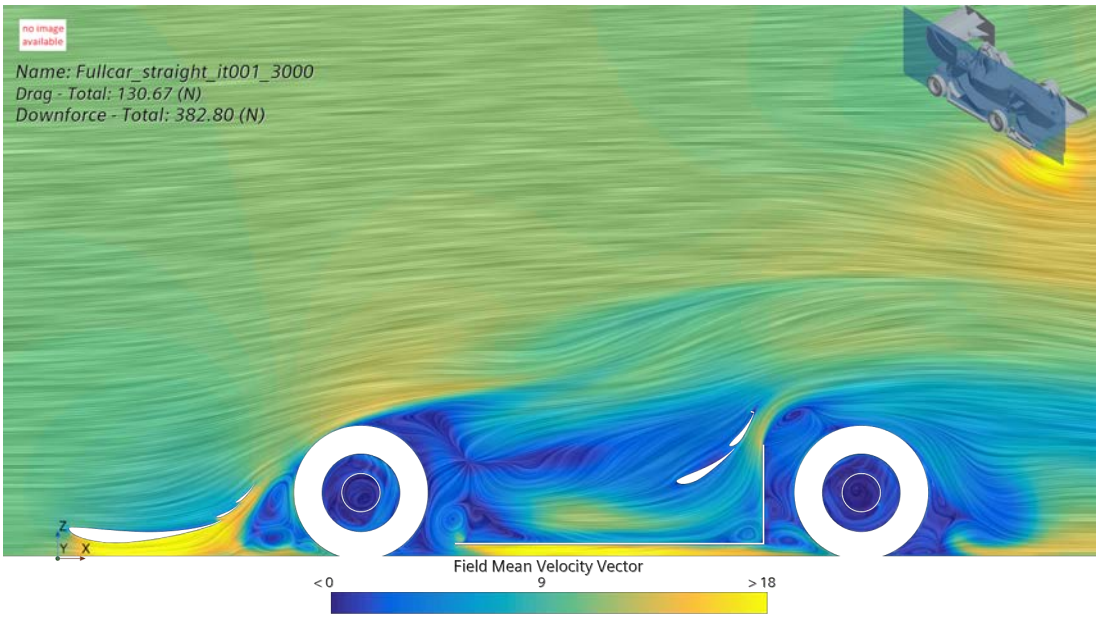

(a) Velocity vector field plot of Baseline at y = 0.625 m plane

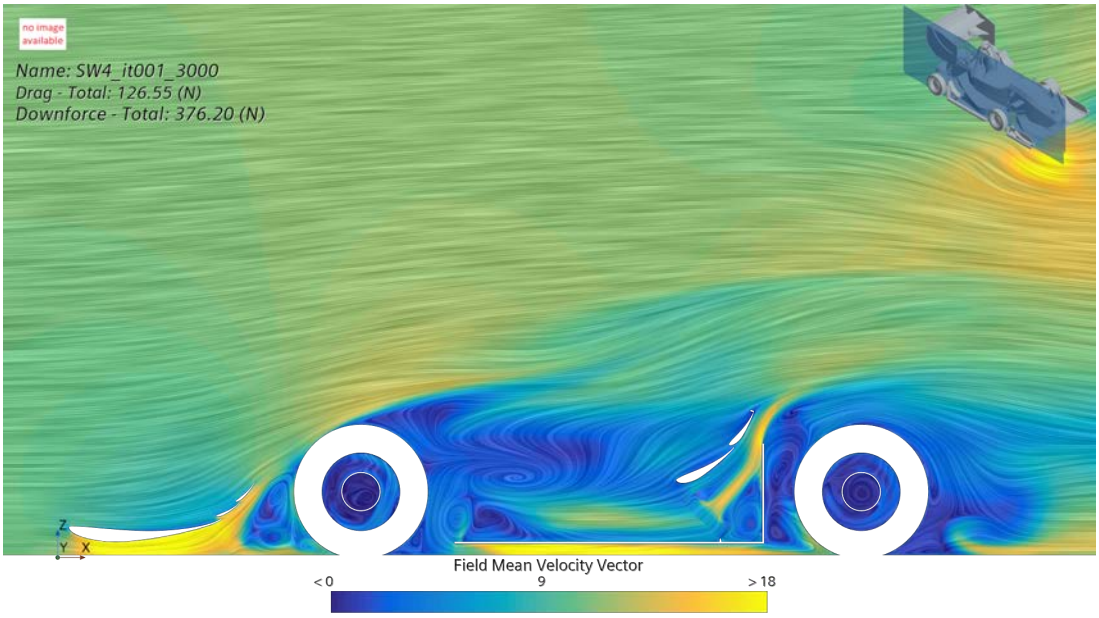

(b) Velocity vector field plot of SW4 it001 at y = 0.625 m plane

Figure 4.27: Velocity vector field plots for Baseline and SW4 it001

Simulation	$-F_z$ **Body/Diffuser**	$-F_z$ **FW**	$-F_z$ **Side Wings**	$-F_z$ **RW**	$-F_z$ **Total**
Baseline	56.1 N	133.3 N	98.6 N	106.8 N	382.8 N
SW Concept 4	58.8 N	131.0 N	105.1 N	93.2 N	376.2 N

Table 4.12: Results for Side Wing Concept 4 it001

This concept was overall not a positive contribution to the performance of the car. It did increase downforce on the side wings, and slightly helped the diffuser. However, the air flow to the rear wing was affected negatively, incurring a net loss of the total downforce.

4.2.6 Potential Concept 5

There is also potential for a fifth concept where the properties of concept 1 and concept 3 are combined. The two concepts both utilize air along the outside edge of the side structures, concept 1 pushing air along it from the front tyres and concept 2 by pulling air from it into the end of the main segment. The potential concept could be seen as an iteration of concept 3 where the fans keep their positions but in the location where the fans are positioned in concept 1, the fans are simply replaced by a hole. The concept is shown in Figure 4.28. Because the air naturally flows in the direction of the hole there is a possibility that a similar effect of concept 1 can be achieved without the fan. Furthermore the two concepts, 1 and 3, utilize different effects in different locations. There is a possibility that these can work simultaneously, independent of each other. A simplified version of this concept was simulated resulting in the plot compared to the baseline as seen in Figure 4.29.

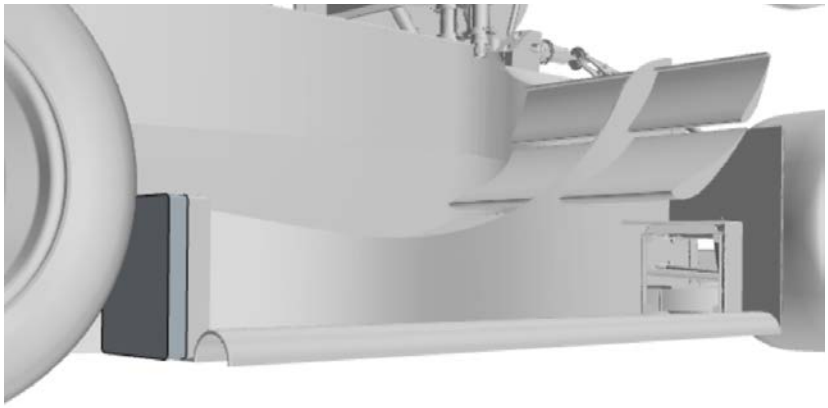

Figure 4.28: CAD of Potential Side Wing Concept 5, where the fan is seen to the left and the hole through the stagnation plate to the right

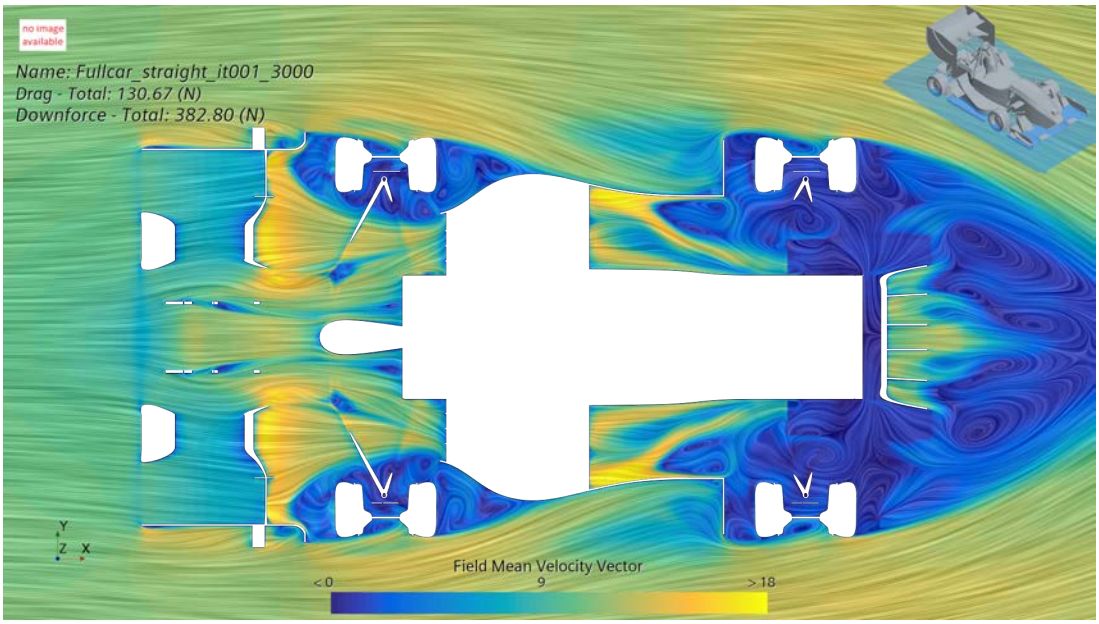

(a) Velocity vector field plot of Baseline at z = 0.15 m plane

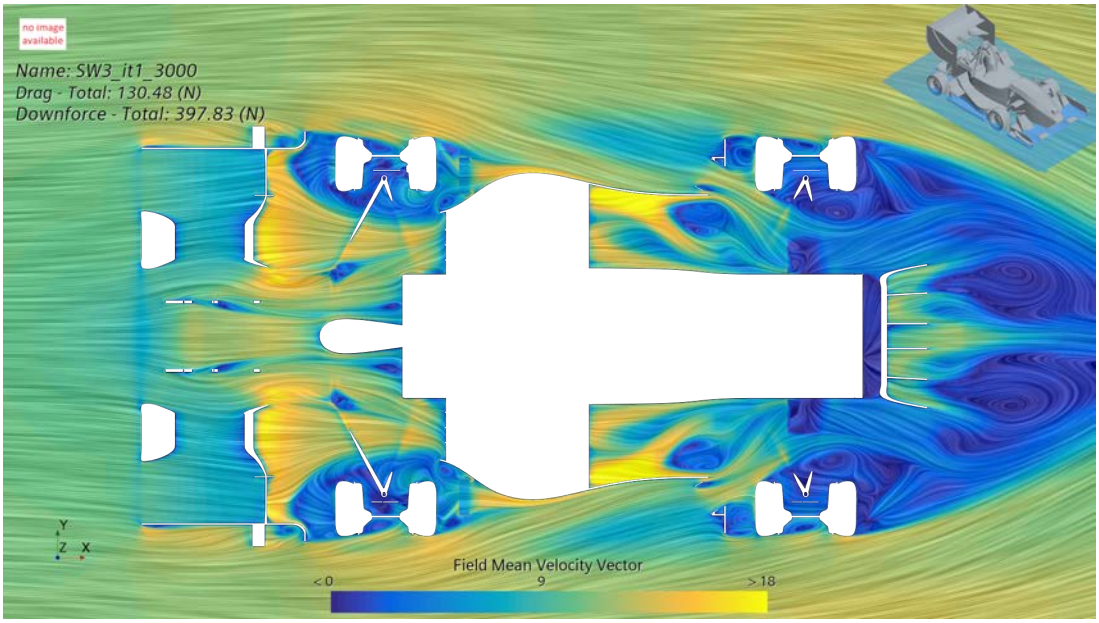

(b) Velocity vector field plot of SW5 it001 at z = 0.15 m plane

Figure 4.29: Velocity vector field plots for Baseline and SW5 it001

When the fan was moved from the stagnation plate to the new position for simulation of this concept, the original fan mounting bracket was accidentally left in the stagnation plate. This caused the flow to separate around the bracket. Looking at Figure 4.30c, this slightly disturbs the airflow around the hole in the side structure. The stagnation plate in front of the rear wheels is designed to outwash the air flow in order to not cause turbulence

around the rotating wheels which disturbs the airflow. However, by looking at concept 1 in Figure 4.30a, it is seen that an inwash design could be beneficial when utilizing a hole in the side structures. A redesign of the endplate allowing inwash and a more seamless integration along the sidewall could result in more downforce being generated by the side wing. This could possibly be done by constructing the endplates at an angle and smoothing out the transition from sidewing to hole by removing mountings from it and possibly angle the edges of the hole.

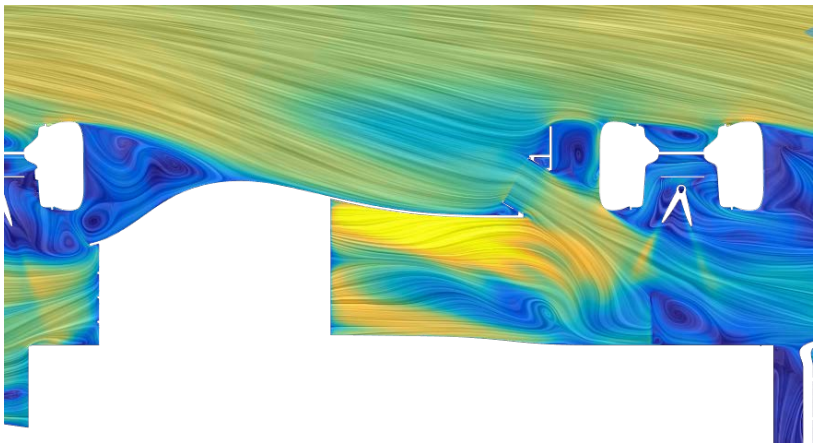

(a) Velocity vector field plot of SW1 it001 at z = 0.15 m plane

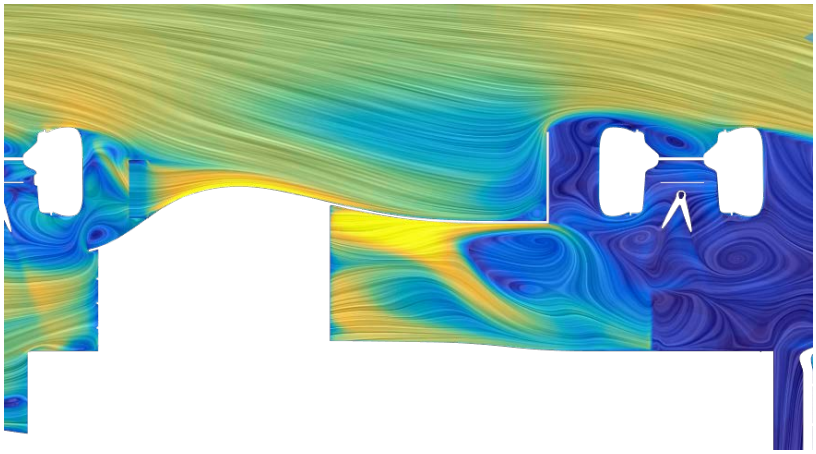

(b) Velocity vector field plot of SW3 it001 at z = 0.15 m plane

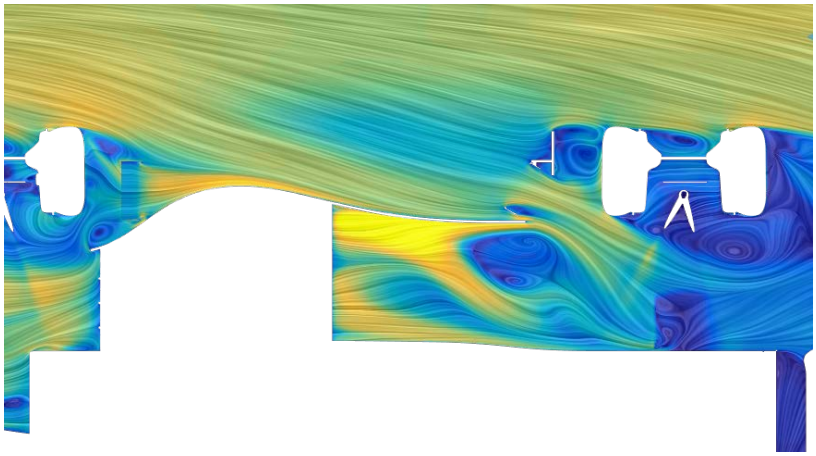

(c) Velocity vector field plot of SW5 it001 at z = 0.15 m plane

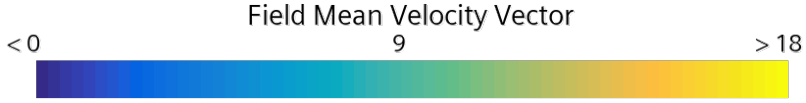

(d) LIC reference scale

Figure 4.30: Velocity vector field plots for SW1 it001, SW3 it001 and SW5 it001

As seen in Table 4.13 the total downforce achieved in this simple simulation is 397.8 N, which is close to each of the two concepts it is based on (398.5 N and 398.9 N for concepts 1 and 3 respectively).

Simulation	$-F_z$ Body/Diffuser	$-F_z$ FW	$-F_z$ Side Wings	$-F_z$ RW	$-F_z$ Total
Baseline	56.1 N	133.3 N	98.6 N	106.8 N	382.8 N
SW Concept 5	65.0 N	136.1 N	114.5 N	92.9 N	397.8 N

Table 4.13: Results for Side Wing Concept 5 it001

4.3 Diffuser

In this section, diffuser concepts will be presented and discussed. A total of four concepts will be introduced, each featuring a different solution aimed at increasing overall downforce with the help of a diffuser

4.3.1 Concept 1 Suction to increase expansion

The goal with this concept was to lower the pressure under the car. To make this happen, the idea was to increase the expansion rate of the diffuser while maintaining an attached flow.

In the baseline case, the flow is attached and no separation occurs. Therefore, the first step was to increase the expansion rate of the diffuser. A total of four simulations were carried out (see Table 4.14). The reason the strakes were removed is to not divide the diffuser into segments. The purpose of the strakes is to keep out turbulent, low energy air (see Section 2.4.3), however, this clashes with the purpose of the fan. The fan is intended to give momentum to the flow but it was believed that the strakes acting as walls will prevent the fan from reaching the outer segments of the diffuser. It would therefore minimize the effect of the fan.

Expansion raito		$-F_z$ Body/diffuser
1.60	Basline with strakes	56.1 N
3.08	No strakes	58.2 N
3.48	No strakes	59.2 N
4.06	No strakes	56.0 N
4.66	No strakes	55.9 N

Table 4.14: Downforce generated by the body/diffuser with varying expansion rates

The fourth simulation, with 4.66 in expansion ratio, lead to a separation which can be seen in Figure 4.31

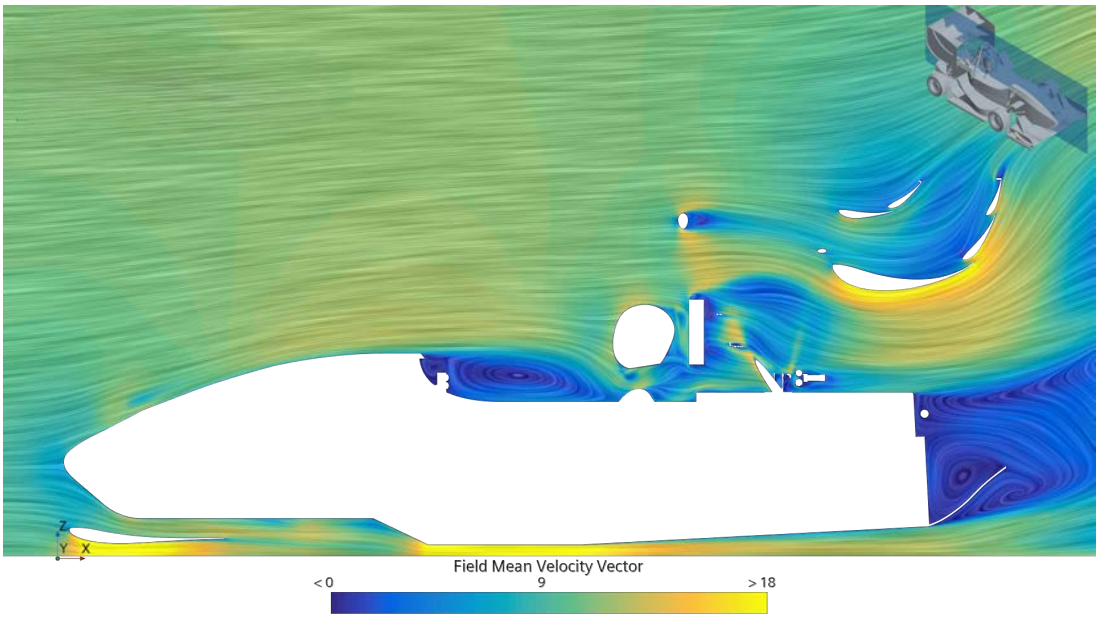

Figure 4.31: Velocity vector field plot of a diffuser with an expansion rate of 4.66

To re-attached the flow, the following concept is presented, see Figure 4.32. The aim is to create a low pressure region on the top part of the diffuser by introducing fans.

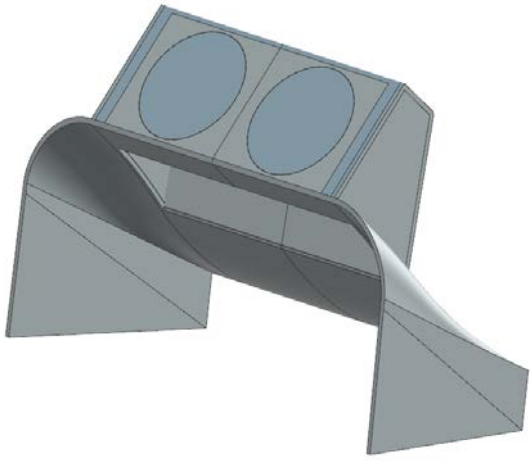

Figure 4.32: CAD of Diffuser Concept 1 iteration 1

The result of the concept was as follows.

Concept	$-F_z$ Body/Diffuser	$-F_z$ Side Wings	$-F_z$ RW	$-F_z$ FW	$-F_z$ Total
Baseline	56.1 N	98.6 N	106.8 N	133.3 N	382.8 N
Suction to increase expansion	57.0 N	107.2 N	110.2 N	133.0N	395.7

Table 4.15: Results for Diffuser Concept 1 it001

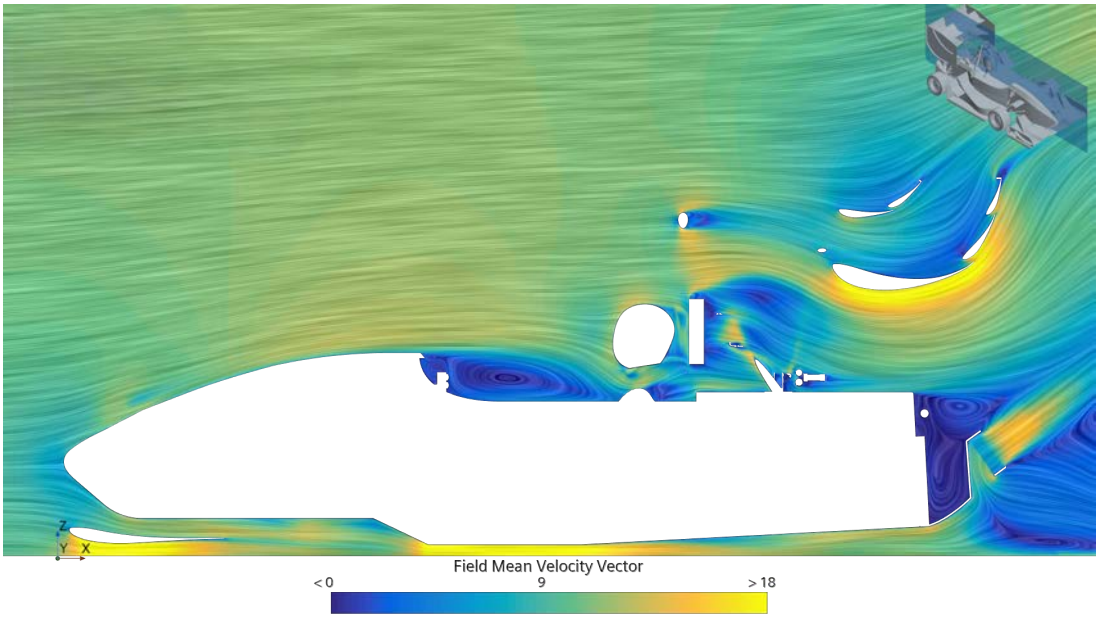

Figure 4.33: Velocity vector field plot of DF1 it001 at y = 0.075 m plane

The general purpose was fulfilled, as shown in Figure 4.33. The flow remains attached to the diffuser, and the outflowing air is directed upward at an angle.

By comparing the boundary pressure coefficient plot under the car, it can be observed that the concept's goal, to reduce the pressure beneath the car, has been partially achieved. Although the downforce in the body/diffuser region has decreased, the side wing shows an increase in downforce. Figure 4.37a displays a broader dark blue area around the lowest part of the floor, compared to Figure 4.50a, extending toward the main segment of the side wing, which explains the shift in performance metrics.

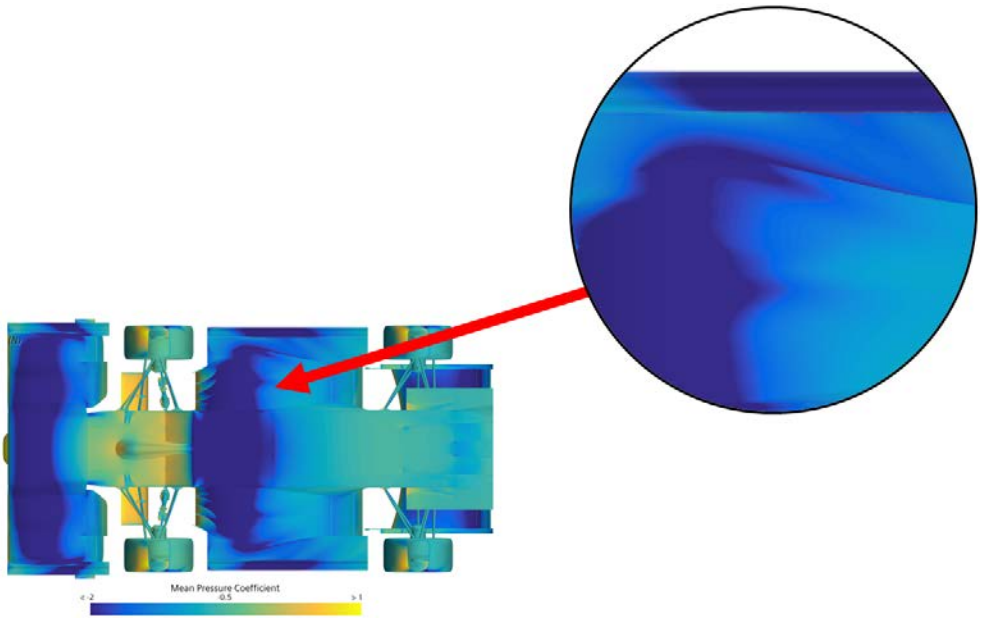

(a) Pressure Coefficient plot for Baseline at y = 0.0 m plane

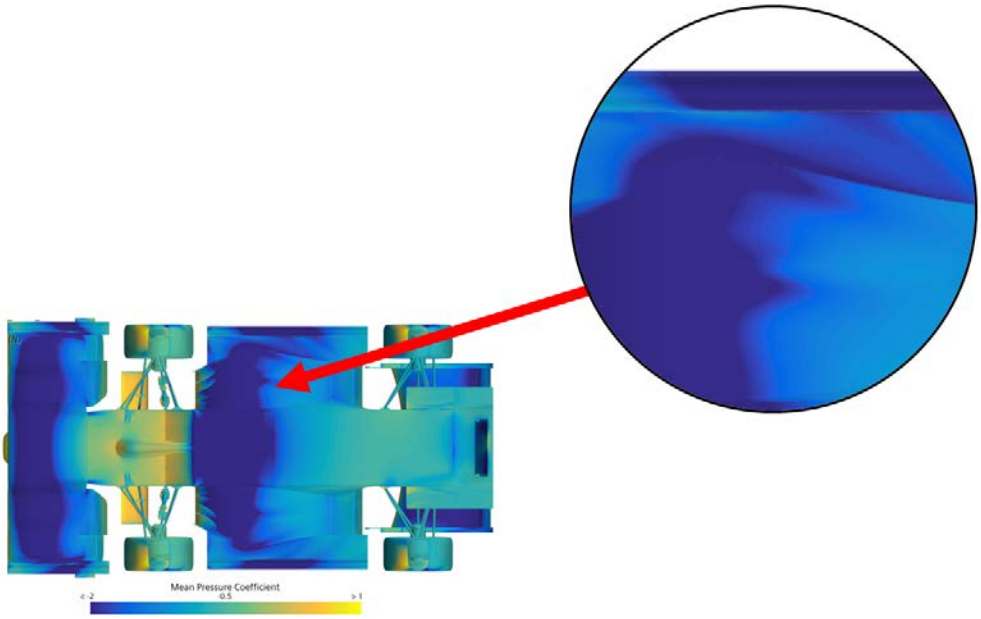

(b) Pressure Coefficient plot for DF1 it001 at y = 0.0 m plane

Figure 4.34: Pressure Coefficient plots for Baseline DF1 it001

Examining the diffuser profile in Figure 4.33, it becomes apparent that the diffuser is somewhat angular. However, further refinement of the diffuser shape was not pursued, as the primary objective of the concept was already met.

4.3.2 Concept 2 Suction to increase expansion with upward flow

From Table 4.15, it can be seen that the concept led to an increase in rear wing performance. This was not the initial intention, but it inspired a new concept: to maintain suction from the diffuser while directing the airflow toward the rear wing to energize the boundary layer on the rear wing.

To realize this idea, the same diffuser as in Concept 2 was used, the main difference lies in the shape of the duct, especially the angle of the outflowing air. Figure 4.35 illustrates the differences between Concept 2 and Concept 3.

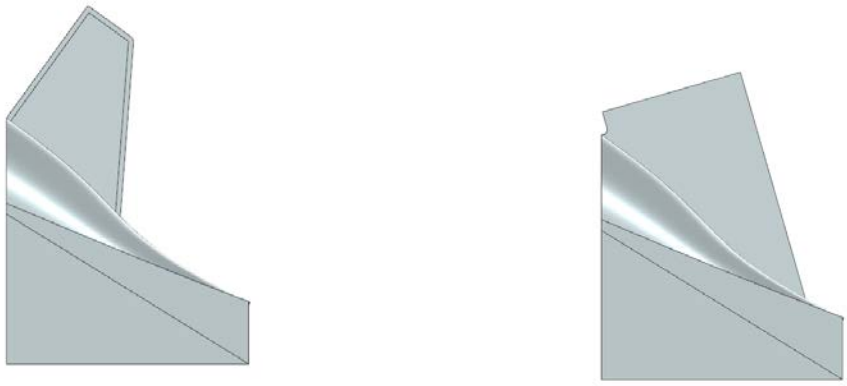

(a) CAD Diffuser Concept 1, Suction to increase expansion

(b) CAD of Diffuser Concept 2, Suction to increase expansion with upward flow

Figure 4.35: CAD of Diffuser Concept 1 and Diffuser Concept 2

Looking at Figure 4.36, the general concept appears to function as intended. It draws air through the diffuser to maintain flow attachment, and the outflowing air interacts with the airflow beneath the rear wing. However, the data presented in Table 4.16 shows a significant decrease in the downforce generated by the rear wing. This indicates that the primary objective of the concept was not achieved. Although the downforce generated by the body and diffuser increases slightly, the total downforce is still lower compared to the previous concept.

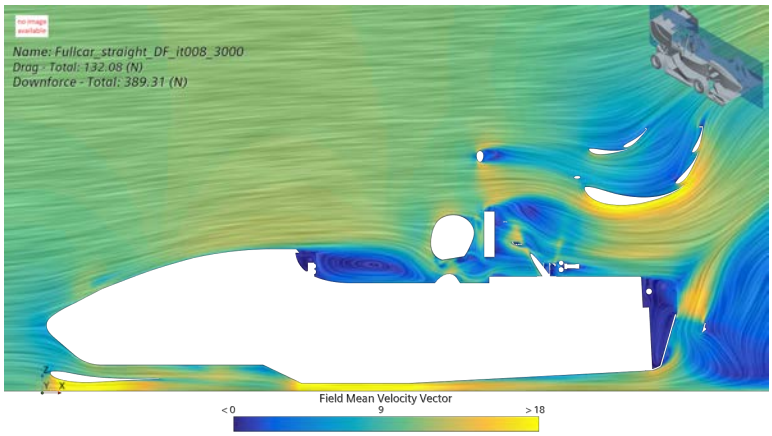

Figure 4.36: Velocity vector field plot of DF2 it001 at y = 0.075 m plane

Simulation	DF Body/Diffuser	$-F_z$ FW	$-F_z$ Side Wings	$-F_z$ RW	$-F_z$ Total
Suction to increase expansion	57.0 N	133.0 N	107.2 N	110.2 N	395.7 N
Suction to increase expansion with upward flow	59.5 N	132.8 N	108.5 N	101.4 N	389.3 N

Table 4.16: Results for Diffuser Concept 2 it001

The exact cause of the significant reduction in rear wing downforce is unclear, but one hypothesis is that the rear wing is operating near its maximum capacity. This means that introducing more energy into the flow, from the fan, directed at the rear wing does not necessarily enhance its performance unless the geometry is modified. Note that this might not be the case when the car is moving at a lower velocity.
To increase the downforce generated by a wing, the pressure difference across its surface must be increased. However, as illustrated in Figure 4.37 , the pressure difference actually decreases compared to concept one Suction to increase expansion.

With this in mind, this concept will not be further developed.

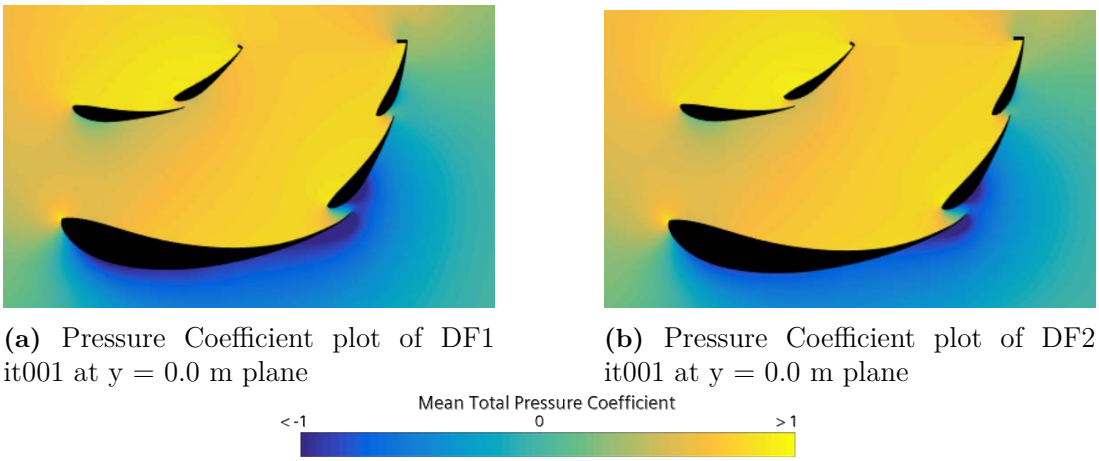

(a) Pressure Coefficient plot of DF1 it001 at y = 0.0 m plane

(b) Pressure Coefficient plot of DF2 it001 at y = 0.0 m plane

Figure 4.37: Pressure Coefficient plots of DF1 it001 and DF2 it001

To iterate this concept further, the need to change the geometrical shape of the rear wing is necessarily. But that is above what this project should deal with. With this in mind, this concept will not be further developed

4.3.3 Concept 3 Inside-suction

The idea behind this concept is to directly suck air from the underfloor through the fan and out of the diffuser. The sucking of the fan was intended to decrease the pressure upstream of the diffuser and the blowing was meant to help increase the expansion rate of the diffuser. The diffuser expansion that was chosen is it004 (see Table 4.14). What makes this concept unique is that it directly transfers air through a crucial part of the diffuser and there was a concern whether this would stall the flow because of the rather low power and quite large size of the fan.

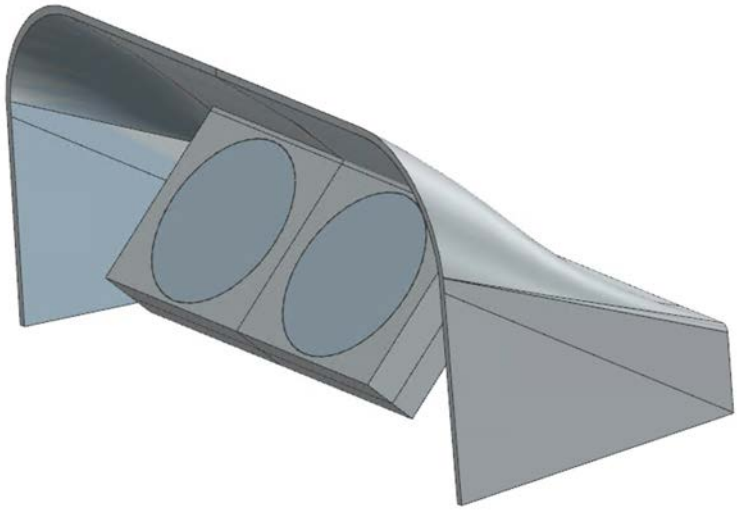

Figure 4.38: CAD of Diffuser Concept 3

Simulation	$-F_z$ **Body/Diffuser**	$-F_z$ **FW**	$-F_z$ **Side Wings**	$-F_z$ **RW**	$-F_z$ **Total**
Baseline	56.1 N	133.3 N	98.6 N	106.8 N	382.8N
inside-suction	58.6 N	131.7 N	107.0 N	100.3 N	386.0 N

Table 4.17: Results for Diffuser Concept 3

Unfortunately, the result was not great, as the total downforce only increased by 0.8% (see Table 4.17. The LIC picture below (Figure 4.39a) is positioned where the fan is moving the most air. When examined closely the fan is not fully attached to the diffuser and it can be seen that the flow seperates quite early. This is partly because the fan is sticking out from the diffuser but also the fact that the diffuser geometry is not optimized. The geometry of the diffuser was made with limited knowledge of what the best profile and expansion rate for a diffuser is and especially when there is a fan inside of it. A concept like this would need a significant amount of iterative work which is something that is not a possibility in this project. It was also a delimitation to not change much with the main segments as can be read further in Section 1.4.

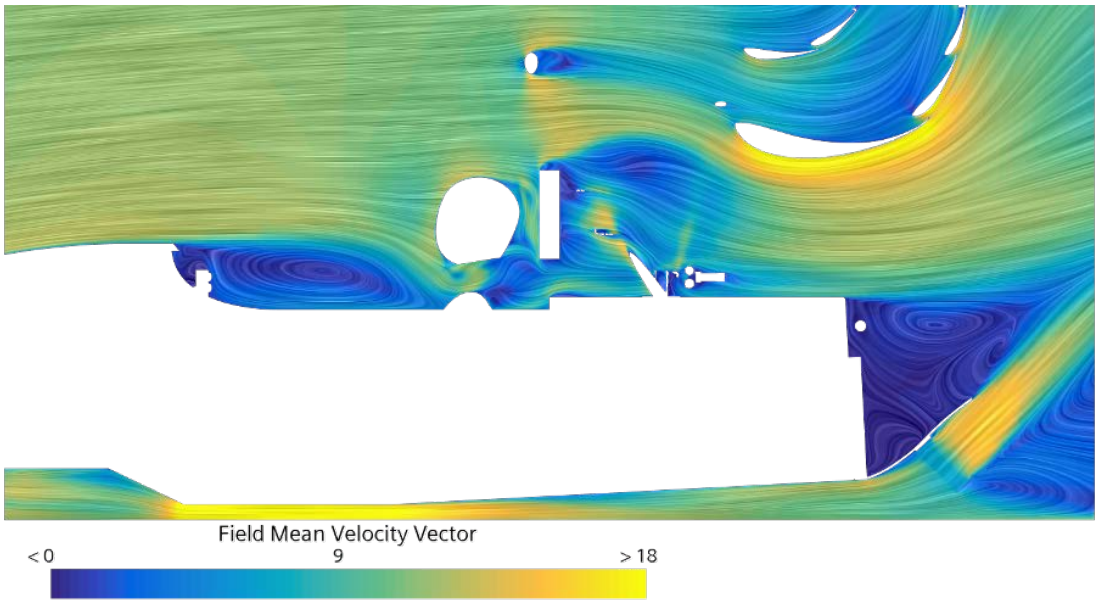

(a) Velocity vector field plot for DF3 it001 at y = 0.075 m plane

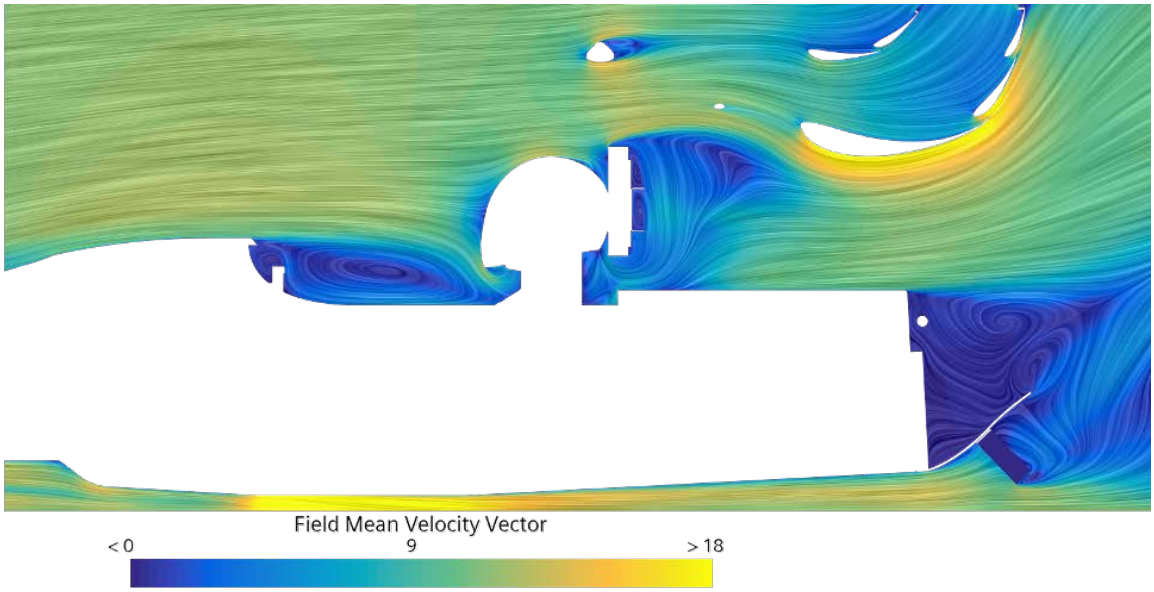

(b) Velocity vector field plot for DF3 it001 at y = 0.0 m plane

As seen in Figure 4.40, the pressure distribution is not as evenly distributed over the surface. This means that the surface of the diffuser is not being used to its potential and only a small part of the diffuser is creating downforce. The seperation at the start of the diffuser is also costing a lot since it is where the most downforce is created. This is because the biggest difference in pressure is achieved here.

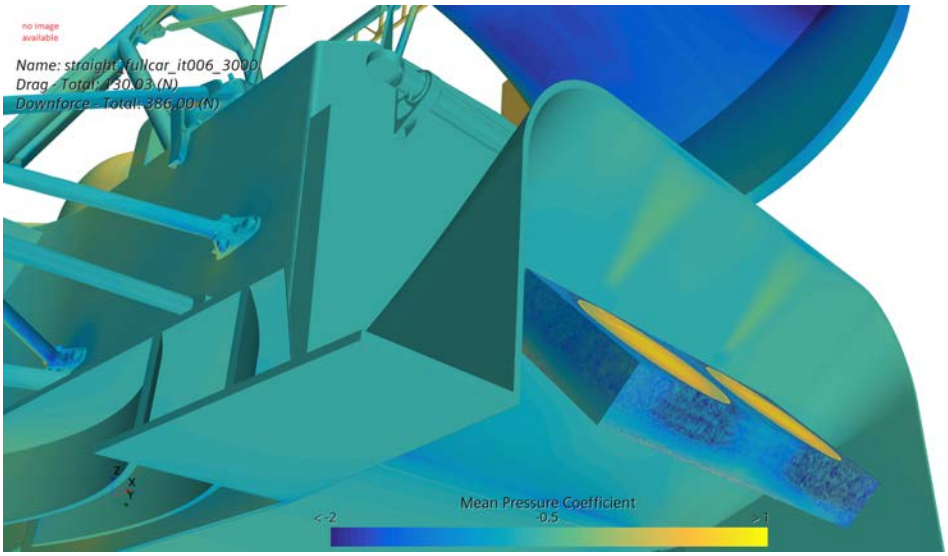

Figure 4.40: ISO Pressure Coefficient plot of "inside-suction" concept

The downforce generated in the body/diffuser region increased by 4.5% and it is that low partly due to the flow getting stalled by the fan as seen in 4.39b. This concept was also ruled out because of the inability to make cooling in this location efficiently.

4.3.4 Concept 4 Virtual Wall

All of the diffuser concepts saw an increase in SW downforce and with this final diffuser concept the idea was to take advantage of of that mechanism while simultaneously helping the diffuser. The fan can be seen in Figure 4.41 with its suction thought to increase the velocity under the SW. The blowing of the fans was intended to create low pressure air that would redirect turbulent wheel wake from the low pressure underfloor to the fan which would then act as a virtual wall. Additionally, this was thought to complement and enhance the functionality of the outwashing device on the footplate of the diffuser seen in Figure 4.41, giving it more energy to work with.

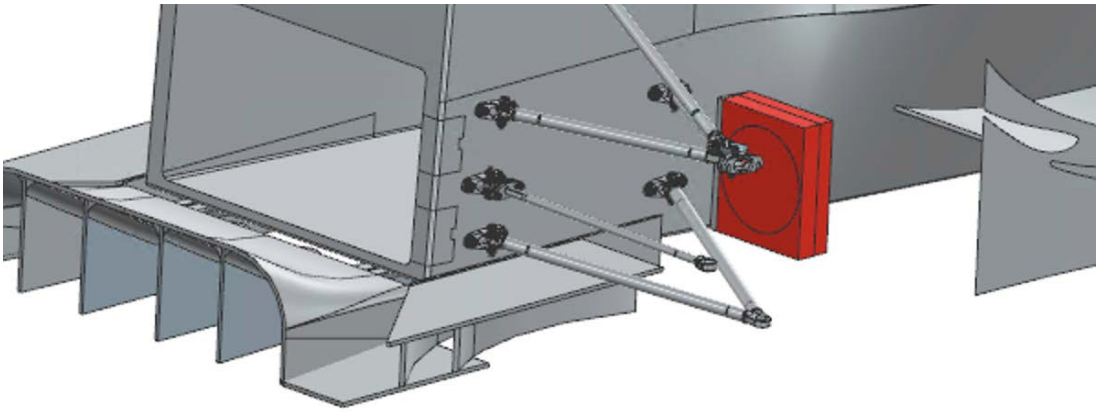

Figure 4.41: CAD of Diffuser Concept 4, "Virtual Wall" iteration 1

4.3.4.1 Iteration 1

For the first iteration, the total downforce increased by around 3.2%. Looking at the velocity vector field plots in Figure 4.42b it can be observed that the fan is creating a high-momentum jet. It seems to somewhat redirect the flow from the underfloor but not enough which can be seen by looking at the wake from tyres spinning around this area. When comparing the two velocity vector field plots in Figures 4.42a and 4.42b it can be seen that less air with low velocity is entering the underfloor which could be the reason for the increase in downforce for the diffuser.

Simulation	$-F_z$ **Body/Diffuser**	$-F_z$ **Side Wings**	$-F_z$ **RW**	$-F_z$ **FW**	$-F_z$ **Total**
Baseline	56.1 N	98.6 N	106.8 N	133.3 N	382.8 N
Virtual Wall	59.8 N	110.0 N	104.6 N	133.2	395.0 N

Table 4.18: Results for Diffuser Concept 1 it001

The blowing of the fan seems to do an adequate job but not enough to completely block the wake entering the underfloor, meaning that it can be further optimized. Looking at the numbers in Table 4.18 it seems to do a good job in terms of SW while also keeping FW, RW loss at a minimum.

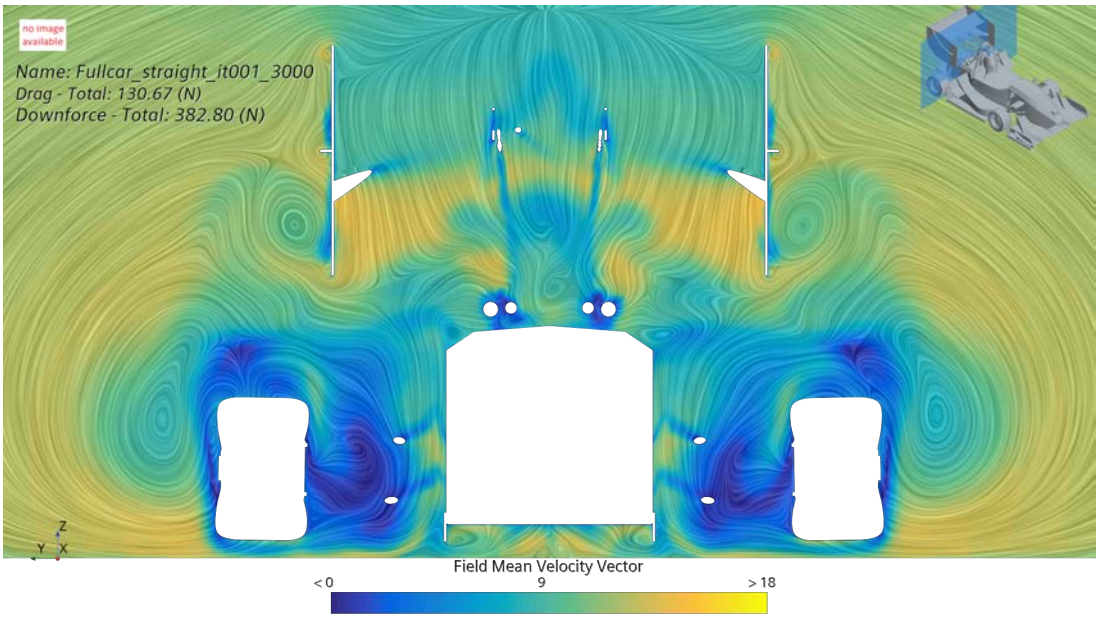

(a) Velocity vector field plot for Baseline at x = 3.0 m plane

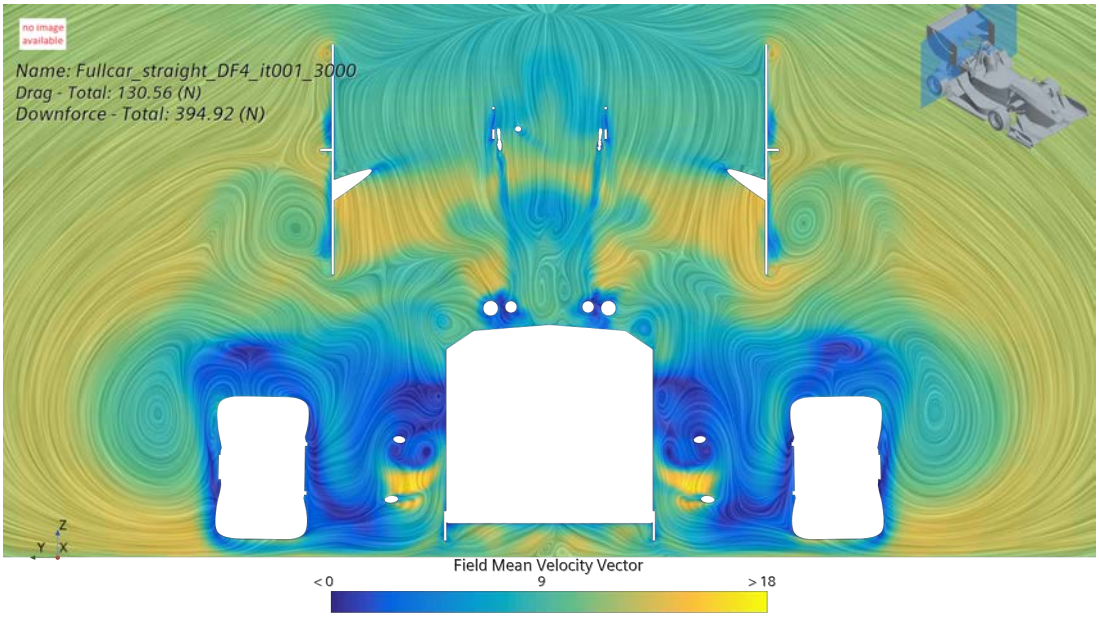

(b) Velocity vector field plot for DF4 it001 at x = 3.0 m plane

Figure 4.42: Velocity vector field plots for Baseline and DF4 it001

4.3.4.2 Iteration 2

For the second iteration on the concept, the target was to redirect the outgoing flow to better achieve the original ambition of creating a seal to the underfloor with a jet of high energy air. This was made by adjusting the angle of the fan-radiator assembly. Having

previously been horizontally placed, they were now angled in a way that the outgoing air was directed downwards as seen in Figure 4.43.

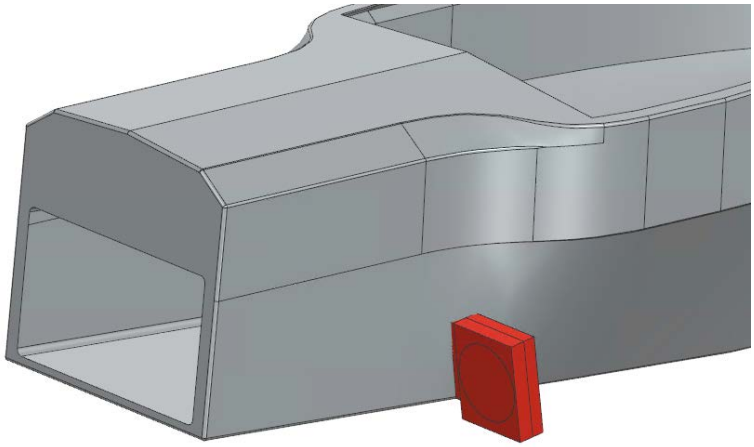

[H]

Figure 4.43: CAD of Diffuser Concept 4, "Virtual Wall" iteration 2

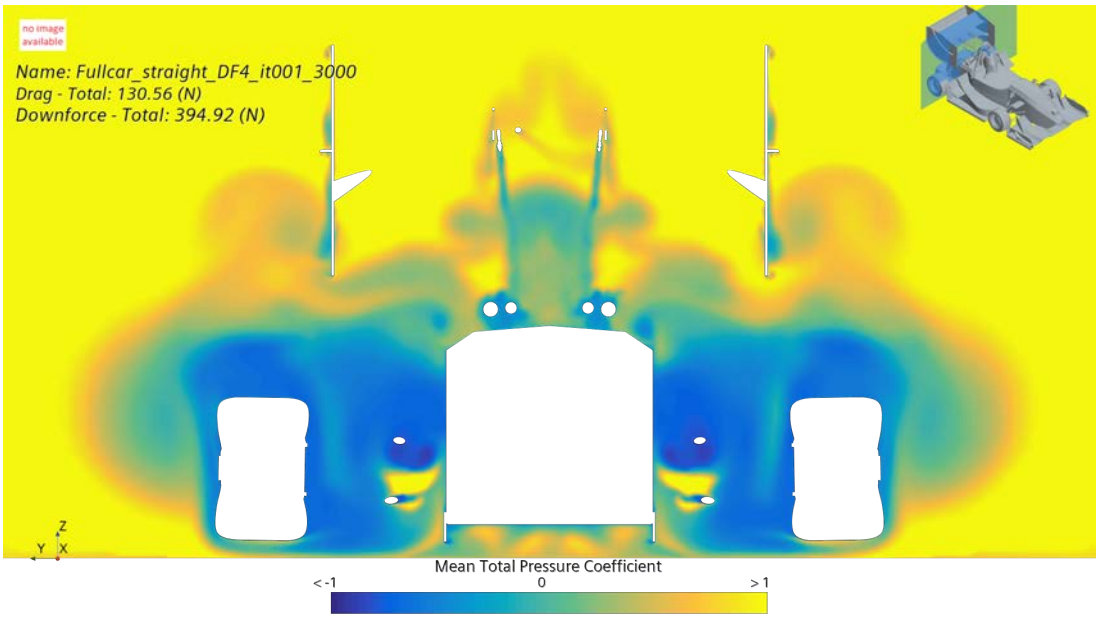

(a) Total Pressure Coefficient plot for DF4 it001 at x = 3.0 m plane

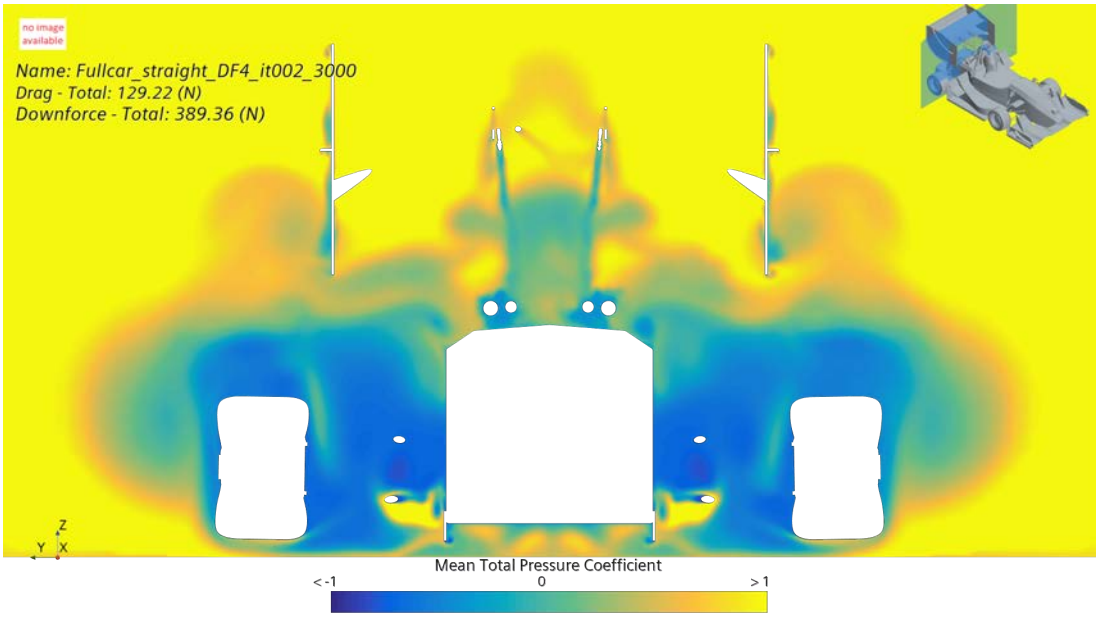

(b) Total Pressure Coefficient plot for DF4 it002 at x = 3.0 m plane

Figure 4.44: Total Pressure Coefficient plots for DF4 it001 and DF4 it002

As concluded in the previous section, the placement of the high energy jet was such that it did not achieve the planned functionality. Comparing Figures 4.44a and 4.44b the outflow direction change of the fan-radiator assembly lowered the placement of the high energy jet slightly, but not to the point that was initially sought after. The ambition remains to place the jet between the ground plane and the lower plane of the monocoque in the

z-direction.

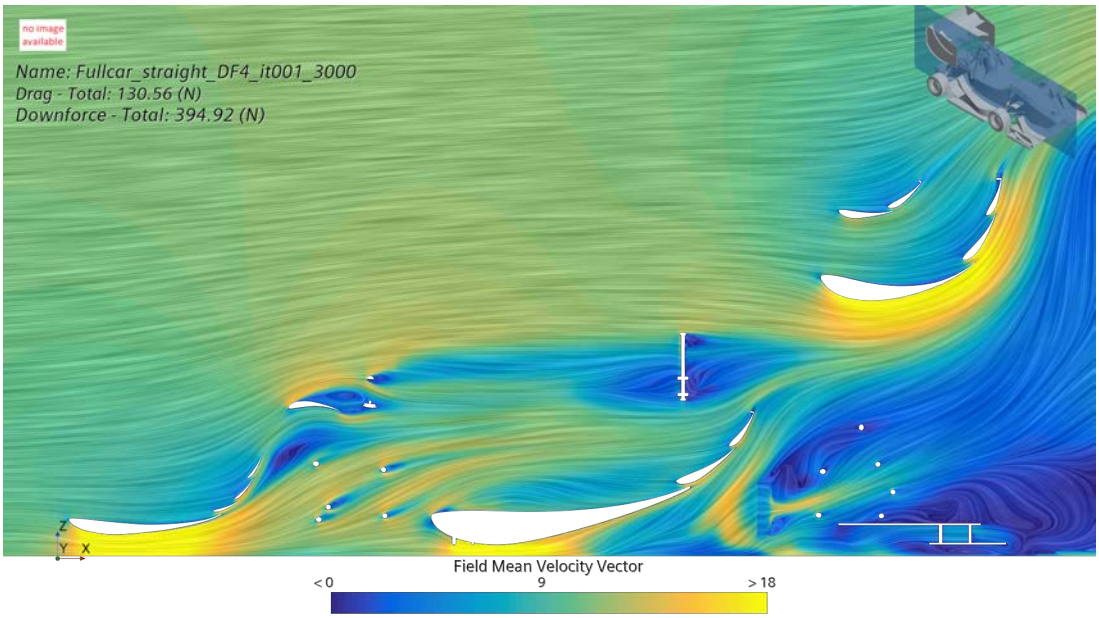

(a) Velocity vector field plot for DF4 it001 at y = 0.350 m plane

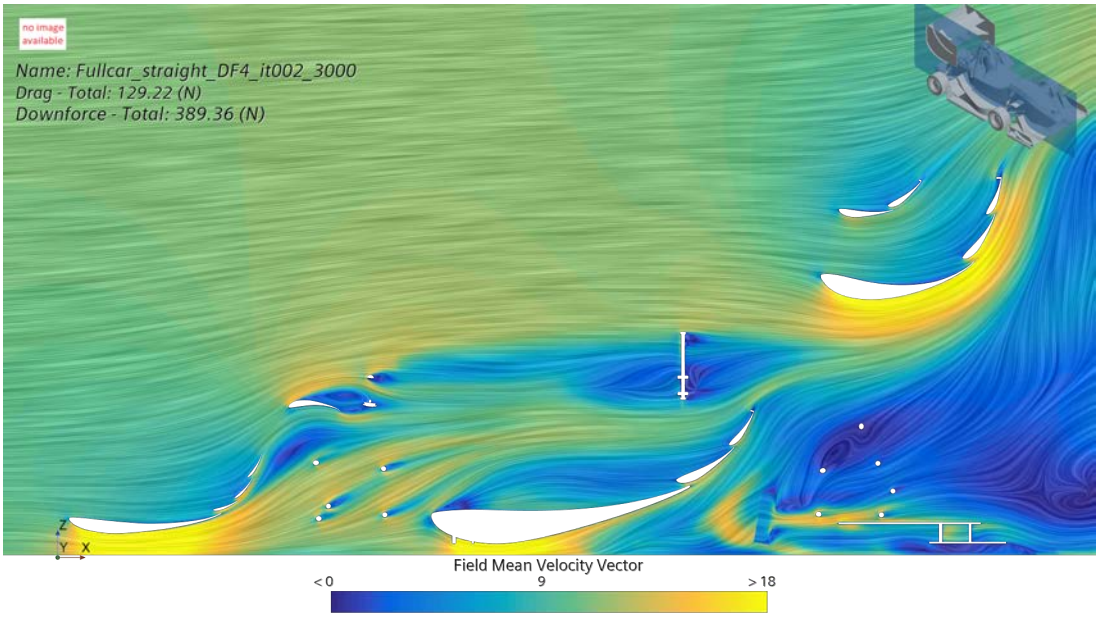

(b) Velocity vector field plot for DF4 it002 at y = 0.350 m plane

Figure 4.45: Velocity vector field plots for DF4 it001 and DF4 it002

Additionally, observing Figures 4.45a and 4.45b it becomes evident that the angle at which the fan-radiator assembly sucks the air affects the flow on several locations around the side wings. Firstly, the fan seems to suck air from the boundary layer of the suction side, meaning that the energy levels are reduced. Due to this, a larger region of recirculation

can be observed on the suction side of the upper side wing flap. Furthermore, a larger separation region on the leading edge of the side wing main segment is observed in Figure 4.45b which could be a result of the overall compromised flow around the side wings.

Simulation	$-F_z$ **Body/Diffuser**	$-F_z$ **Side Wings**	$-F_z$ **RW**	$-F_z$ **FW**	$-F_z$ **Total**
Baseline	56.1 N	98.6 N	106.8 N	133.3 N	382.8N
DF4 it001	59.8 N	110.0 N	104.6 N	133.2 N	394.9 N
DF4 it002	59.4 N	106.8 N	102.4 N	132.6 N	389.4 N

Table 4.19: Results for Diffuser Concept 4 it002

While the overall performance is still increased compared to the baseline, both the overall, and part-specific downforce figures are worse for the second iteration of the concept as seen in Table 4.19. Judging by the previously shown pictures, this is to be expected as the change of outflow angle did not give the sought after results for the outgoing flow. In the meantime, the flow around the side wings was compromised as a result of the alteration. A conclusion from this iteration is that a horizontal inlet angle is to be preferred over the angle in this concept. This means that ducts have to be placed either at the inlet or outlet to manage the objective of the concept and achieve the desired position of the high energy jet. Something which will be tried in coming iterations.

4.4 Rear Wing

In this section, results of concepts and iteration in the Rear Wing region are discussed. The concepts primarily revolved around enhancing the rear wing performance, but proved to have an effect on several other devices.

4.4.1 Concept 1 - RW upwash

The first concept for the RW was based on trying to accelerate the flow on the suction side of the RW flaps. If the fan can be placed at an advantageous position, flow separation can also be delayed. Another intention with the concept was reducing wheel wake leaking into the diffuser. The potential problem with the concept was finding a good position that is good for both cooling and airflow. The decision was made to place them at the rear end of the monocoque as seen in Figure 4.46 below.

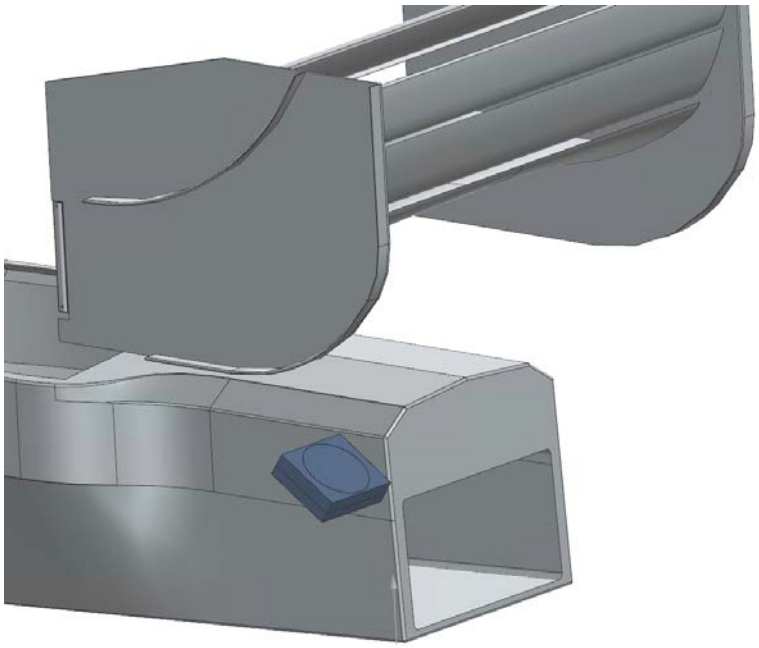

Figure 4.46: CAD of Rear Wing Concept 1, RW upwash

Observing the results in Table 4.20 the overall results are similar in terms of downforce, with a notable decrease in performance on the rear wing. The major parts benefiting are the body/diffuser and the side wings. From the velocity vector field plot in Figure 4.47, the enhanced performance of these parts looks to be a result of the way the fan inlet is directed. The suction is thought to serve a twofold purpose as it could potentially work as an alternative attraction for wake from the rear wheels as opposed to the flow in the diffuser, as well as enhancing the massflow through the side wings. The significant loss on the rear wing however, must imply that the air from the fan is interfering with the flow of the RW and it possibly has to do with the angle of the incoming air. Another theory is that the sucking of the fan is causing more massflow to the inlet of the side wing upstream. Conservation of mass means that if air is being taken from one place it must decrease in another and since little to no surrounding air is introduced it is valid point. The fact that the SW and diffuser is gaining compared to baseline supports the argument that more massflow is being transported to the SW.

Simulation	**-F_z Body/Diffuser**	**-F_z Side Wings**	**-F_z RW**	**-F_z FW**	**-F_z Total**
Baseline	56.1 N	98.6 N	106.8 N	133.3 N	382.8 N
Rearwing Upwash	61.8	111.9 N	87.9 N	132.0 N	381.6 N

Table 4.20: Results for Rear Wing Concept 1

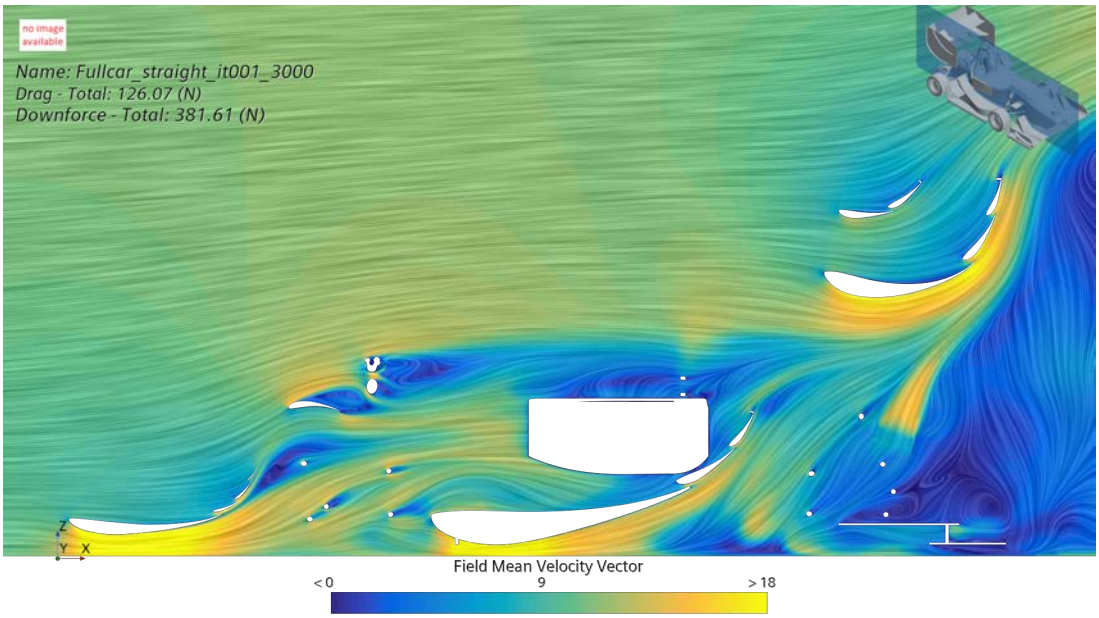

Figure 4.47: Velocity vector field plot for RW1 it001 at y = 0.3 m plane

It can be concluded that the sucking of the fan is doing a good job with reducing wake coming in the diffuser and also helping the SW. Only one iteration for this concept was done since it was not doing what was intended. Instead, it became inspiration for Concept 2 on the rear wing, which will be explained in Section 4.4.2 and here the blowing is done in front of the wing to not disturb the suction side.

4.4.2 Concept 2 - Headrest mounted fan

The second concept for the rear wing was based on mounting the fan and radiator assembly in close proximity to the headrest of the car. Looking at Figure 4.48 showing a Velocity vector field-plot of the baseline in the xy-centerline plane, one can find a relatively large region of stationary air behind the head rest.

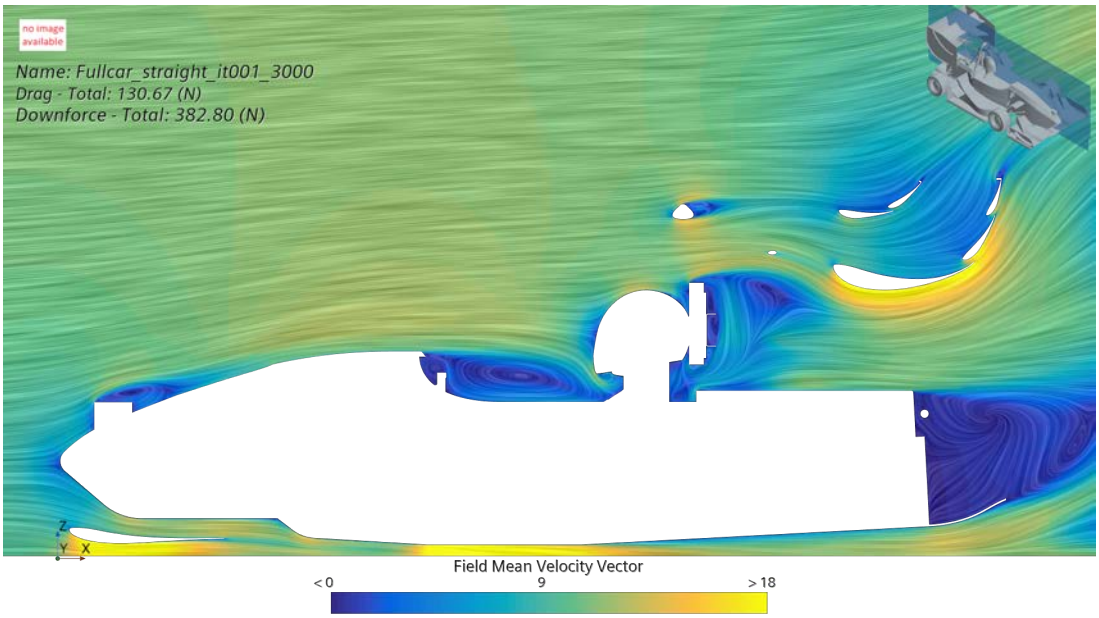

Figure 4.48: Velocity vector field plot for Baseline at y = 0.0 m plane

This is to be expected as the head rest consists of a flat plate with no effort to keep the flow attached behind with something like a cover. The flow is separating from the leading edge of the head rest with the wake region growing in the vertical direction potentially affecting the flow to the main segment of the rear wing. In order to minimize the extent of the wake region, this concept places the fans behind the head rest, with the ambition to eject high energy flow in place of the previous wake.

4.4.2.1 Iteration 1

The geometry of the first iteration can be seen in Figure 4.49 where the inlet duct is placed behind the head rest. Being stacked vertically, the ambition with the placement of the fans was to replace the previously turbulent wake air, with higher energy flow . As the flow coming of the head rest directly affects that of the rear wing main segment, increasing the energy in the flow was thought to benefit the performance of the rear wing. The inlet duct was designed in a way that it complied with the geometrical constraints of the region, while allowing for air to enter through the sides and top section. Additionally a diffuser-like inlet was added inside the duct behind the head rest in order to slow down the incoming flow in a controlled manner before it reached the radiator.

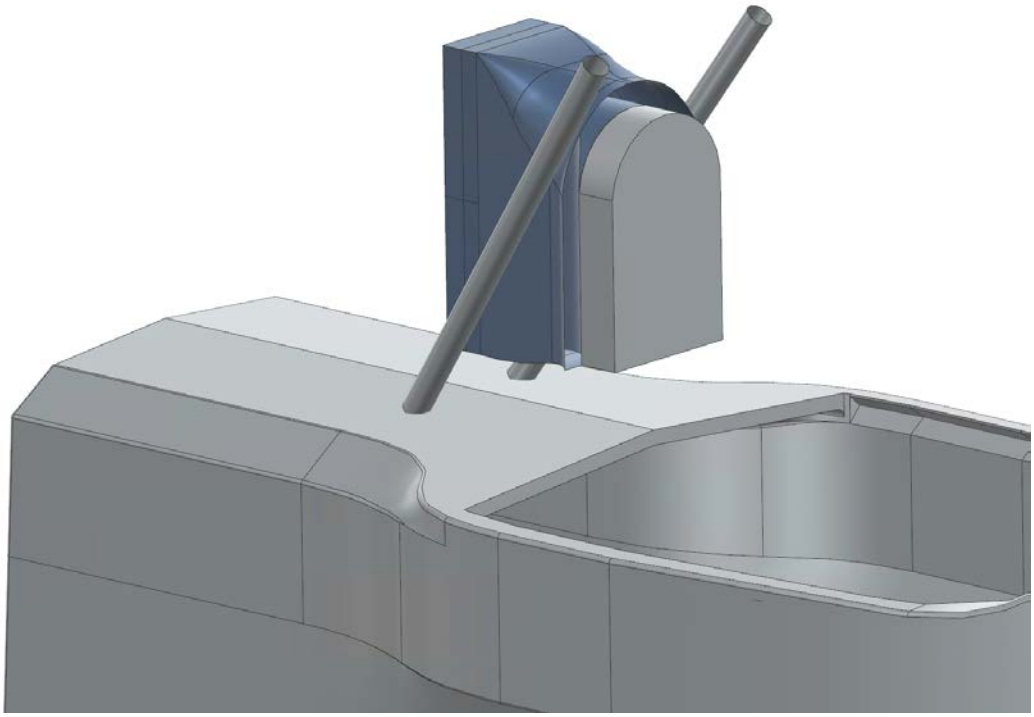

Figure 4.49: CAD of Rear Wing Concept 2 Iteration 1

Simulation	**-F_z Body/Diffuser**	**-F_z Side Wings**	**-F_z RW**	**-F_z FW**	**-F_z Total**
Baseline	56.1 N	98.6 N	106.8 N	133.3 N	382.8 N
RW2 it001	57.5 N	103.9 N	95.7 N	131.7 N	377.2 N

Table 4.21: Results for Rear Wing Concept 2 it001

Looking at the losses from the head rest region in Figure 4.50 one finds that while the top fan injects high energy air in the boundary layer of the rear wing main segment, a region of total pressure losses occurs between the outlet flows of the two fans. Judging by the figures, this means that the energy from the lower fan is not utilized by the rear wing to the same extent, and is just adding energy to a region where it is not utilized by another aerodynamic device. Furthermore it can be seen that the topmost part of the rear facing surface of the fan-radiator assembly causes some losses. In both cases this is thought to be caused by the fact that the fan outlets do not cover the entire surface. This means that only a limited part of the surface ejects energy to the flow, and the extent to which the energized flow mix with the other flow coming of the rear facing surface seems to be relatively low. Looking at Table 4.21 the iteration caused the rear wing to lose approximately 11% of its downforce, while the overall loss was around 0.4% compared to the baseline.

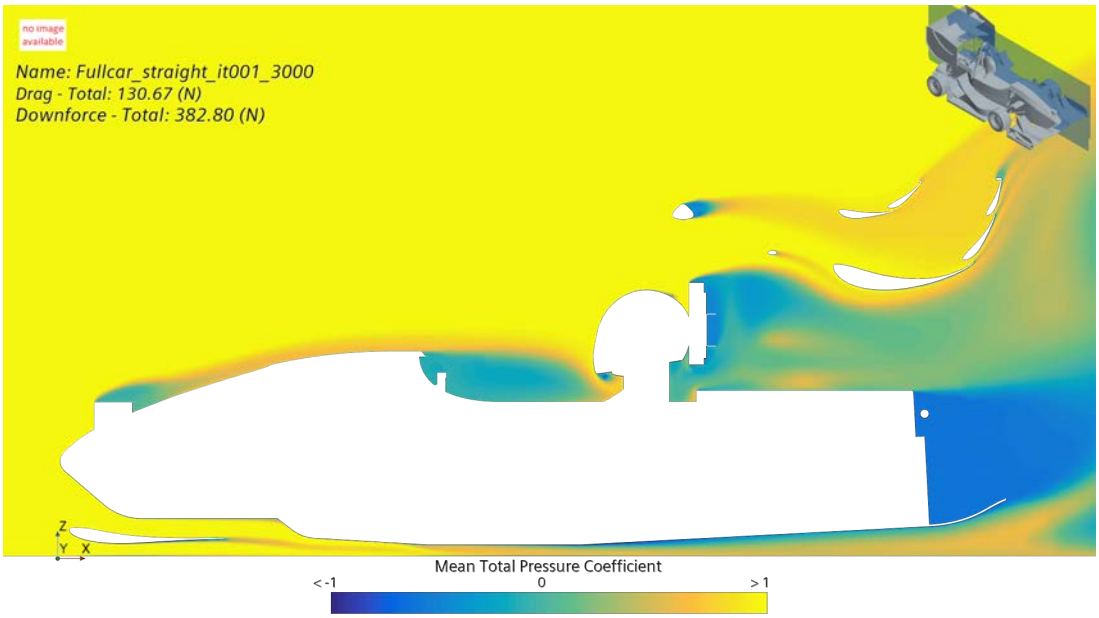

(a) Pressure Coefficient plot for Baseline at y = 0.0 m plane

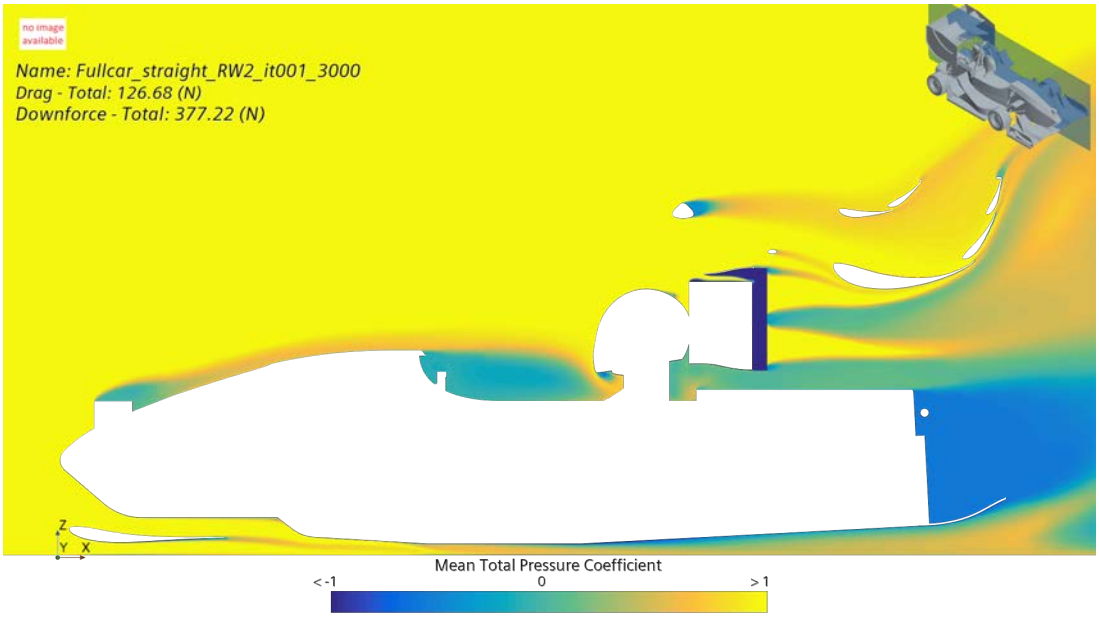

(b) Pressure Coefficient plot for RW2 it002 at y = 0.0 m plane

Figure 4.50: Pressure Coefficient plots for Baseline and RW2 it001

While the performance of the initial iteration on the concept was worse compared to the baseline, it was seen as a good starting point for further development. The isolated rear wing downforce figures were worse looking at Table 4.21, and so were the overall downforce figures. Other than some losses from the fans themselves, one potential cause for the the lack of performance was thought to be the relative blockage that the new

assembly caused to the oncoming airflow to the rear wing main segment. While the duct made up for some of the blockage by sucking air at the top most part and ejecting it through the fan, the following vertical expansion in the front duct, and the height-wise placement of the fan-radiator assembly could be acting as a blockade for the oncoming flow and prevent ambient flow of high total pressure to enter the suction side of the rear wing main segment. Additionally, the direction of the outgoing air from the lower fan was thought to be of no real benefit to the overall performance.

4.4.2.2 Iteration 2

To address some of the previously mentioned problems with the first iteration on the concept, a rear duct was added with two major ambitions. The first of which being to concentrate the flow coming of the rearmost part of the fan-radiator assembly and design the duct in such a way that the low energy flow from the regions outside the fan outlets, can mix with the high energy air from the fans. With this, the thought was to have an outlet without the regions of losses seen in the first iteration. The second ambition was to manage the angle at which the outgoing flow was interacting with the boundary layer of the rear wing main segment. Knowing that this part of the flow is a sensitive to changes and a decisive factor in the functionality of the rear wing, it was thought that some degree of iterative work was needed to perfect the functionality of the concept, but that the iteration in this case rather aimed at evaluating the core functionality of the outlet concept.

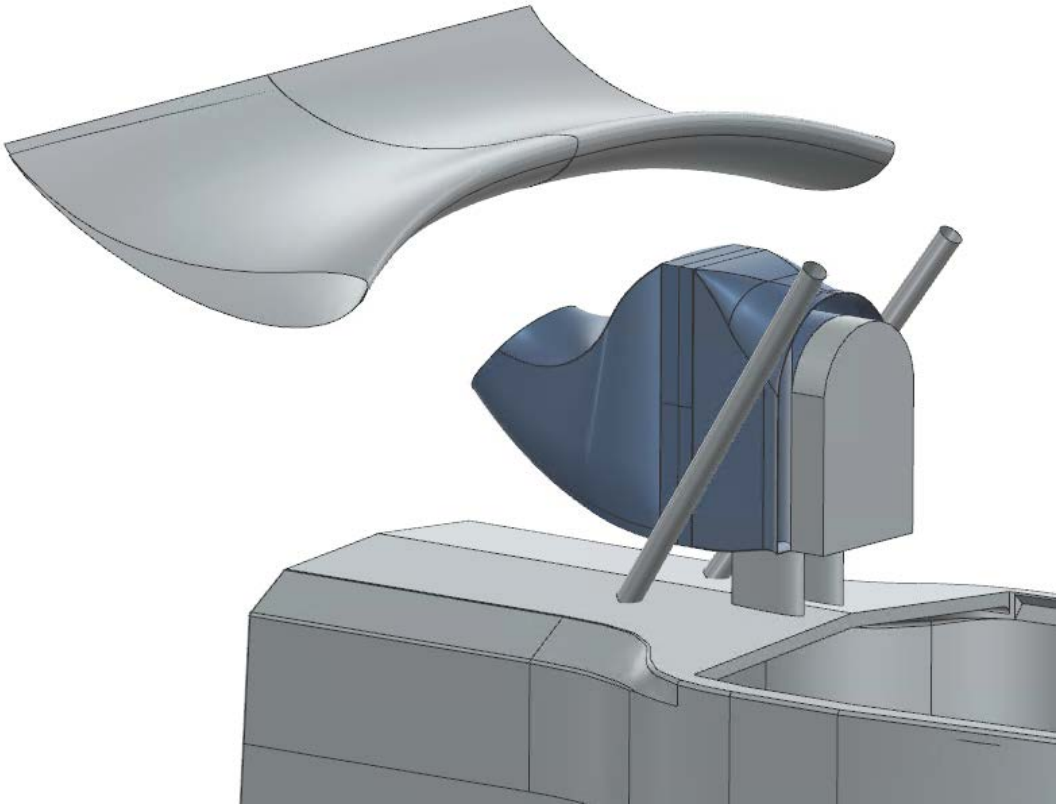

Figure 4.51: CAD of Rear Wing Concept 2 Iteration 2

Simulation	**-F_z Body/Diffuser**	**-F_z Side Wings**	**-F_z RW**	**-F_z FW**	**-F_z Total**
Baseline	65.1 N	98.6 N	106.8 N	133.3 N	382.8 N
RW2 it001	57.5 N	103.9 N	95.7 N	131.7 N	377.2 N
RW2 it002	60.3N	105.9 N	95.0 N	131.7 N	381.3 N

Table 4.22: Results for Rear Wing Concept 2 it002

When looking at Figures 4.52 and 4.53, it can be concluded that the ambition of merging the fan's outflow was achieved and that the mixing of the turbulent air worked as expected. With that, the air entering the boundary layer is mostly free of turbulence as seen in Figure 4.53. From the same figure, it's also noted that the duct combats the wake that was previously coming of the fan-radiator assembly. With all this being said, the introduction of the strong jet of high energy air seems to affect the regular airflow going to the suction side of the main segment, where a larger region of stagnated flow on the leading edge is noted in Figure 4.52 as compared to the baseline. The disturbance to the regular flow is confirmed by slightly lower downforce figures for this iteration as compared to the first.

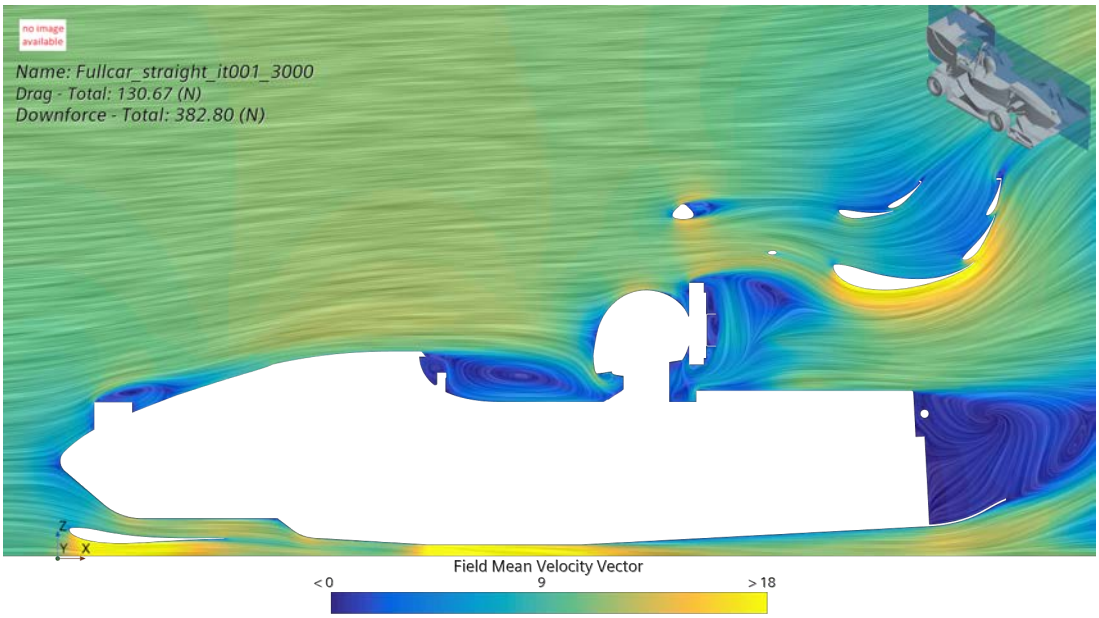

(a) Velocity vector field plot for Baseline at y = 0.0 m plane

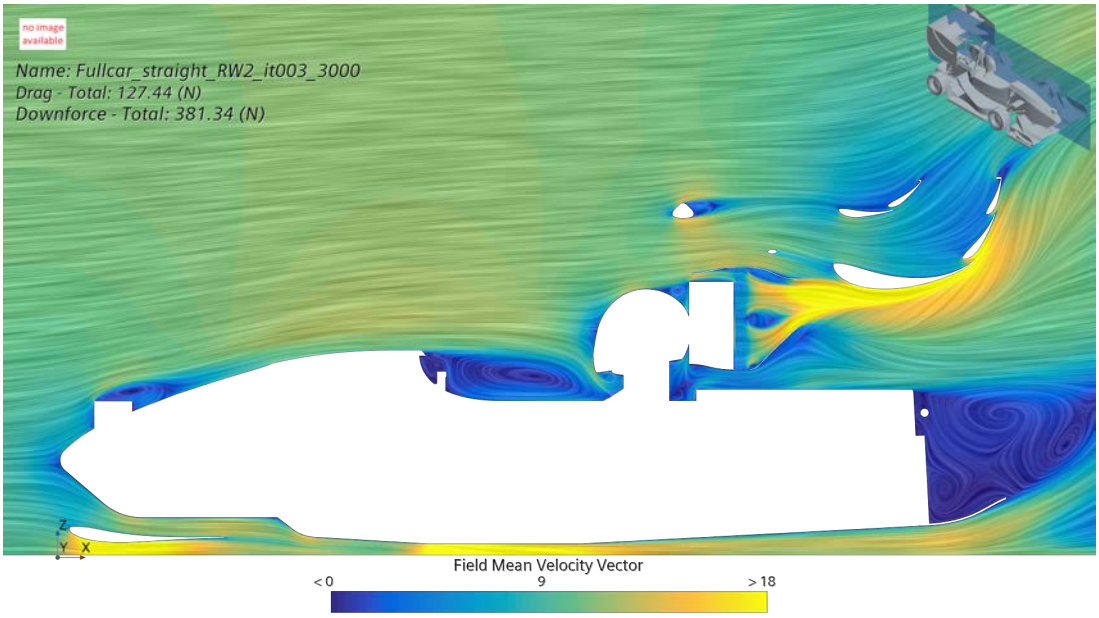

(b) Velocity vector field plot for RW2 it002 at y = 0.0 m plane

Figure 4.52: Velocity vector field plots for Baseline and RW2 it002

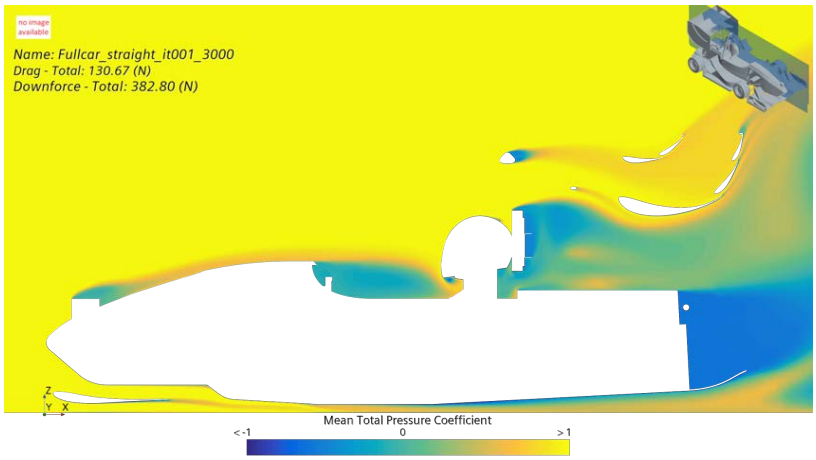

(a) Total Pressure Coefficient plot for Baseline at y = 0.0 m plane

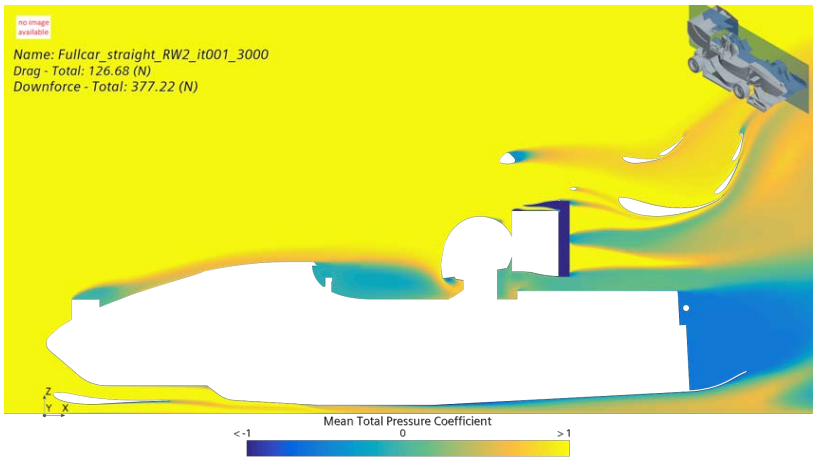

(b) Total Pressure Coefficient plot for RW2 it001 at y = 0.0 m plane

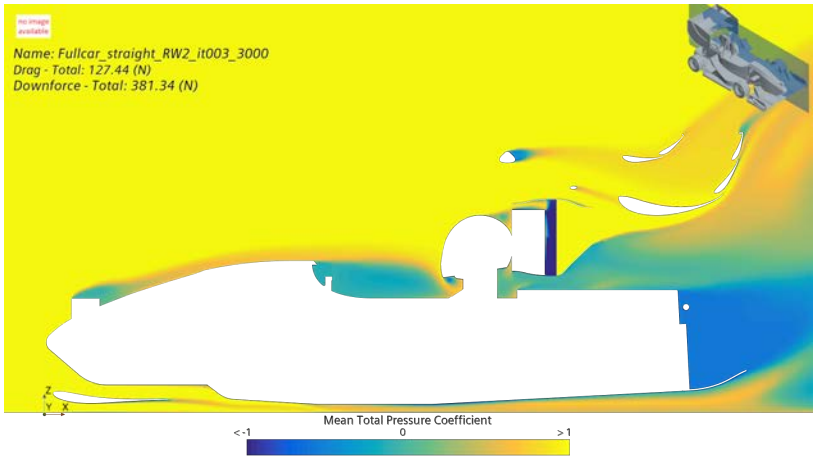

(c) Total Pressure Coefficient plot for RW2 it002 at y = 0.0 m plane

Figure 4.53: Total Pressure Coefficient plots for Baseline, RW2 it001 and RW2 it002

Although the quality of the outgoing air from the fan-radiator is improved in terms of losses, the introduction of a rear duct highlights the rear wing main segment's sensitivity to disturbances. Comparing the region's pressure fields in Figure 4.54, the disturbances in the pressure field on the suction side of the main segment become apparent, especially on the leading edge. One conclusion from the previous iteration was the disturbance on the main segment flow as a consequence of the hight wise placement of the assembly. Having not adjusted the vertical position of the assembly, this iteration further shows a sensitivity to disturbance in the longitudinal direction. Repositioning the assembly while keeping within the geometrical constraints in the region will be the primary target for coming iterations.

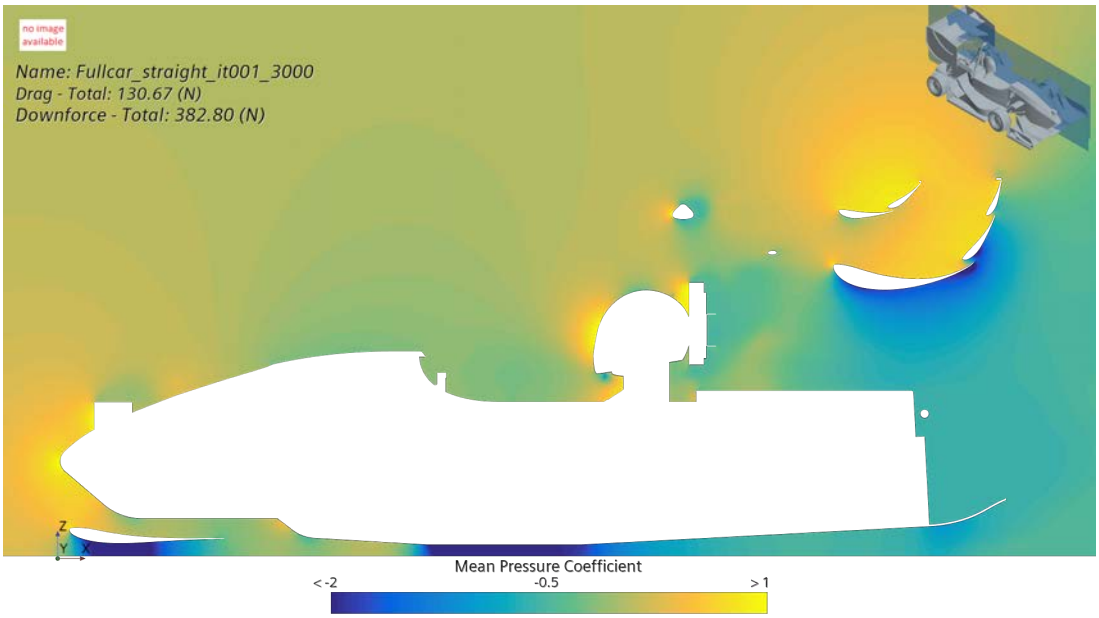

(a) Pressure Coefficient plot for Baseline at y = 0.0 plane

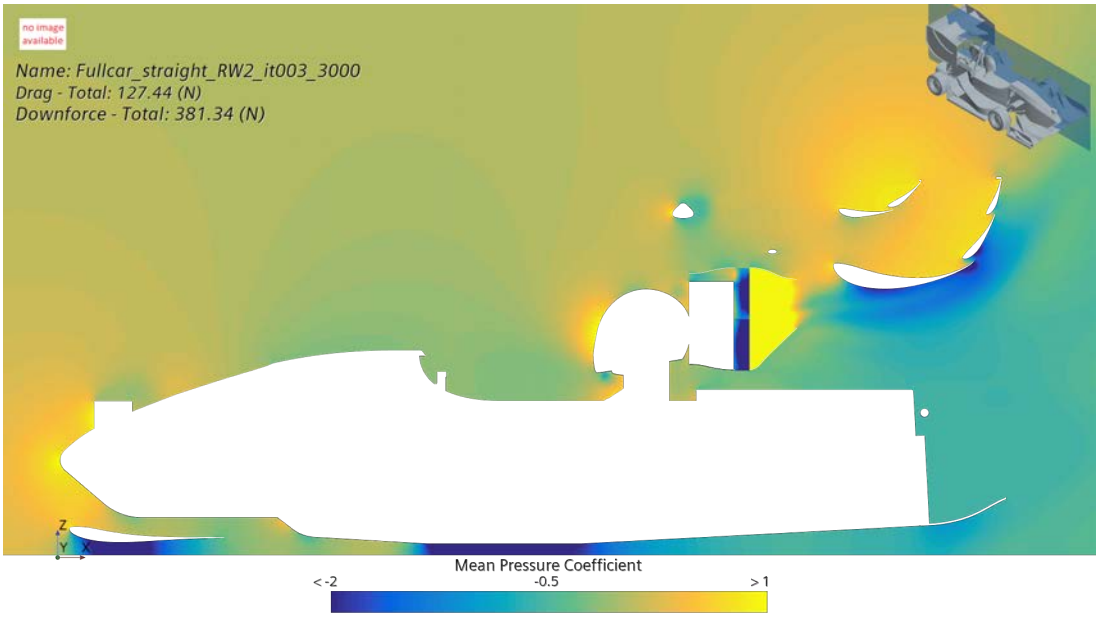

(b) Pressure Coefficient plot for RW2 it002 at y = 0.0 m plane

Figure 4.54: Pressure Coefficient plots for Baseline and RW2 it002

While thought to be effective, another conclusion of the concept is that directly injecting high energy air in the flow on the suction side of the main segment in the way that a duct of this design does, is of no real benefit to the performance of the rear wing. This is proven by the numbers in Table 4.22 showing slightly worse numbers for the rear wing compared to the previous iteration, and significantly worse numbers compared to the

baseline. Comparing the pressure fields in Figure 4.54 once again, no distinct difference in terms of lower overall pressure is observed. Additionally, no major separation occurs in the baseline as seen in Figure 4.50a meaning that the need for extra energy in the boundary layer even for the top flap is minimal.

4.4.2.3 Iteration 3

As the previous iteration proved the direct injection of high energy air in the boundary layer of the main segment to be of no real use, the third iteration on the concept introduced multiple changes. To combat the previous issues of the assembly disturbing the flow to the main segment, the suction region of the front duct was adjusted so that the side and bottom parts of the duct formed the major suction regions. The top-most surface of the duct was made tangent with the head rest resulting in no additional vertical blockage of air going to the main segment. In the longitudinal direction, the front-most plane of the frontal duct was made tangent with the front surface of the head rest to allow for more clearance between the rear duct and the main segment.

For the rear duct, the outlet was relocated further down and its direction adjusted to be horizontal. Additionally, a wing element was added downstream of the outlet with a relatively steep AoA. The ambition being to redirect the majority of the high energy air to the boundary layer of the top flaps where the pressure differential between the suction and pressure sides is not as prominent. This, in addition to the local downforce generated by the winglet element. Working in a region of aggressive upwash, in addition to the high energy airflow from the fans, it was thought that the winglet would manage the high AoA's without separating. The final design of the concept can be seen in Figure 4.55

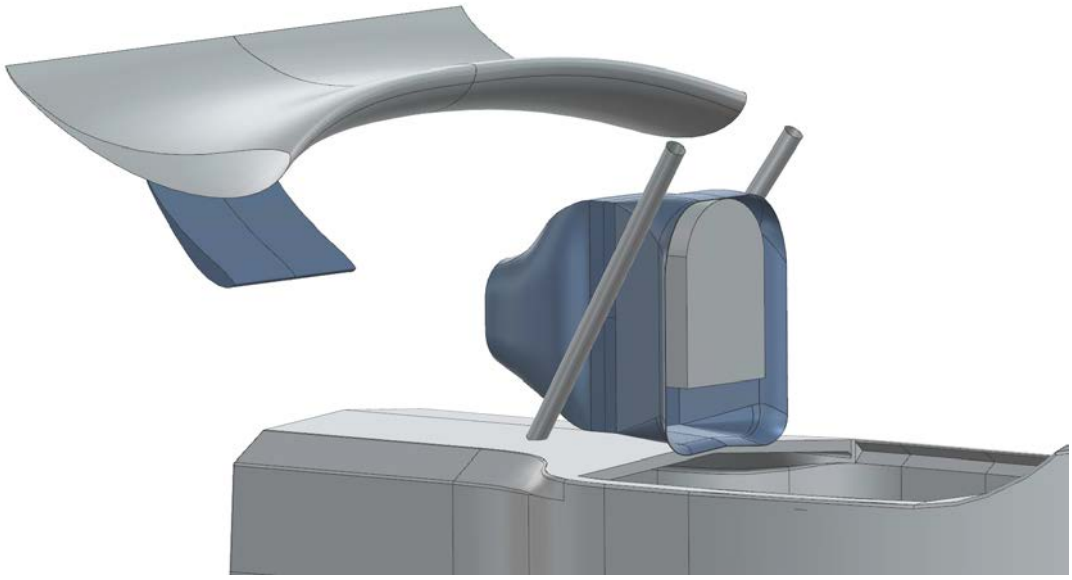

Figure 4.55: CAD of Rear wing Concept 2 Iteration 3

Simulation	-F_z Body/Diffuser	-F_z Side Wings	-F_z RW	-F_z FW	-F_z Total
Baseline	56.1 N	98.6 N	106.8 N	133.3N	382.8 N
RW2 it001	57.5 N	103.9 N	95.7 N	131.7 N	377.2 N
RW2 it002	60.3 N	105.9 N	95.0 N	131.7 N	381.3 N
RW2 it003	60.0 N	104.5 N	101.5 N	132.4 N	386.9 N

Table 4.23: Results for Rear Wing Concept 2 it003

Looking at Figure 4.57, it is observed that the added wing element successfully deflects the outgoing air as previously ambitioned. Knowing that the ideal way in which to deflect the air requires some iterative work, this is seen as an adequate demonstration of the concept's capability. While the steep downwash on the top of the rear duct amounts to some losses, it is thought to made up for by the increased distance to the rear wing main segment. This thought is further cemented when following the direction of the flow in Figure 4.56 where it to a larger extent follows the perimeter of the main segment suction side as compared to Figure 4.52. Additionally, the previously mentioned enlarged stagnation region on the leading edge of the main segment that could be seen in the previous iteration, has now reverted to a similar position and size compared to that of the baseline, where the wing was working in less disturbed airflow. This is signaling that the revised position of the rear duct has improved and/or restored the functionality of the wing as compared to the previous iteration.

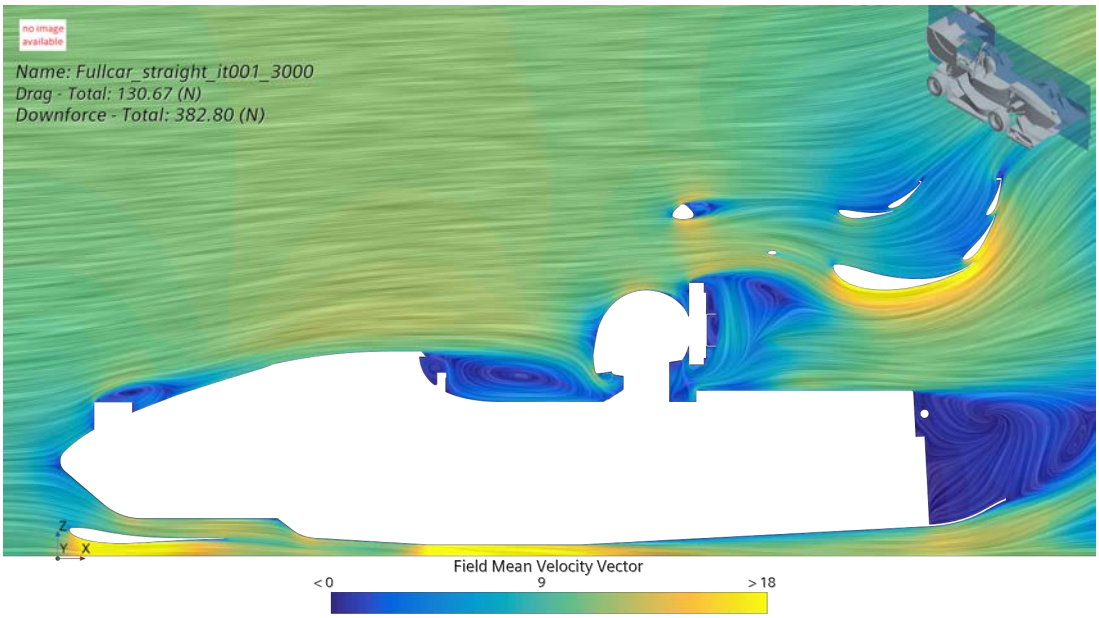

(a) Velocity vector field plot for Baseline at y = 0.0 m plane

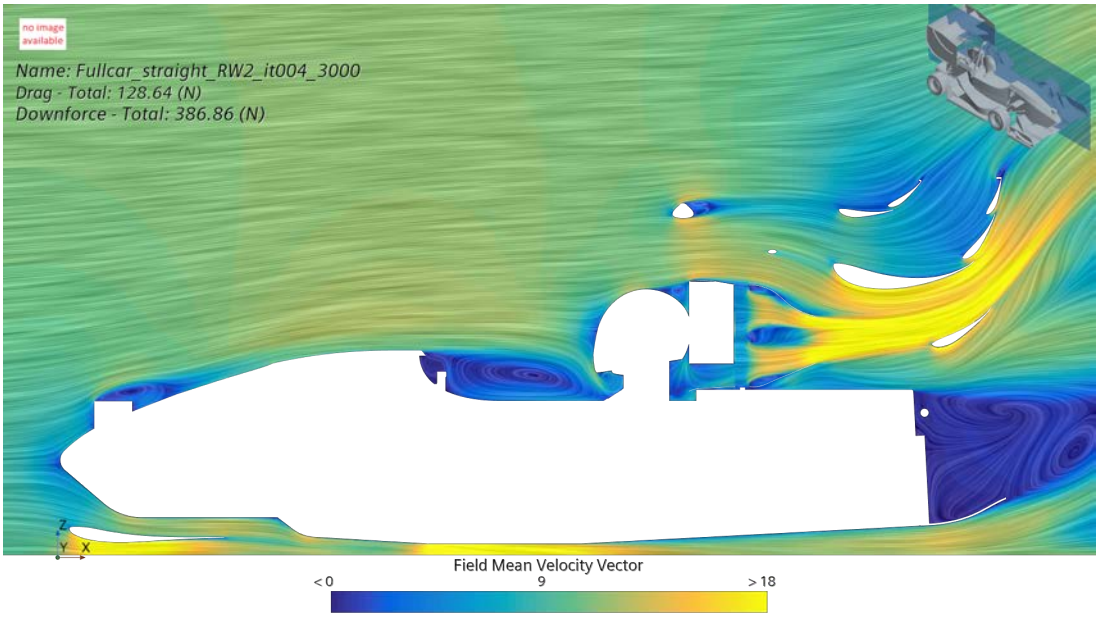

(b) Velocity vector field plot for RW2 it003 at y = 0.0 m plane

Figure 4.56: Velocity vector field plots for Baseline and RW2 it003

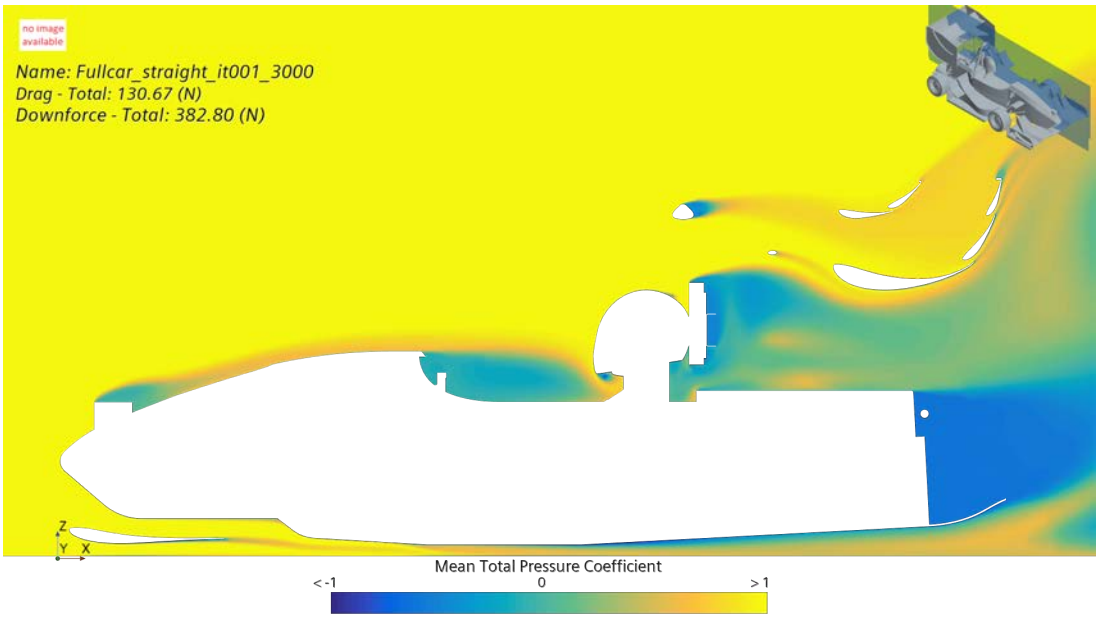

(a) Total Pressure Coefficient plot for Baseline at y = 0.0 m plane

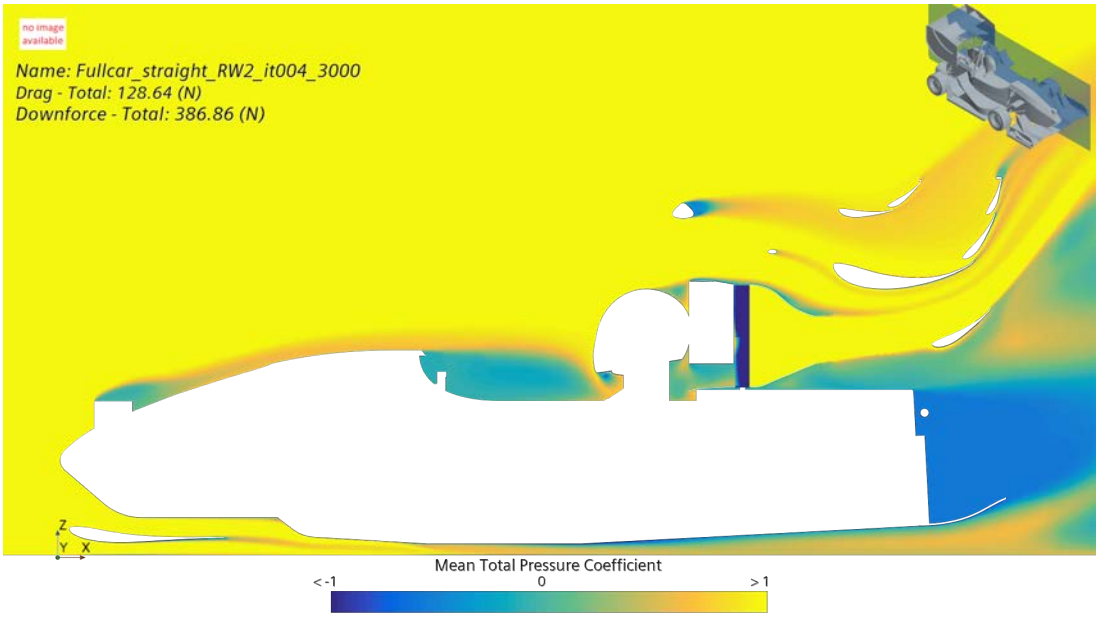

(b) Total Pressure Coefficient plot for RW2 it003 at y = 0.0 m plane

Figure 4.57: Total Pressure Coefficient plots for Baseline and RW2 it003

As previously shown, the rear wing is functioning relatively well even without the added energy from a fan outlet. This point is further proven when looking at the pressure distribution of the rear wing on the baseline compared to the current iteration in Figure 4.58. While the added wing element in itself is adding some degree of downforce to the overall rear wing package by the pressure difference it experiences on its suction and

pressure side, the magnitude and spread of the low pressure region on the suction side of the main segment is relatively similar. This means that while further improvements to the existing rear wing geometry seems to be difficult to achieve with the fans, their added energy to the airflow behind the driver and head rest could potentially allow for implementation of new wing pieces to the existing package without majorly affecting the existing devices.

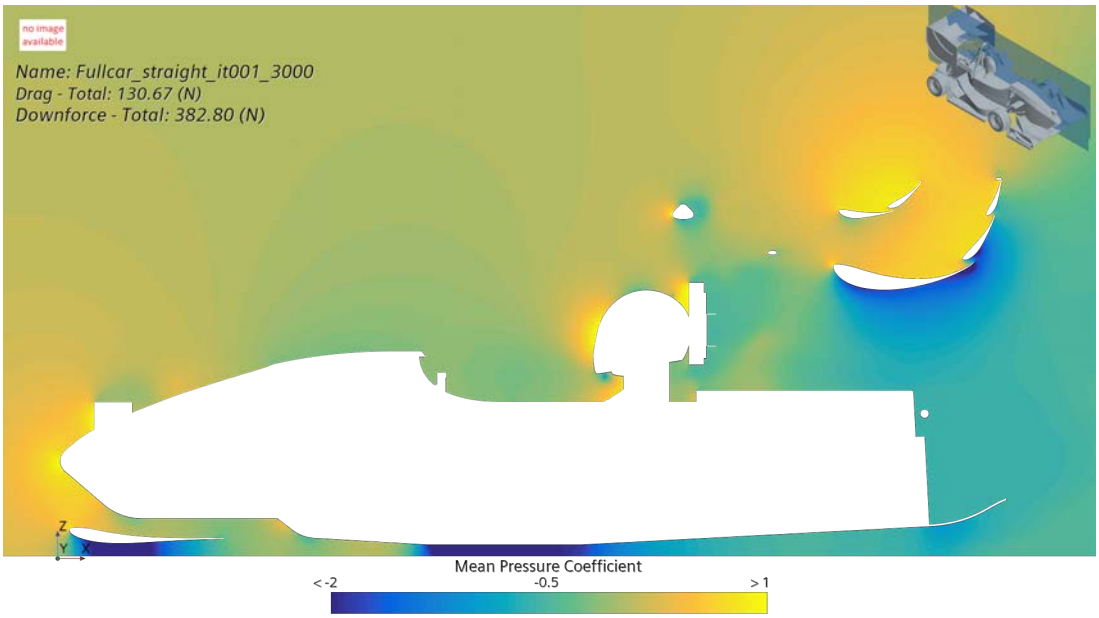

(a) Pressure Coefficient plot for Baseline at y = 0.0 m plane

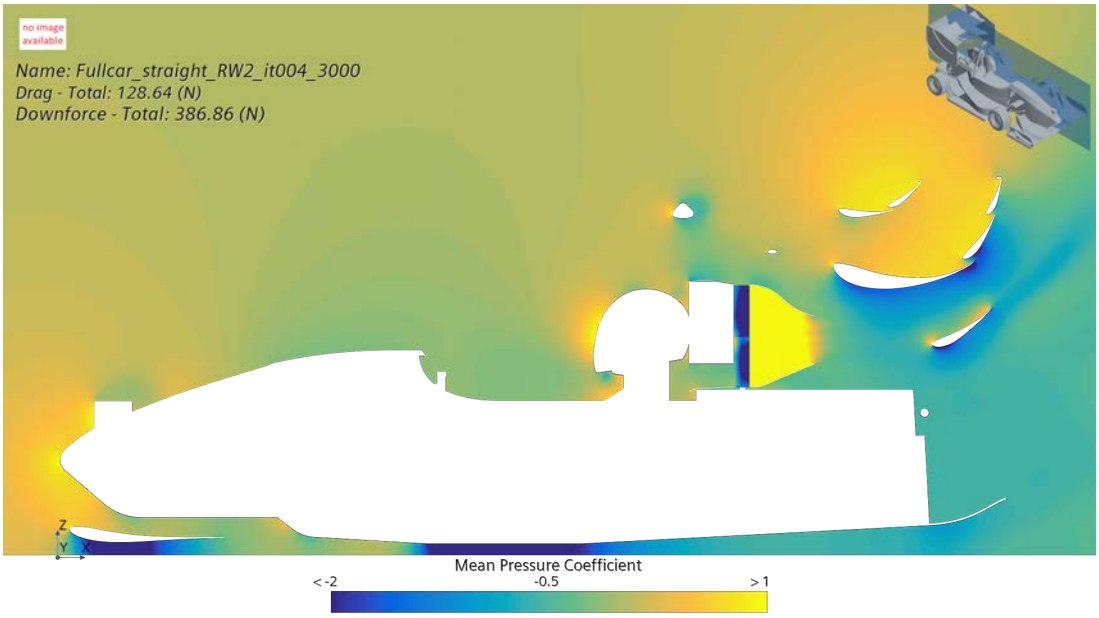

(b) Pressure Coefficient plot for RW2 it002 at y = 0.0 m plane

Figure 4.58: Pressure Coefficient plots for Baseline and RW2 it003

Finally it can be concluded that the revised duct geometry allowed for more flow to the main segment with less disturbance. The ducts kept to the geometrical constraints of the region, while maintaining an outlet jet of high energy air to the surrounding airflow. Looking at Table 4.23 the performance of the rear wing is still worse compared to the baseline. It should be noted however, that the downforce from the added winglet is

not counted towards the rear wing downforce number in this case and only to the total downforce. While the airflow to the rear wing for the iteration looks to be similar to that of the baseline, the loss of rear wing performance further shows its sensitivity to changes in the region. Simultaneously though, the overall downforce is still increased compared to the baseline with the underfloor and diffuser gaining the most. This could be a consequence of the added winglet as it introduces a strong upwash in the region between the rear wing and diffuser which in turn might affect the air exiting the diffuser and prolongs flow attachment.

5
Overall Discussion

While the previous section was centered around result and discussion of individual concepts and iterations, this section will in broader terms discuss fan placement in the different specified geometric regions. Trends and similarities observed between concepts in the regions, as well as conditions for fan placement will be the main focal points.

5.1 Front Wing

This section is based upon the results and discussions in Section 4.1. Despite designing and simulating four front wing concepts, one of which having three iterations, very few positive results were found. As explained in Section 3.1.1, there were initial doubts about the front wing's potential. These doubts were proven correct, but the results can be used for learning and to exclude the front wing from further developments.

There were a few main issues with most front wing concepts that hindered potential performance. The lack of space was a big issue for all concepts designed in this study. This led to potentially good concepts having to be scrapped due to the lack of space for the fans and radiators, as these required a certain size. This caused the radiators and fans having to be placed in undesired areas to be able to design the concept. This led to the fan and radiator package being placed too close to the suction side of the front wing in concept 1 and 2. On both occasions, this meant that the flaps stalled and therefore lost downforce. It also meant that some negative effects on concept 4 it003 were observed. Several front wing concepts rely on the concept of outwashing. This is a concept commonly used on formula cars with larger wheelbases. As described in Section 4.1.3, those concepts focus on outwash causing a suction effect on ambient air and therefore the idea is to improve performance with the newly introduced air. The short wheelbase of a formula student car proved to be too short for the achieved pressure difference to be able to cause enough suction on the ambient air. However, there were a main issue that plagued not only every concept but the idea of a fan on the front wing itself. The concept of using a fan to enhance aerodynamic performance is to inject energy into the air and therefore be able to increase to downforce. As explained in Section 2.4.1, the front wing always receives clean energized air. This means that there is a very marginal gain in energy that can be introduced into the airflow. Since there are several areas further downstream that lack energized air, the fans could be better utilized in other areas. Therefore, there are no reasons to further develop any front wing concepts mentioned in Section 4.1 and probably no other concepts either, as they have too many fundamental issues. See the results compared to the baseline in Figure 5.1 below.

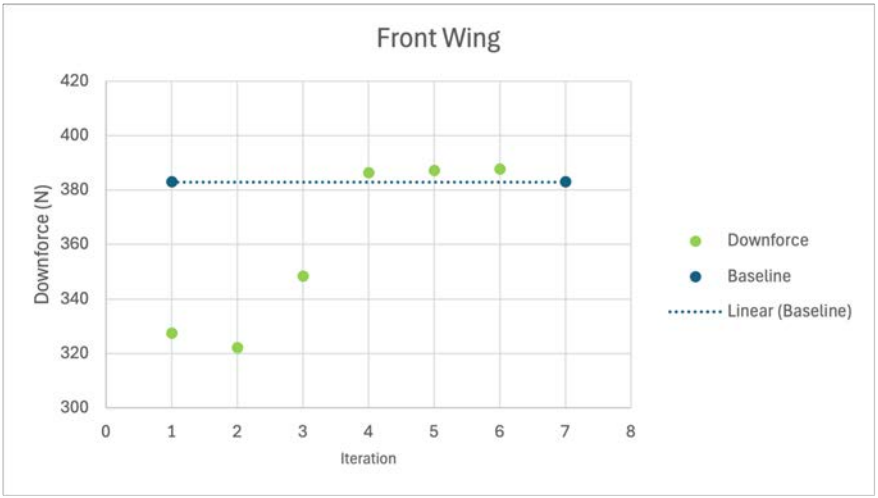

Figure 5.1: Plot of Total Downforce Results for all conducted simulations on the Front wing

The mass flow through the radiator was generally slightly below the value achieved by the CFS current solution. However, since the downforce produced by the front wing concepts was not large enough to allow implementation on the real car, no changes were required.

5.2 Side wings

This section is based upon the results and discussions in Section 4.2. In general, the results from the side wing concepts were positive with a net gain in downforce from most concepts and iteration. Figure 5.2 shows the results in terms of total downforce for all iterations on the different side wing concepts.

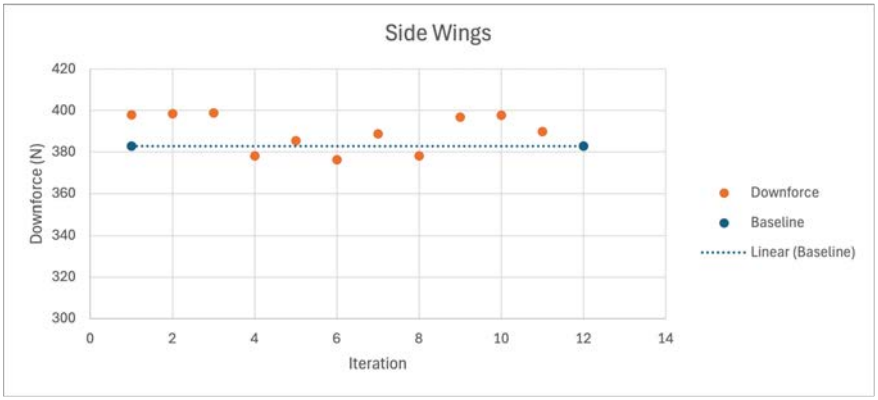

Figure 5.2: Plot of Total Downforce Results for all conducted simulations on the Side Wings

The side wings consists of two multi element wings on each side of the car located close to the ground. While the concept functions without the addition of fans, increasing the

mass flow through the wing was thought to constitute an opportunity to enhance the performance of the component. Additionally, when having no limit on the power for fans, this was the preferred method for other teams to increase the downforce of the vehicle. The results of concept 2 as well as the results from the first iteration of concept 4 for the diffuser, showed that the method could still prove to be beneficial. While not as powerful as previously without the fan power limit, it's still a viable option for fan implementation. One flow pattern observed throughout the various concepts and iterations was the in-wash along the outside of the side wing main segment, behind the front wheels, which turned out to be crucial for the performance of the side wings. This could be seen when altering the angle of the fans in concept 3 where outwahsing air
Something about the synnergy between the floor and the side wings
Two of the concepts, concept 1 and concept 3 saw a significant gain in downforce with concept 3 seeing a small gain after the second iteration. Concept 4 was the only concept where no gain was visible. The simulations of concept 4 did not show any sign of the desired effects, hence no further iterations were made. Concept 2 however saw a negative effect on the performance after the first iteration but flaws of the implementation were clearly visible in the pictures extracted from the simulation hence a second iteration was made. The second iteration did not show as large of a performance advantage as expected or desired but there were no clear flaws to the implementation of the concept, although optimization could be made in order to reach further performance benefits in terms of downforce. A plausible reason to the lack of performance from concept 2 could simply be the lack of power. The concept was thought to be a concept with high potential but the gained performance was limited.

The two high-performing concepts were concepts 1 and 3 were concept 1 is the currently implemented concept on the Chalmers Formula Student car and concept 3 made use of the stagnated air in the front tyre wake. The performance increase from concept 3 was higher than expected and was partly due to being well integrated with the other parts of the car, showing an increase in downforce in both the diffuser, front wing and side wings. A simplified version of a concept 5 was also simulated, testing a combination of concepts 1 and 3. The simulation showed a minimal decrease in performance from the two individual concepts, showing that a well implemented concept has potential of gaining more performance. Lastly, the rear wing has shown to be very sensitive to change in airflow around the side wings. The rear wing saw negative effects in downforce from every side wing concept.
Additionally, all of the side wing concepts mentioned above complied with the by CFS specified requirement for airflow through the radiators, implying that they are all viable for implementation in that regard.

5.3 Diffuser

Overall the results from the diffuser look promising. Four concepts were made in total, where three of them attempted to increase the expansion ratio with help from the fan. The last one was an attempt at sealing the underfloor and maintaining a low pressure. A majority of the concepts saw an increase in SW performance while the diffuser had minimal gain in downforce (between 1.6% and 6.6%). This might sound surprising but it

should be mentioned that the flow around an aerodynamic package is complex and it can sometimes be hard to look at components individually. Looking at any of the pressure plots of the floor, like the ones in Figure 4.37, it becomes evident that the regions of lowest pressure for the side wing and the underfloor coincide. While not totally unexpected, this implies that an effort to lower the pressure in the underfloor most likely also will affect the lowest pressure of the side wings. A point further cemented when more carefully comparing the two pressure plots in Figure 4.37, where the added suction from the fans on the diffuser largely affects both components.

Concepts 1, 2, and 3 for the diffuser were all based on the diffuser it004 expansion ratio (see Table 4.14). This is something to build on since it is in no way optimized and it was made with limited knowledge. The concept with the most downforce was concept 1 "Suction to increase expansion" with 395.7 N. Only one iteration of this concept was made so its safe to say that it can be further optimized. Concept 4 "Virtual Wall" was another interesting concept that came close with 394.9 N but it proved to be a challenge to further optimize the initial iteration, which in its initial state could be seen as more of a side wing concept. Concept 2 "Suction to increase expansion with upward flow" was in a way a development of concept 1 but it failed somewhat in what it was intended to do, which was to help the RW. These concepts were in turn similar to concept 4 on the front wing, all aimed at lowering the pressure in the underfloor. While the front wing concept aimed at pushing air through the floor, the main objective was still the same. Placing the fan-radiator assembly upstream had some effects on the airflow though, as the geometry of the assembly meant some losses coming of it and entering the floor. As the diffuser concepts placed the fans downstream on top of the diffuser out of the underfloor flow, utilizing suction to reach the same objective, the issues with losses were avoided. While the mounting geometry of the fan-radiator assembly can still be perfected to minimize losses in the diffuser region, this fundamental property of the diffuser concepts deemed them more promising.

On this subject, experimenting with different diffuser profiles with the added fans, and evaluate their potentially effects on the result could be an interesting next step. The diffuser downforce for each iteration can be seen in Figure 5.3. The result looks promising since only one iteration was carried out for these concepts (except for concept 4) and therefore it is believed that more performance could be found by iterating on the geometry. Furthermore, all diffuser concepts comply with the specified mass flow requirement through the radiator, meaning that further work in the region can be centred around finding aerodynamic performance without worrying about the mass flow parameter.

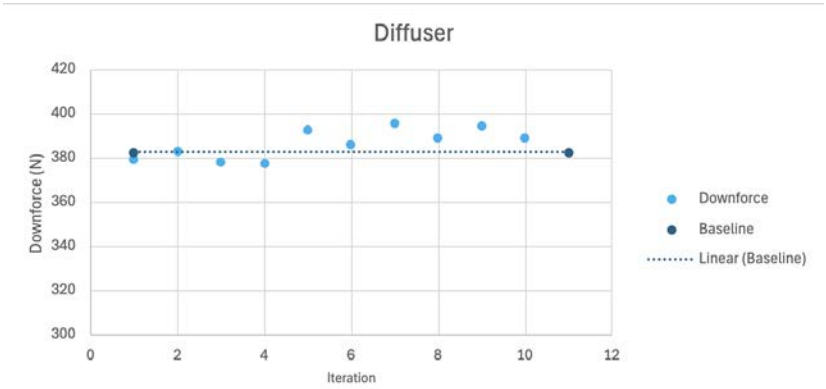

Figure 5.3: Plot of Total Downforce Results for all conducted simulations on the Diffuser

5.4 Rear Wing

Below, a general discussion regarding the result for the rear wing will be carried out. Two concepts were simulated with results mostly harming the performance of the isolated rear wing part but some iterations proving improved performance for the aero package as a whole. Figure 5.4 shows the total down force for each conducted simulation on the rear wing.

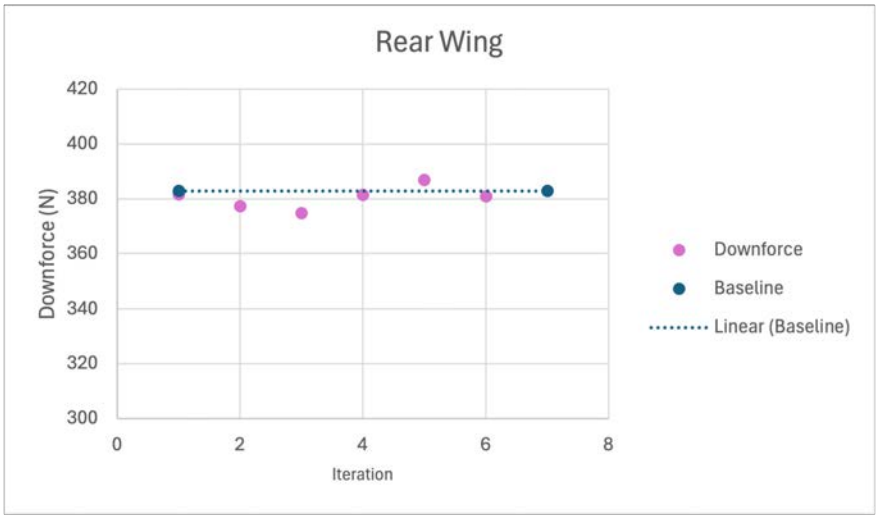

Figure 5.4: Plot of Total Downforce Results for all conducted simulations on the Rear Wing

With the rear wing being located high up compared to other aerodynamic devices on the car, it mostly receives air of ambient pressure and velocity. This is not to say that it is independent of the other devices on the car and as previously seen in results for concepts aimed at improving another part, the performance of rear wing often deteriorate. One

theory is that introducing low pressure zones at new points downstream in the airflow has an effect on the overall flow distribution and can in some cases mean that less air is going towards the rear wing. This is especially true on some of the side wing concepts where rear wing performance have decreased significantly. On the same note it has been found that the rear wing is sensitive both to alterations in the oncoming flow and in the flow on the suction side. The second point is thought to be a result of the rear wing already being a relatively well functioning aerodynamic device. The first concept as well as some iterations in the second concept aimed to inject more energy in the boundary layer as a measure to reduce the risk of separation as well as lowering the pressure on the top flap. When looking at comparisons like the one in Figure 4.58 however, the pressure fields on the suction sides are remarkably similar meaning that the injection of high energy air in the boundary layer makes little to no difference. As no separation occur in the first place, no real benefits are found considering that ambition either. It should be noted that the simulations are carried out in a straight line scenario with no consideration of pitch. Injecting high energy air in the boundary layer could potentially reduce pitch sensitivity on the rear wing, but that is outside the confinements of this project. The same is true of potential geometry changes which could've been made possible with the new energy, but that is once again considered in this project. As mentioned in the conclusions in Section 4.4.2.3, the functionality of the current geometry means that the energy could be used towards potential new geometry in the region as showed by the added beam wing in the same concept. While new geometry could have an influence on the performance on the existing one, it is still thought to be a successful way of increasing overall performance in the region. While the first concept proved to decrease rear wing performance, it showed to be beneficial for both the body/diffuser and side wings as seen in Table 4.20. This is another key takeaway from working in this region. The strong upwash from the rear wing has an impact even on flow relatively far away. With a lot of stationary air and global upwash, the aerodynamic devices in the region and their individual performance becomes notably dependent on each other. This means that learning and understanding the synergies between the parts in the region is key to design devices that work well together. Knowing where to inject new energy and in which direction is therefore important not only for the targeted part, but for all devices in the region. For a project like this, where the number of iterations on each concept are relatively few, it's difficult to acquire the required understanding of the flow patterns in the region, but if it would be decided to place a fan in the region, understanding the synergies between the devices and the flow patterns in the region should be prioritized.

5.5 Sources of error

In this section, the possible sources of error are discussed and explained. Every study have sources of possible errors, it is therefore important to thoroughly investigate what these are and how then can be prevented or minimized.

5.5.1 Simplifications and general sources of error

This study is meant to be comparable to the current fan and radiator placement used by CFS. It is therefore important that the CAD and simulations are representable and

comparable. One source of error is the CAD used for the radiator and fan package. In reality, the fans have a set geometry. The fan CAD used in most simulations was based on approximate measurements of the actual fan. Due to heavy space constraints, some front wing concepts were required to use a slightly smaller geometry. This causes the mass flow through the fans to decrease, as the fans are defined with power per area unit. Therefore, the results of the front wing could be slightly misleading. However, since the results were negative and that having slightly higher mass flow was deemed to not drastically improve the results, the difference in fan radius was considered irrelevant.

The radiators were simplified in STAR-CCM+ by being defined as a porous region instead of the actual geometry. The real radiator geometry would both require unnecessary CAD work for the group as the geometry is quite complex. This would also require adding a large number of cells, leading to longer meshing and simulation times. These simplifications were deemed acceptable since CFS currently uses this setup. Similar simplifications were made with regard to the fans as well. In STAR-CCM+ the fans could be defined as a geometric volume rotating with a specified rotations per minute. This was also considered redundant, as this would lead to increased simulation times and no guarantee that it would decrease the error. One simplification that in further studies probably should be reconsidered is the fact that the air exiting the fans is relatively laminar, as the fans only inject energy into the air. In reality, fans cause a vorticity that could change the results.

In this study, mountings and coolant tubing were determined not to be discussed as it would cause CAD times to increase. The radiators require two tubes, both of which would disturb the airflow. If the fans require mountings, it would increase the weight and further disturb the airflow. This means that the actual result of the concepts may be slightly worse than the simulations made in this study. Therefore, more simulations must be made before implementing any of the mentioned concepts on the actual car.

5.5.2 CFD uncertainty

CFD modeling involves using a discretized domain to solve the equations numerically. In other words, the problem is approximated in order to be solvable. Even though the approximation with some work in the model can be very close to reality, an error of some magnitude will always remain. The size of the error can be affected by a number of factors.

One factor is the chosen physics model. The aim for it is to match the airflow behaviour that the car will endure at competition. However, there are many environmental factors that can make the flow differ in behaviour and a significant risk that the competition conditions do not match those of the simulations.

Another factor is the chosen settings for the mesh. The finer the mesh, the smaller the resulting error will be. However, with limited computational resources, it has had to be accepted to use rougher meshes in some areas and that the use of a mesh overall results in an approximation in calculations.

To conclude, the use of computer based simulations overall means an approximation in

calculations when the intended application of the project is on a real race track. Even though the aim in manufacturing the car is to match the CAD model, there will be differences in shapes and surface finishes when the car is later on built. It can therefore not be fully concluded that a concept that performs in the simulations will work as well on the actual race track.

6
Conclusion

In this chapter, conclusions are drawn from the results presented in the previous chapters. This includes analysing the conceptual potential in terms of implementation on the Chalmers Formula Student car.

From Section 5 and Figure 6.1, it becomes evident that the most promising areas of implementation for the fans are the side wings and the diffuser. The conclusion is based on most concepts showing promising results both in comparison to the non-fan baseline and the by CFS implemented concept (SW1). It should once again be mentioned that the concepts evaluated in this project have been tested through a maximum of 5 iterations, which implies that a lot of iterating work can still be done to enhance the performance for each concept. This iterative work has been carried out for the CFS concept (SW1), which is one factor in its results. However, when analyzing the results from some of the less iterated concepts for the side wing and the diffuser, it becomes evident that some performance is still to be found, but that the fundamental functionality and thought behind them benefits the overall airflow of the vehicle.

The concepts for the side wings aimed at enhancing the mass flow through as well as lowering the pressure under the side wings were in general successful as the interaction between the low pressure zone under the floor and the side wing was strong. This meant that a concept aimed at lowering the pressure on the suction side of the side wing main segment also affected the region of low pressure under the floor. Similarly, some diffuser concepts that were designed to reduce the pressure under the floor also greatly affected the side wings, as the suction effect induced by the fans meant that the coinciding low pressure region of the side wing main segment was affected.

From the matrix in appendix C, the best concept with regards to performance and implementability is the third side wing concept. Placed at the leading edge of the side wing floors, the aim of the fan-radiator assembly is to extract air from the front tyre wake region that would have otherwise entered the side wing main segment. The air is then ejected along the floor towards the outer flaps of the side wings placed downstream. Other than showing promising numbers in terms of performance, this concept is thought to be of relative ease to implement on the car, with the placement on the side wings proven to be a viable location. Additionally, no new concept specific geometry like ducts are needed to find the base performance of the concept. While further iterations might show that this kind of geometry can enhance the concept's performance, it has a high base performance to begin with.

As discussed in Section 5.5, there are several simplifications made and before implementing any of the mentioned concepts on the real car, further simulations must conducted to verify that the performance found is translatable to a real world implementation. The given simplifications include, but are not limited to mounting and hoses connecting to the radiator.

As discussed in Section 5 and shown in Appendix C, was the general radiator mass flow greater than the current CFS solution (SW1). Although the current mass flow is sufficient, an increased mass flow would be beneficial to the car. The concepts were therefore considered to have a great mass flow and no alterations would be required to achieve the desired mass flow on the real car.

In summary, it is evident that the concept of using radiator fans for aerodynamic gains is significant. However, more precise simulations are required to determine with certainty what the best concept is for such implementation.

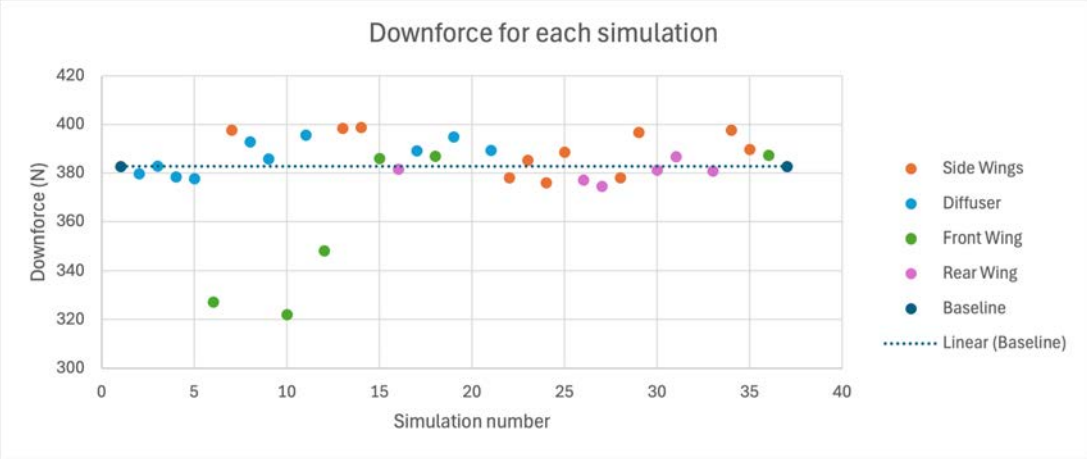

Figure 6.1: Plot of the resulting downforce for each simulation

Bibliography

[1] Formula Student Germany. (2025) Formula student rules 2025. Hämtad 2025-01-28. [Online]. Available: https://www.formulastudent.de/about

[2] ——. (2025) Formula student rules 2025. Hämtad 2025-01-28. [Online]. Available: https://www.formulastudent.de/fileadmin/user_upload/all/2025/rules/FS-Rules_2025_v1.1.pdf

[3] D. Mclean, *Understanding Aerodynamics: Arguing from the Real Physics*. Wiley-Blackwell, 2012.

[4] J. Katz, *Race Car Aerodynamics: Designing for Speed*. Massachusetts, MA, USA: Bentley Publishers, 1995.

[5] A. Ogawa, S. Mashio, D. Nakamura, Y. Masumitsu, M. Minagawa, and Y. Nakai, "Honda r&d aerodynamic analysis of formula one vehicles," Honda R&D Co., Ltd., Tech. Rep., NA.

[6] S. L. Dixon and C. A. Hall, *Fluid Mechanics and Thermodynamics of Turbomachinery*, 7th ed. Oxford, UK: Butterworth-Heinemann, Elsevier, 2014, pages 1–2.

[7] Glenn Research Center - NASA, *Navier-Stokes Equations*, NASA, last updated: 2021, Accessed on: Apr. 22, 2025. [Online]. Available: https://www.grc.nasa.gov/www/k-12/airplane/nseqs.html

[8] R. Eymard, T. Gallouët, and R. Herbin, "Finite volume methods," in *Handbook of Numerical Analysis, Volume 7: Solution of Equation in (Part 3), Techniques of Scientific Computing (Part 3)*, J. L. Lions and P. Ciarlet, Eds. Elsevier, 2000, pp. 713–1020. [Online]. Available: https://hal.science/hal-02100732v2

[9] CD-adapco, *STAR-CCM+ User Guide, Version 11.02*, CD-adapco, 2016, accessed on: Apr. 8, 2025.

[10] Siemens Digital Industries Software, *Simcenter STAR-CCM+, version 2021.1*, 2021, available: https://www.plm.automation.siemens.com/global/en/products/simcenter/STAR-CCM.html.

Appendix A

Implementation category	Frequency
Frontwing	0
Sidestructures	21
Ground effect	4
Rearwing	10
No implementation	1
N/A	9
Diffuser	4

Fan placement	Frequency
Frontwing	0
Side wing main segment	3
Rear	8
Rear angeld vertical	16
N/A	3
In front of side wing flaps	5
Stagnation plates	11
Rear angeld horizontal	2
No fan	1

https://www.formulastudent.de/pr/pictures
https://media.formulastudent.de/keyword/car_035

Skidpad points	CIA
50	14
44.8	5.78
39.19	5.43
38.62	4.119
35.44	4.9
31.25	5.05
28.4	4.38
21.35	4.8
19.61	4.78
13.37	3.95
2.5	3.9
0	4.7
0	4.49
0	6.65

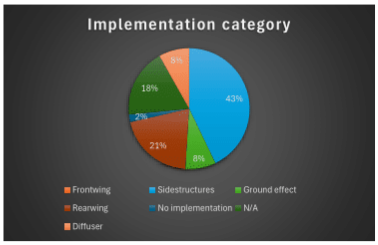

DNF/DSQ results not included below:

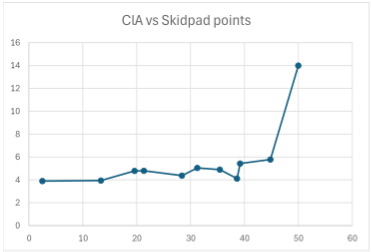

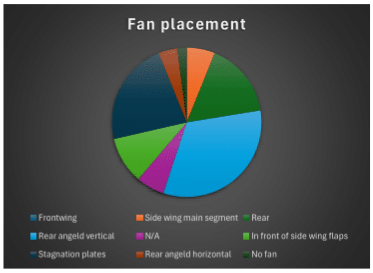

Not including TU Dresden below:

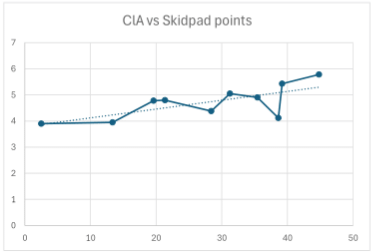

Figure .2: Results from study about current fan placement on top 50 FS teams.

Appendix B

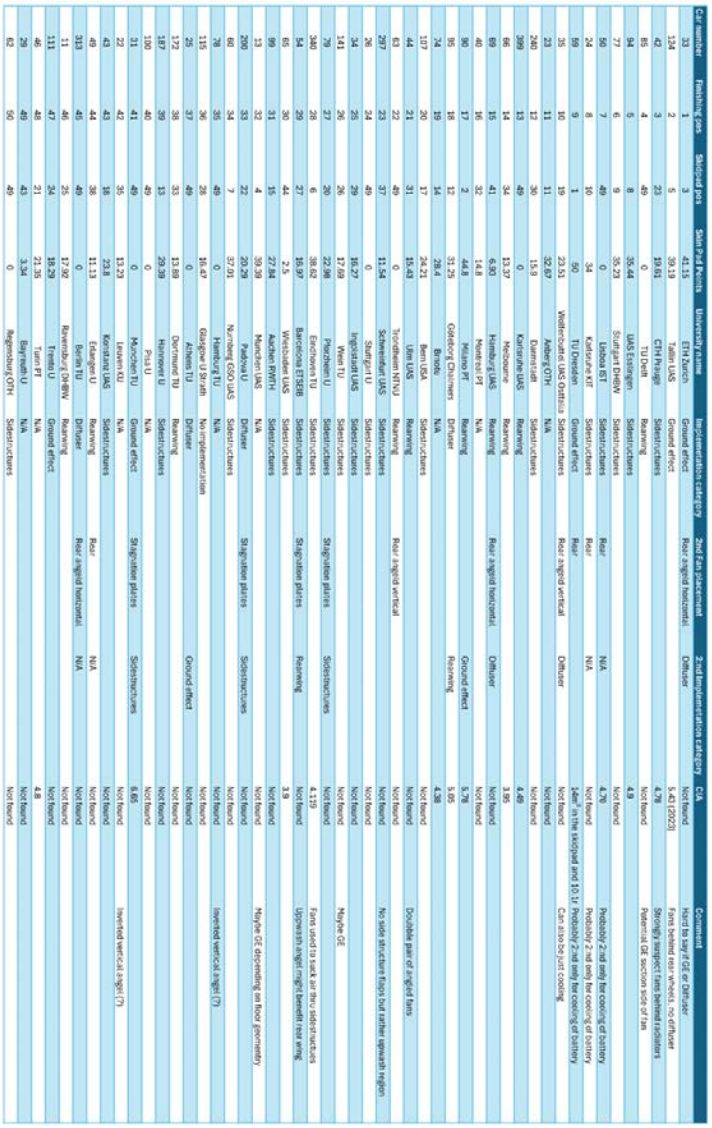

Car number	Finishing pos.	Skidpad pos.	Skidpad Points	University name	Implementation category	2nd Fan placement	2nd Implementation category	CIA	Comment
33	1	3	41.15	ETH Zurich	Ground effect	Rear angled horizontal	Diffuser	Not found	Hard to say if GE or Diffuser
124	2	5	39.19	Tallin UAS	Ground effect			5.43 (2022)	Fans behind rear wheels, no diffuser
42	3	23	19.61	CTH Provgi	Sidestructures			4.76	Strongly suspect fans behind radiators
85	4	49	0	TU Delft	Rearwing			Not found	Potential GE suction side of fan
84	5	8	35.44	UAS Esslingen	Sidestructures			4.9	
77	6	9	35.23	Stuttgart DHBW	Sidestructures	Rear	N/A	Not found	
50	7	49	0	Lisboa IST	Sidestructures	Rear	N/A	4.76	Probbably 2 rad amby fan cooling of battery
24	8	10	34	Karlsruhe KIT	Sidestructures	Rear	N/A	Not found	Probbably 2 rad amby fan cooling of battery
59	9	1	90	TU Dresden	Ground effect	Rear	Diffuser	14m in the stepped and 10.1r	Probbably 2 rad amby fan cooling of battery
35	10	19	23.51	Wolfenbuttel UAS Ostfalia	Sidestructures	Rear angled vertical	Diffuser	Not found	Can also be just cooling
23	11	11	32.87	Aalberg OTH	N/A			Not found	
240	12	30	15.9	Darmstadt	Sidestructures			Not found	
399	13	49	0	Karlsruhe UAS	Rearwing			4.49	
66	14	34	13.37	Melbourne	Rearwing			3.95	
69	15	41	6.90	Hamburg UAS	Rearwing	Rear angled horizontal	Diffuser	Not found	
40	16	32	14.8	Madeira PT	N/A			Not found	
90	17	2	44.8	Milano PT	Rearwing		Ground effect	5.78	
95	18	12	31.25	Göteborg Chalmers	Diffuser		Rearwing	5.05	
74	19	14	28.4	Brno TU	N/A			4.38	
107	20	17	24.21	Bern UAS	Sidestructures			Not found	
44	21	31	15.43	Ulm UAS	Rearwing			Not found	Doubler pair of angled fans
63	22	49	0	Trondheim NTNU	Rearwing	Rear angled vertical		Not found	
297	23	37	11.54	Schweinfurt UAS	Sidestructures			Not found	No side structure flaps but rather sepwash region
26	24	49	0	Stuttgart U	Sidestructures			Not found	
34	25	29	16.27	Ingolstadt UAS	Sidestructures			Not found	
141	26	26	17.69	Wien TU	Sidestructures	Stagnation plates	Sidestructures	Not found	Maybe GE
79	27	20	22.98	Pforzheim U	Sidestructures			Not found	
340	28	6	38.62	Eindhoven TU	Sidestructures	Stagnation plates	Sidestructures	4.119	Fans used to suck air thru sidestructures
54	29	27	16.97	Barcelona ESEIB	Sidestructures	Stagnation plates	Rearwing	Not found	Upwash might benefit rear wing
65	30	44	2.5	Wiesbaden UAS	Sidestructures			3.9	
99	31	15	27.84	Aachen RWTH	Sidestructures			Not found	
13	32	4	39.39	München UAS	N/A			Not found	Maybe GE depending on floor geometry
200	33	22	20.29	Piešťany U	Diffuser	Stagnation plates	Sidestructures	Not found	
60	34	7	37.01	Nürnberg GSO UAS	Sidestructures			Not found	
78	35	49	0	Hamburg TU	N/A			Not found	Inverted vertical angel (?)
115	36	28	16.47	Glasgow U Strath	No implementation			Not found	
25	37	49	0	Athens TU	Diffuser		Ground effect	Not found	
172	38	33	13.88	Dortmund TU	Rearwing			Not found	
187	39	13	29.39	Hannover U	Sidestructures			Not found	
130	40	49	0	Pisa U	N/A			Not found	
31	41	49	0	München TU	Ground effect	Stagnation plates	Sidestructures	6.85	
22	42	35	13.23	Leuven U	N/A			Not found	Inverted vertical angel (?)
43	43	38	11.3	Kaiserslautern UAS	Sidestructures			Not found	
49	44	48	1.3	Stuttgart U	Diffuser	Rear	N/A	Not found	
313	45	48	1.3	Esslingen U	Diffuser	Rear angled horizontal	N/A	Not found	
11	46	25	17.93	Rosenheim UAS	Rearwing			Not found	
111	47	24	18.29	Trento UNI	Ground effect			Not found	
46	48	21	21.35	Turin PT	N/A			4.8	
28	49	43	3.34	Bayreuth U	N/A			Not found	
62	50	49	0	Regensburg OTH	Sidestructures			Not found	

Figure .3: Study about current fan placement on top 50 FS teams.

Appendix C

Concept		1 Base	2	3	4	5	6	7	8	9	10	11	12	13	14	15
Criteria	Weight factor (1-5)	Score (-3 to +3)														
Massflow	1	−3	−3	3	3	−3	2	3	3	0	3	3	3	3	2	3
Ease of Implementation	3	3	−3	−3	−2	2	1	2	2	2	2	−3	2	2	−2	2
Drag force	1	0	1	0	3	0	0	2	2	0	−1	0	0	0	1	2
Downforce	5	0	−2	−1	−2	1	3	−2	0	3	3	1	2	2	1	−1
Manufacturability	2	3	−1	−1	0	2	3	2	2	2	1	0	2	1	−1	2
	Total	**12**	**−23**	**−13**	**−10**	**12**	**26**	**5**	**15**	**25**	**25**	**−1**	**23**	**21**	**0**	**10**
	Rank	7	15	14	13	7	1	10	6	2	2	12	4	5	11	9

1	Basline	Mass flow
2	FW Ground effect near wall mommentum	0,146
3	FW Ground effect and outwash	0,300
4	FW Outwash	0,254
5	FW Enhanced Underfloor Massflow	0,173
6	SW Accelerate low energy wheel wake along side structures	0,245
7	SW Accelerate air over stagnation plate	0,268
8	SW Ground effect in side wing main segment	0,268
9	SW Airflow through stagnation plate	0,229
10	DF Suction to increase expansion	0,252
11	DF Inside-suction	0,264
12	DF Virtual wall	0,263
13	DF Suction to increase expansion	0,256
14	RW Powered head rest	0,240
15	RW Mono upwash	0,262

Dragforce	Downforce	Value
125	395	3
127	391	2
129	387	1
131	383	0
132	387	−1
133	375	−2
134	371	−3

Mass flow	Value
0,25	3
0,24	2
0,23	1
	0
0,21	−1
0,2	−2
0,19	−3